Ph.D. Dissertation

2011

Effects of antagonists of luteinizing hormone- and growth hormone-releasing hormone on experimental benign prostatic hyperplasia and prostate cancer

Ferenc G. Rick, M.D.

Department of Anatomy
University of Pécs, School of Medicine
Pécs, Hungary

Department of Pathology
University of Miami, Miller School of Medicine
Miami, Florida, USA

Head of Postgraduate Education:	László Lénárd, M.D., Ph.D., D.Sc.
Program leader:	Valér Csernus, M.D., Ph.D., D.Sc.
Mentors:	Magdolna Kovács, M.D., Ph.D., D.Sc.
	Zoltán Rékási, M.D., Ph.D.
Advisors:	Andrew V. Schally, Ph.D., M.D.hc(Multi), D.Sc.hc
	Norman L. Block, M.D., F.A.C.S., D.A.B.U.

Ferenc G. Rick, M.D.

Effects of antagonists of luteinizing hormone- and growth hormone relasing hormone on experimental benign prostatic hyperplasia and prostate cancer

Mentors:

Magdolna Kovacs, M.D., Ph.D., D.Sc., Professor

and

Zoltan Rekasi, M.D., Ph.D., Professor

Department of Anatomy
University of Pecs, School of Medicine
Pecs, Hungary

Advisors:

Andrew V. Schally, Ph.D., M.D.hc (Multi), D.Sc., Professor

and

Norman L. Block, M.D., F.A.C.S., D.A.B.U., Professor

Department of Pathology, Divisions of Hematology/Oncology and Endocrinology, Department of Medicine
University of Miami, Miller School of Medicine
Veterans Affairs Medical Center and South Florida Veterans Affairs Foundation for Research and Education
Miami, Florida, United States of America

The work described in this thesis was supported by the Medical Research Service of the Veterans Affairs Department, Departments of Pathology, and Medicine, Division of Hematology/Oncology of the Miller Medical School, University of Miami and AEterna/Zentaris GmbH through South Florida Veterans Affairs Foundation for Research and Education (all to A.V.S.), the L. Austin Weeks Endowment for Urologic Research (N.L.B.), and the Hungarian National Sciences Foundation Grant OTKA K068452 (Z.R.).

© Copyright 2011, F. G. Rick

All rights reserved. No part of this work may be reproduced in any form by any electronic or mechanical means without permission in writing from the author.

Contents:

Abbreviations

5AR2 = 5α-reductase type 2

α_{1A}-AR = α1A-adrenoreceptor

AR = androgen receptor

BPH = benign prostatic hyperplasia

BOO = bladder outlet obstruction

CET= Cetrorelix

COX = cyclooxygenase

DHT = dihydrotestosterone

EGF = epidermal growth factor

FGF = fibroblast growth factor

GH = growth hormone

GHRH = growth hormone-releasing hormone

GHRH-R = growth hormone-releasing hormone receptor

IFN-γ = interferon-γ

IGF = insulin-like growth factor

IL = interleukin

LH = luteinizing hormone

LHRH = luteinizing hormone-releasing hormone

LHRH-R = luteinizing hormone-releasing hormone receptor

LUTS = lower urinary tract symptoms

NF-κβ = nuclear factor-kappa beta

PSA = prostate specific antigen

STEAP = six-transmembrane epithelial antigen of the prostate

SV1 = splice variant 1 of GHRH-R

TE = testosterone enanthate

TGF-β = transforming growth factor-β

1. Introduction and background

1.1. Benign prostatic hyperplasia

Benign prostatic hyperplasia (BPH) is an extremely common urinary tract disorder that can be described clinically or pathologically. Clinical BPH is commonly viewed as benign enlargement of the prostate, which contributes to an array of urinary voiding difficulties that can range from bothersome lower urinary tract symptoms (LUTS) to significantly impacting quality of life among older men (1). Pathologic BPH is the histological determination of non-neoplastic new prostatic growth in adult men. Autopsy studies have revealed that the prevalence of pathologic BPH increases markedly after the 4th decade and is found in up to 90% of men over age 80 (2). The high prevalence of BPH in older men has led some to consider prostatic hyperplasia to be a ubiquitous result of aging (3). The precise molecular mechanisms underlying the induction, maintenance, and development of clinical sequelae resulting from BPH are incompletely understood (4).

1.2. Clinical BPH

The human prostate consists of four separate histologic zones: central, peripheral, transition, and anterior fibromuscular (5). While prostate cancer is found mostly in the peripheral zone, virtually all clinically significant BPH develops in the transition zone of the prostate (6). Macroscopic growth of the transition zone can cause narrowing of the urethra as it passes through the prostate, leading to a bladder outlet obstruction (BOO), which may affect the flow of urine. In men, the prostate is the most common cause of obstruction. BPH and subsequent BOO contributes to a variety of urinary voiding problems that can significantly impact quality of life and are commonly known as LUTS (7). In large studies of men with BPH and LUTS, no strong correlation was found between prostate size, symptoms and urinary flow rates (1). However, serum prostatic specific antigen (PSA) does correlate with prostate volume, and men with larger prostates and elevated serum PSA are at higher risk of experiencing more significant symptoms, including ultimate progression to acute urinary retention (1). LUTS include bladder storage symptoms such as increased urinary frequency, urgency, and nocturia; difficulty starting the stream of urine decreased urinary flow and incomplete emptying are generally attributed to problems with bladder emptying (8). Other significant causes and contributing factors to LUTS are age-related declines in detrusor function and systemic medical conditions (8,9). In contrast to earlier times in man's history, with contemporary treatment strategies, BPH is now an atypical direct cause of mortality. Experiencing an acute urinary retention and nocturia are clinical markers of increased mortality risk that likely represent the high comorbidity of BPH with other systemic medical conditions (4,10). Taken together with high morbidity and financial burden, BPH and LUTS are serious medical matters.

1.3. Pathological BPH

Pathologically, BPH is characterized by hyperplastic epithelial and stromal growth that combine into microscopic and macroscopic nodules in the prostate gland (11). There are five generalized types of BPH nodules: (1) fibromyoadenomatous (common), (2) fibroadenomatous, (3) fibrous/fibrovascular, (4) fibromuscular, and (5) muscular (uncommon) (12). More frequently, BPH is described as epithelial (containing mostly prostate epithelial cells), mixed (containing stromal and epithelial cells), and stromal (containing mostly stromal cells) (13). The initial nodules that develop in BPH are found in the periurethral region and are typically stromal, composed of fibrous tissue mixed with some smooth muscle (12). Infrequently, BPH nodules may be found in the peripheral zone, which is palpable with digital rectal examination, and are typically composed of epithelial glandular elements (14). The lack of glandular elements in stromal BPH nodules, and the observation of zonal differences in the initiation of BPH nodules suggest a distinct etiology of stromal nodules compared to BPH with glandular components. When the transition zone enlarges macroscopically, due to BPH nodular growth, it can obstruct the flow of urine through the prostatic urethra and hence contribute to LUTS. Understanding the key molecular mechanisms for how distinct BPH nodules develop and are associated with LUTS is essential to developing clinical management tools for these diseases.

1.4. Theories of the etiology of BPH

The precise molecular etiology of BPH is complicated and unknown, but several theories have been proposed. Hyperplastic growth in BPH has been credited to embryonic reawakening (6), an imbalance between androgen/estrogen signaling (3,15), tissue remodeling in the aging prostate (16), epithelial-mesenchymal transition (17), stem cell defects (18), hypoxia (19), chronic inflammation (20), overexpression of stromal and epithelial growth factors (21) or by other obscure factors (Figure 1).

One prominent theory of BPH pathogenesis was proposed by McNeal and is termed the embryonic reawakening theory (6). In 1978, McNeal posited that prostatic hyperplasia represents an awakening of hormonally-mediated developmental processes (6). Through precise study of 63 autopsy prostates, he noted that BPH nodules arose from the transition zone (6).

Consistent with this observation, Cunha demonstrated that androgen regulation and paracrine interactions were necessary for prostate glandular development and maintenance, establishing the key role of stromal–epithelial cell interactions in the prostate (22). A hormonal etiology involving dysregulation of stromal–epithelial cell interactions is recognized as important for BPH development, but the precise pathogenesis remains to be elucidated.

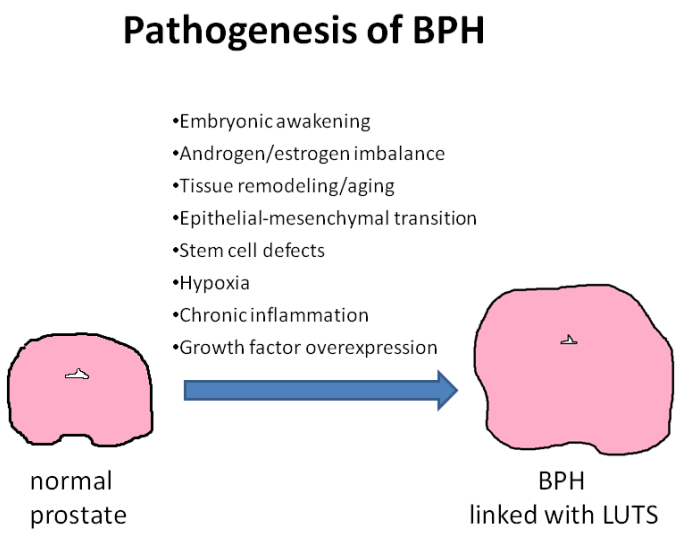

Figure 1. A schematic showing the confluence of factors for the development of BPH

Androgens, in particular DHT, are widely accepted as essential for the growth and development of the human prostate (3). Although an association between concentrations of androgens in the blood or prostate and risk of BPH or LUTS cannot be consistently demonstrated in epidemiological studies (23), it is believed that androgens play a permissive role in BPH pathogenesis (3). Androgen ablation by orchiectomy or suppression of the pituitary–testicular axis effectively reduces prostate volume and improves symptoms caused by BPH, but also leads to adverse effects unacceptable to many patients.

Increasing evidence from epidemiological, animal and in vitro studies supports a role for estrogens in the pathogenesis of BPH (3). Most epidemiological studies have shown an association between circulating estrogen levels and the risk of BPH or LUTS, and many experimental studies have reported estradiol stimulation of prostate stromal cell proliferation in vitro (24,25). Studies of human prostate tissues have indicated differential localization of ER subtypes in the two main cell compartments of the prostate. Expression of ERα and ERβ has been identified mainly, though not exclusively, in the prostate stroma and epithelium respectively, which suggests that they play different roles in prostate physiology (26). To date, animal and in vitro studies have shown that ERα and ERβ mediate the proliferative and apoptotic effects of estrogens on prostate cells, respectively (27). Current evidence suggests that estrogens and androgens interact with one another in regulating prostate cell growth in vivo (3).

Age is an associated factor for the development of both histologic and clinically significant BPH. Although nearly all men will develop histologic BPH with age, it is thought that BPH initiation occurs in younger men (30 years of age) (2). Furthermore, younger men develop BPH but at much lower rates compared to aged men (2). It is presumed that there is no single pathomechanism, but a

synergistic effect of multiple events within biological communication systems (nerve-, endocrine-, immune system) during the aging process of the organ (16). These events are predominantly changes in prostate cell–cell interactions and alterations of highly specialized cell types responsible for tissue homeostasis and function. In particular, life-long stress, pleiotrope mechanisms/factors and noxes on metabolically highly active epithelia seem to be main triggers for initiation of BPH and organ enlargement (16).

Alonso-Magdalena *et al* proposed that BPH is not a proliferative disease of the stroma but the result of accumulation of myofibroblasts and smooth muscle cells, as a consequence of epithelial proliferation and epithelial-mesenchymal transition (EMT) (17). This phenomenon involves changes in gene expression that disrupt epithelial polarity and establish a mesenchymal phenotype, with concomitant alterations in cytoskeletal organization, cell adhesion, and production of extracellular matrix. The TGF-β/Smad3 is a key signaling pathway associated with the induction and maintenance of EMT (28).

Lin et al demonstrated mesenchymal stem cell markers on primary stromal cells from BPH patients, which have strong proliferative potential and ability to differentiate to myogenic, adipogenic and osteogenic lineages (18).

A recent study revealed that prostatic stromal cells respond to hypoxia by upregulattion of secretion of several growth factors such as VEGF, FGF-2, FGF-7 and TGF-β, suggesting that hypoxia can trigger prostatic growth (19).

An emerging body of evidence suggests that inflammation may play a key role in the development and progression of BPH (20,29). Clinically, several cross-sectional studies have proposed that a relationship exists between the presence of inflammatory infiltrates and an increase in prostate volume. Di Silverio *et al.* reported that presence of chronic inflammation increased as prostate volume augments, from 9% in prostates of 30-39 milliliters (mls) to more than 60% in prostates of 80-89 mls (30). A minor correlation was observed between presence of prostatic inflammation and lower urinary tract symptoms (LUTS) in participating men in the Reduction by Dutasteride of Prostate Cancer Events (REDUCE) trial (31). This minor correlation between prostatic inflammation and presence of LUTS may be expected given the relatively modest correlations that have been found between prostate volume and LUTS (32) . Additionally, in a Wistar rat model, administration of an immunostimulator resulted in epithelial proliferation (33).

Recent reviews of the pathogenesis of BPH highlighted the differential expression of cytokines and growth factors in BPH tissue suggesting a role for inflammation in the propagation of BPH (16,34). An up-to-date outline of the current state of knowledge in regard to the impact of inflammation on the pathogenesis of BPH was reported by Kramer *et al.* (20). Chronic inflammatory infiltrates, mostly composed of activated T cells and macrophages, are often associated with BPH nodules (35,36). Infiltrating T cells and macrophages are responsible for the production of cytokines

(IL-2 and IFNγ), which are believed to support fibromuscular growth through cascades of proinflammatory cytokines and growth factors (21,37,38), leading to LUTS (39). Migration of T cells into the area is accomplished by increased production of proinflammatory cytokines such as IL-6, IL-8, IL-15 and IL-17 (16,20,40,41). Subsequently, surrounding cells are killed by unknown mechanism and are replaced by fibromuscular nodules (42).Various growth factors such as FGF-2, FGF-7, IGF-I, IGF–II, TGFβ and VEGF, are also involved in the pathogenesis of BPH (21,43).

Recent evidence from cell culture systems and immunohistochemical and mRNA analyses of BPH tissues on expression profiles of growth-regulatory proteins and cytokines has provided insights into the potential role of these growth factors and cytokines in the pathogenesis of BPH. Several stromal and epithelial growth factors and inflammatory cytokines have been reported to be overexpressed in BPH tissues or BPH-derived stromal cells (21). These include members of the fibroblast (e.g. FGF-2, FGF-7, FGF-9), insulin-like (e.g. IGF-1 and IGF-2), transforming growth factor families (e.g. TGF-β1 and TGF-β2), and angiogenic factors (e.g. VEGF-A) and downstream effector molecules as well as a variety of interleukins (e.g. IL-2, IL-4, IL-8 and IL-17) that, working together, could lead to abnormal stromal and epithelial cell growth within the transition zone of the prostate (21,43).

1.5. Models of BPH

There are many *in vitro* and *in vivo* models of BPH available, each has its own strengths and weaknesses (Table 1) (4,44). The best organism to evaluate BPH is man; however, there are ethical issues that make human BPH studies difficult. Additionally, human genetics, socioeconomic backgrounds, and lifestyles are highly variable between populations. Finally, the cost associated with human research is high. For these reasons and others, use of humans is not ideal for early stages of BPH research (4).

Table 1. Benefits and drawbacks of various BPH models

Model	Benefit	Drawback
Xenograft	Human cells, BPH types	Immune function, genetics, SE
Tissue recombination	Human cells, SEI, *in vitro* and *in vivo*	Immune function, SE
Chimpanzee	Anatomy,spontaneous, *in situ*	Genetics, SH, cost, anatomy
Dog	Literature, spontaneous, *in situ*	Genetics, SH, cost, anatomy
Rat	*In situ*	Genetics, anatomy
Mouse (transgenics)	Pathway analysis, *in situ*	Lacks multifactorial initiation, anatomy

Key: stromal-epithelial interactions (SEI); special housing (SH); secondary events (SE)

Adapted from Nicholson et al. Differentiation (2011) DOI: 10.1016/j.diff.2011.04.006

Human xenografts (45) or human tissue recombination xenograft models (46) have been developed and studied extensively. The use of xenografts is particularly well suited for studies evaluating maintenance or treatment of BPH, however, with all xenograft studies several drawbacks apply. They are less suitable for researching the development and prevention of BPH. Additionally,

use of immunocompromised mouse or rat hosts make xenograft studies less appealing for evaluating BPH in the context of an intact immune system. Lastly, although no animal model can evaluate LUTS directly, analysis of secondary complications due to BPH (e.g. BOO) is not possible with xenograft models.Tissue recombination, a technique that utilizes epithelia and stroma from various species or organs, has successfully been used for the study of a wide range of normal and pathogenic states (4,47). In this regard, Barclay and colleagues utilized tissue recombination methods using benign human prostatic epithelial cells (BPH-1 cell line (48)) and human stroma from BPH or normal prostates (46). In those experiments it was found that BPH stroma significantly increased epithelial proliferation relative to control normal stroma, but importantly, malignant transformation did not occur in the BPH tissue recombinants (48). These data are consistent with the important growth promoting role of stroma in BPH. There are distinct advantages of utilizing tissue recombination technology in BPH research. First, human cells can be employed; second, cells are commonly grown in culture first and then recombined and grown in mouse hosts. While the cells are in culture it is possible to manipulate gene expression (e.g. use of shRNA or forced expression of gene of interest) and hence evaluate its consequences, such as growth and differentiation. Furthermore, in vitro experiments can be inexpensively performed as proof of principle prior to in vivo experiments. Lastly, tissue recombination is especially useful in evaluation of stromal–epithelial interactions, which are likely to play a central role in the manifestation and maintenance of BPH.

Models where spontaneous BPH occur are highly desirable because they likely recapitulate the underlying pathophysiology of human disease. The only animals other than man that develop spontaneous BPH are dogs (4,44) and nonhuman primates such as chimpanzees (49). The logistics and costs of carrying out such experiments with these species are typically high, and as such they are used less frequently. Another limitation of spontaneous models is a lack of genetic manipulation, which restricts the use of these models for key mechanistic questions.

Like man, dogs and rodents have hormone responsive prostates making them particularly important in BPH research. The administration of androgens and estrogens to recreate a hormonal environment similar to men as they age, reliably produces prostatic growth in dogs (50) and Wistar, Brown Norway and Sprague-Dawley rats (44,51). Key research utilizing these models have significantly moved the field of BPH research forward although prostate anatomy in dogs and rats differs significantly from the human prostate. In particular, these prostates may grow outwardly and away from the prostatic urethra, making prostatic growth less likely to cause obstruction and affect urine flow, a key feature of human BPH. As such, BOO due to BPH has not been sufficiently described in these models. Possibly the biggest obstacle to the utilization of many BPH models is the lack of genetic manipulation. The ability to alter the genetics of cells, tissues, and whole organisms has greatly advanced the scientific understanding of molecular mechanisms in developmental biology, cancer, and many other disciplines. Although transgenic rats and dogs are possible (4), they are

unlikely to surpass the mouse in availability of genetically altered pathways. Further complications with the usage of dog and rat hormone induction models are the associated cost and special housing needed for these studies. Certainly many aspects of dog and rat models, as with all models, have and will continue to move the field of BPH research forward; however, new genetically tractable models of BPH with putative ‘‘LUTS’’ are needed.

The best genetically workable organism for BPH and BOO research is the mouse, in which gain and loss of function are easily regulated. In general, mouse models for BPH have been poorly received due to their prostatic anatomy which is similar to the rat; therefore, the challenges of modeling human BPH are similar to those encountered with rats and dogs. The prostatic lobes of the mouse, although hormonally responsive, grow outwardly from the urethra into the abdominal cavity. Thus, it is intuitive that regardless of prostate size, it may be impossible for BPH related BOO and subsequent ‘‘LUTS’’ to occur. There are several BPH transgenic mouse models (4), however, it should be recognized that effects of one gene on the induction of multi-factorial disease(s) such as BPH are likely only to enhance the knowledge of the particular pathway or process evaluated.

1.6. Therapy of BPH

A number of treatment options exist for the care of men with clinical sympthoms due to an enlarged prostate. The standard of care for BPH is treatment with α-blockers, 5α-reductase inhibitors (e.g. finasteride), surgery, or a combination there of (1). Drugs that block α-1 adrenergic receptors are effective in BPH mainly by blocking sympathetically mediated contraction of prostatic smooth muscle, relieving BOO, and leading to improved urine flow. α-1 adrenergic receptors are present throughout the smooth muscle of the male urinary tract, and at the level of the spinal cord, ganglia and nerve terminals, and therefore, are likely to have a wide spectrum of favorable effects on these extra-prostatic sites (Nitti, 2005). While α-blockers are effective at improving LUTS for many patients, they do not affect prostate growth and therefore do not decrease the risk of BPH complications such as acute urinary retention and the need for surgical intervention (52). Hormonal treatment of BPH with 5α-reductase inhibitors blocks the conversion of testosterone to DHT, shrinks the prostate and results in improved urinary flow rates, underscoring the well-known dependence of BPH on DHT. The gold-standard surgical treatment for BPH is transurethral resection of the prostate (TURP) which relieves obstruction by removing BPH nodules in the transition zone; however, a variety of minimally invasive surgical approaches exist (7). Some patients do not respond well to these standards of care and it is difficult to predict which patients will respond to a particular treatment. Furthermore, the efficacy and acceptability of other hormonal treatments, such as antiandrogens or LHRH agonists, is low and can be associated with side-effects of androgen ablation, such as hot flushes, decrease of potency and libido and negative effects on bone and other tissues (53). Thus, there remains a need for advances

and improvements in treatment and prevention of BPH and LUTS based on a better understanding of their pathophysiology.

1.7. LHRH antagonists and BPH

LHRH antagonists inhibit the reproductive system through competition with endogenous LHRH for binding to pituitary LHRH-Rs, thus avoiding the undesirable stimulation and possible disease flare that precedes the receptor desensitization observed with the agonists (Figure 2) (53). Cetrorelix, originally developed in our laboratory in the late 1980's (54), is a highly potent LHRH antagonist that induces an immediate inhibition of the pituitary-gonadal axis (Figure 2). Several clinical studies have shown that therapy with low doses of this LHRH antagonist caused a marked and long-lasting improvement in LUTS, with no impairment of gonadal function in men with symptomatic BPH (55-58). During a long-term follow-up of >1 year after discontinuation of cetrorelix, most patients continued to show a progressive improvement in urinary symptoms, sexual function, a reduction in the IPSS, and an increase in urinary peak flow rate, with only a slight reduction in prostate volume (56). In recent studies, during treatment there was a dose-dependent transient suppression of serum testosterone concentrations, but the levels remained above castration values. After 2 weeks the serum values returned to baseline (57). In experimental studies in rats, low doses of cetrorelix, similar to those used in clinical studies, caused only a partial suppression of the pituitary-gonadal axis and a transient suppression of serum LH and testosterone levels (59). In clinical studies, the therapeutic effect of cetrorelix appears to be independent of testosterone suppression (55-58). However, contradictory results of treatment with cetrorelix have been reported, which showed no difference with placebo (60). Russo et al showed that LHRH antagonist ganirelix counteracts experimental detrusor overactivity in female rats (60). This suggests that LHRH-R regulates bladder function and supports reports of beneficial effects of LHRH receptor blockade in LUTS patients. The improvement in LUTS also could be due to a direct inhibitory effect of cetrorelix on the prostate through prostatic LHRH-Rs in combination with suppression of inflammatory cytokines, growth factors and their receptors (61).Cetrorelix was also shown to inhibit the growth of human prostatic and other cancers xenografted into nude mice with suppression of growth factors EGF and IGF-2 and EGF receptor (62-64). A recent report demonstrated that apoptosis in primary cultures from prostate cancer was induced by LHRH antagonist cetrorelix mediated by extrinsic pathway involving p53 phosphorylation (65).

A recent study from our laboratory has shown that *in vitro* cetrorelix can directly inhibit the proliferation rate of the human BPH-1 prostate epithelial cell line by counteracting growth factors like IGF-I and -II and FGF-2, and downregulating the LHRH receptor and α-adrenergic receptors, as well as transcription factors (66).

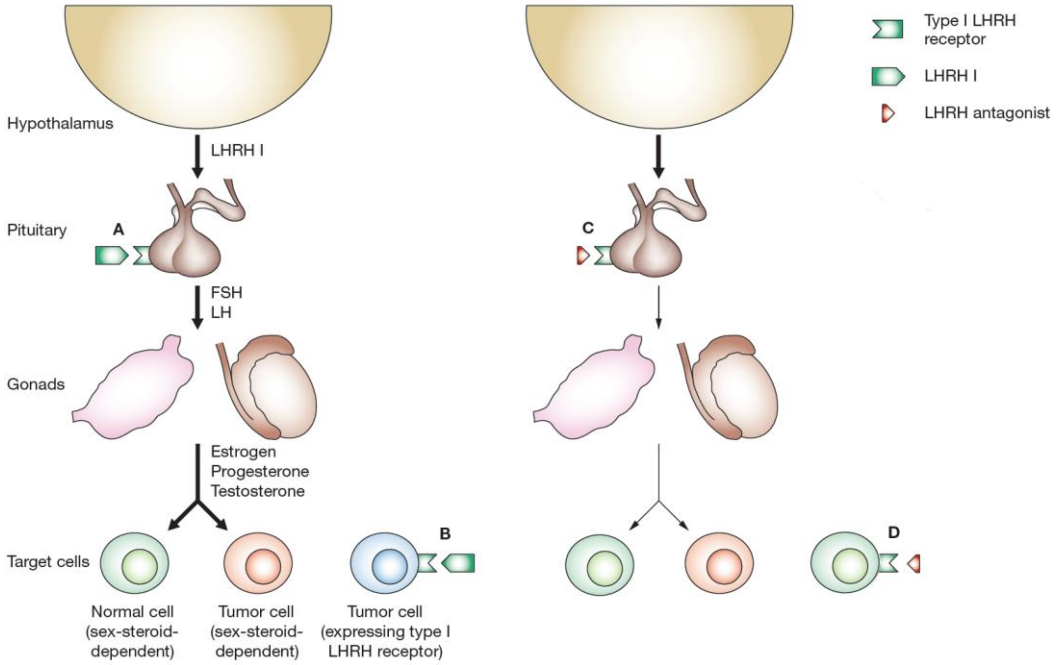

Figure 2. Mode of action of antagonists of LHRH. (A) Type I LHRH secreted by the hypothalamus binds to its receptor in the pituitary and stimulates release of LH and FSH. These hormones, in turn, stimulate release of sex steroids, which can stimulate growth and development of normal and tumor cells. (B) Some tumors express LHRH receptors and can respond to LHRH; cells in these tumors can be sex-steroid-dependent or sex-steroid-independent. (C) LHRH antagonists induce a hypogonadotropic state by competitive blockade of pituitary LHRH receptors. Consequently, levels of FSH and LH, and subsequently levels of sex steroids, are lowered. The decrease in levels of sex steroids inhibits the proliferation of both benign and malignant sex-steroid-dependent cells. (D) On benign cells that express LHRH receptors, antagonists of LHRH might exert some direct effects mediated by these LHRH receptors. Abbreviations: FSH, follicle-stimulating hormone; LH, luteinizing hormone; LHRH, luteinizing-hormone-releasing hormone. Schematic figure is adapted from Engel et al. Nat Clin Pract Endocrinol Metab (2007) 3:157-67).

1.8. GHRH antagonists

The hypothalamic neuropeptide growth hormone-releasing hormone (GHRH) stimulates the secretion of growth hormone (GH) from the anterior pituitary gland upon binding to its receptors (GHRH-R) (67). In turn, GH stimulates the production of insulin-like growth factor 1 (IGF-1), a major anabolic growth factor and a potent mitogen for many cancers (68). GHRH and its pituitary type receptor as well as its truncated receptor splice variants (SV) are expressed in various normal human tissues including prostate, kidney, lung, and liver (69) and on many human cancer cell lines and tumors (67). Pituitary type GHRH-R and SV1 appear to mediate effects of GHRH and its antagonists on tumors (70). GHRH itself acts as an autocrine/paracrine growth factor in human cancers (67,71), including prostate (72).

In order to develop new therapies for cancer, our laboratory has synthesized GHRH antagonists with high antiproliferative activity in numerous experimental cancer models (67). The inhibitory effect of these analogues is exerted in part by indirect endocrine mechanisms through the suppression of GHRH-evoked release of GH from the pituitary, which in turn results in the inhibition of the hepatic production of IGF-I (62). Direct mechanisms involved in the main antitumor effects of

GHRH antagonists appear to be based on blocking the action of autocrine GHRH on tumors and inhibition of autocrine IGF-1/2 (62,67). GHRH antagonists inhibit the growth of androgen-independent human prostatic cancers and also numerous other cancers xenografted into nude mice and suppress tumoral growth factors EGF, FGF-2, IGF-1, IGF-2 and VEGF-A (67,73,74). Recent studies also indicate that GHRH antagonists reduce generation of reactive oxygen species (75), which cause damage to prostatic stroma and epithelium (16).

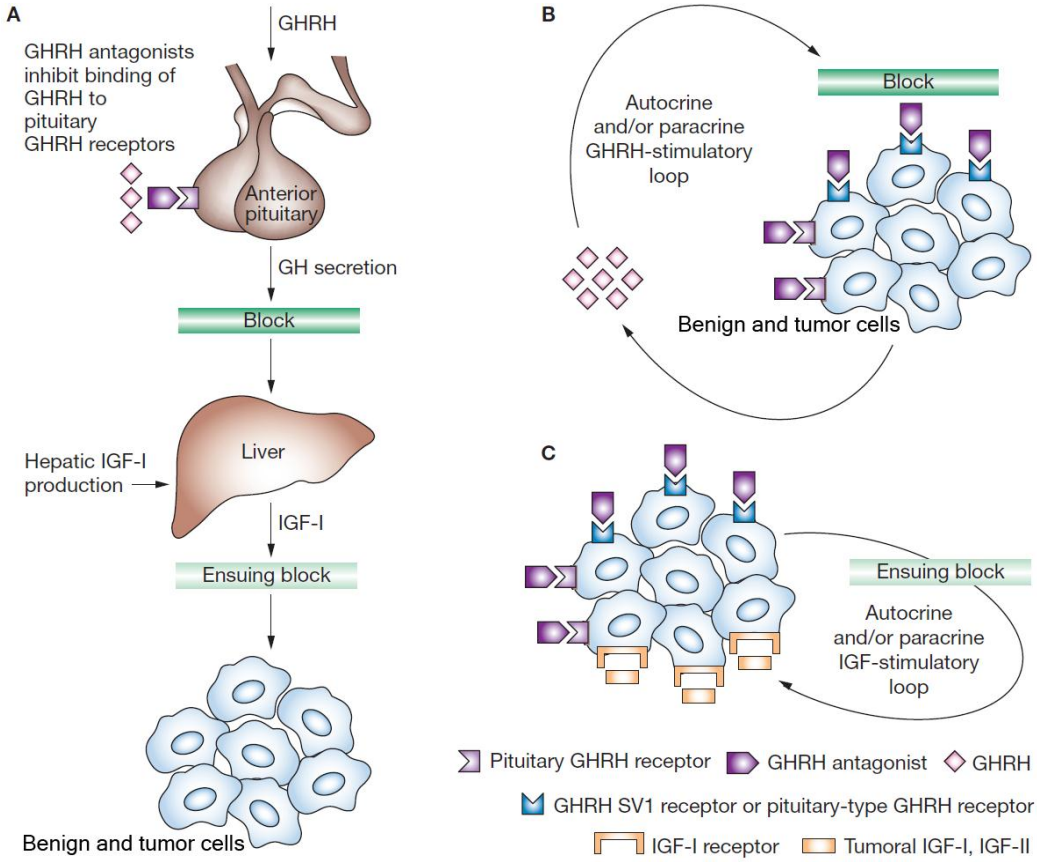

Figure 3. Schematic representation of the three potential mechanisms through which growthhormone-releasing hormone (GHRH) antagonists mediate the inhibition of benign and tumor growth. (A) An indirect action mediated through the suppression of the axis between pituitary GH and hepatic IGF-I. GHRH antagonists block the secretion of GH from the pituitary gland by inhibiting the binding of hypothalamic GHRH to GHRH receptors on pituitary somatotrophs. GH activates liver IGF-I gene transcription and could directly stimulate IGF-I production in some benign and tumor cells. Inhibition of GH results in a decrease of the production of hepatic IGF-I and the lowering in the levels of circulating IGF-I, ultimately leading to inhibition of benign and tumor growth. (B) Direct action. GHRH antagonists competitively inhibit the binding of autocrine or paracrine GHRH to pituitary-type GHRH receptors or GHRH-receptor splice variants on benign and tumor cells. This inhibition blocks the stimulatory effect of locally produced GHRH on cell growth, probably without the involvement of the IGF system. (C) GHRH antagonists can also directly inhibit cell growth by suppressing the autocrine and/or paracrine production of IGF-I or IGF-II by the benign and tumor cells. This effect is probably mediated through pituitary-type GHRH receptors or GHRH-receptor splice variants on the cells. Locally produced IGF-I and IGF-II activate cell proliferation by binding to type I IGF receptors on cells. In some tumors GHRH antagonists can also block the stimulatory effect of local GH on tumor proliferation (not shown). The cell cycle is arrested at the G2-M point, which triggers apoptosis. Abbreviations: GH, growth hormone; GHRH, GH-releasing hormone; IGF, insulin-like growth factor; SV1, GHRH-receptor splice variant 1. Schematic figure is adapted from Schally et al. Nat Clin Pract Endocrinol Metab (2007) 4:33-43.

Our laboratory has recently reported that GHRH and GHRH-R are expressed in BPH-1 cells and that GHRH can strongly influence their growth (76). These findings suggest a role for GHRH as a

locally acting growth factor in BPH and support the merit of further work on the development of GHRH antagonists for the therapy of BPH.

1.9. Prostate cancer

Prostate cancer is the most common noncutaneous malignant tumour in men (77,78). Androgen-dependent prostate cancer constitutes ~70% of all cases of prostate neoplasms (77). The suppression of androgenic activity with surgical orchiectomy or agonists of luteinizing hormone-releasing hormone is considered the most adequate first line treatment for advanced prostate cancer. However, hormonal therapy is successful in only 70% to 80% of cases and the median duration of response is usually only 12 to 24 months (78). Currently the management of metastatic prostate cancer remains a complex and difficult problem because there is no curative treatment. The chemotherapy with docetaxel based combination can lead to significant improvement in survival time. However, median survival does not exceed 20 months from the start of chemotherapy (79). Therefore, there is a great need for new and better therapies.

1.9.1. GHRH antagonists and prostate cancer

On the basis of recent advances in the understanding of the role of neuropeptides and growth factors in the progression of prostate carcinoma and other cancers (77,80), we have developed antagonists of GHRH for the treatment of various cancers including prostate cancer (77,78,81-84). GHRH antagonists inhibit the growth of various human tumours xenografted into nude mice, including androgen-independent prostate cancers (77,81,82,84,85) mainly by direct effects on cancer cells (73,85-88), although indirect effects mediated by the inhibition of the endocrine pituitary GH/hepatic IGF-I axis also occur (81,84,86). The direct effects of GHRH antagonists on cancer cells are mediated through pGHRH-R and splice variants (SV) of the pituitary type of GHRH receptors, which are present on human prostate cancer specimens and on cell lines (69,70,72,73,81,82,87,89,90). In addition to blocking GHRH receptors, antagonists of GHRH also inhibit the tumoral expression of IGF-I and II. These effects contribute to their antiproliferative mechanism (81,82). A decrease of VEGF, FGF, IGF-I and II protein levels and their mRNA expression, and a downregulation of EGF receptors was found after treatment of experimental androgen-independent prostate cancers with GHRH antagonists (73,87,88,91).

Although early GHRH antagonists such as MZ-4-71 or MZ-5-156 significantly inhibited the growth of PC-3 and DU-145 human androgen-independent prostate cancers in vivo (91,92), they were deemed unsuitable for clinical development, as they required high doses and frequent administration (2 x 20 μg/day in nude mice), due to the lack of sufficient potency, protracted activity, and chemical and enzymatic stability. Subsequently, our laboratory developed more potent and longer acting GHRH antagonists, in order to reduce the doses necessary for human therapy and to make the potential clinical use of GHRH antagonists technically and economically feasible (67,84,85). One of

the most potent GHRH antagonists prepared to date is MZ-J-7-138, which was developed by using a number of design criteria, including: (1) replacement of the enzymatically vulnerable Arg and Lys residues present in native GHRH peptide by enzymatically stable alternative residues while also preserving the subnanomolar binding affinities of the analogs to GHRH receptors; (2) replacement of the Asn and Met residues, prone to chemical hydrolysis, by other amino acids; (3) incorporation of a fatty acyl moiety into the molecule in order to enhance its binding to serum albumin, this strategy being employed to reduce the blood clearance due to enzymatic degradation and renal filtration of peptide drugs (67,84,93).

1.9.2. Role of p53 and p21 in prostate cancer

The tumor suppressor gene p53 is mutated in about half of all human cancers (94,95). p53 appears to play an important role in sensing and repairing DNA damage, inhibiting the cell cycle to allow DNA repair, and inducing apoptosis to eliminate severely damaged cells (96). The multifunctional p53 protein, which can act as a transcriptional activator or repressor, is induced by DNA damage, and interacts with proteins involved in DNA replication and repair (96). Mutant p53 (mt-p53) is preferentially expressed in hormone-refractory and metastatic prostate cancer (97-99). A poor response to chemotherapy is clearly associated with mutations in the p53 gene (94). Mt-p53 may have lost the tumor-suppressive functions and acquired additional, new oncogenic "gain-of-function" activities including transactivation of oncogenic targets such as c-myc, anti-apoptotic gene BAG-1, growth-promoting genes such as asparagine synthetase and hTERT, and the multi-drug resistance gp180 protein (MDR1) (100-102). The down-regulation of mt-p53 expression by siRNA in various cancer lines containing endogenous mt-p53 results in a reduction of tumor malignancy (100) and decreases cellular colony growth due to the induction of apoptosis (95). Overexpressed mt-p53 in tumor cells may be a suitable therapeutic target for pharmacological interventions aimed at suppressing its expression *in vivo* (95,102). The expression of wt-p53 in tumors can be also targeted by new experimental therapies aimed to restore or upregulate it (103). Thus, it was shown that the expression of functional wt-p53 protein increased apoptosis and suppressed the growth of human prostate cancer cells (97,104).

The cyclin-dependent kinase (CDK) inhibitor p21 is involved in p53-mediated growth arrest and has been identified as a key factor for the regulation of cell growth (105). Recent studies also indicate to an important anti-apoptotic and pro-survival role of p21 in various cancers including prostatic, colorectal, breast as well as in renal cell carcinomas and melanomas (106-109). Thus a reduction in p21 protein levels by an antisense method sensitized the MDA-PCa-2b and LNCaP prostate cancer cell lines to apoptosis induced by growth factor deprivation and the DNA-damaging agent doxorubicin (106). p21 appears to play a key role in cellular resistance and escape mechanisms

of tumors during treatment with anti-cancer agents including gamma-radiation, doxorubicin, cisplatin, paclitaxel and tamoxifen (106-112).

An increased expression of p21 was found to be associated with androgen independent prostate cancer (113). In clinical studies, p21 expression was identified as an indicator of poor survival in prostate cancer patients (114-116).

In an experimental model of benign prostatic hyperplasia (BPH), GHRH antagonists caused up-regulation of wt-p53 (117); while in small cell lung carcinomas GHRH antagonists inhibited mt-p53 levels (118). Consequently, we investigated the effect of GHRH antagonist MZ-J-7-138 on apoptotic mechanisms including p53, and p21 and growth in human experimental prostate cancers such as androgen independent PC-3 and DU-145 lines expressing mutant p53 and androgen sensitive MDA-PCa-2b line expressing wild type p53.

2. Aims of our studies

2.1. Experimental benign prostatic hyperplasia studies

2.1.1. To show presence of GHRH-R and LHRH-R on rat prostates

2.1.2. To investigate effects of:

- LHRH antagonist cetrorelix
- GHRH antagonists JMR-132, MIA-313 and MIA-459
- combination of LHRH antagonist cetrorelix and GHRH antagonist JMR-132on androgen-induced model of BPH

2.1.3. To explore mechanisms of action of antagonists of LHRH and GHRH, and their combination in experimental BPH

2.2. Human prostate cancer xenograft studies

2.2.1. To investigate the minimum effective dose and dose-response relationship of potent GHRH antagonist MZ-J-7-138 for the treatment of androgen-independent PC-3 prostate cancer in vivo

2.2.2. To assess effect of GHRH antagonist MZ-J-7-138 on tumoral IGF-II and VEGF in PC-3 xenografts in view of evidence from earlier studies that tumor inhibition by GHRH antagonists affects multiple tumoral growth factors and their signaling

2.2.3. To investigate inhibitory effects of GHRH antagonist MZ-J-7-138 on growth of androgen independent human experimental prostate cancer DU-145 and androgen sensitive MDA-PCa-2b

2.2.4. To evaluate the effect of GHRH antagonist MZ-J-7-138 on apoptotic mechanisms including p53, and p21 in human experimental prostate cancer xenografts such as androgen independent PC-3 and DU-145 lines expressing mutant p53 and androgen sensitive MDA-PCa-2b line expressing wilde type p53

3. Materials and methods

3.1. Peptides and reagents

The GHRH antagonists JMR-132, MIA-313, MIA-459 and MZ-J-7-138 were synthesized by solid-phase methodology using Boc-chemistry as described (119). Antagonist JMR-132 had the sequence [$PhAc^{0}$-Tyr^{1}, D-Arg^{2}, Cpa^{6}, Ala^{8}, Har^{9}, $Tyr(Me)^{10}$, His^{11}, Abu^{15}, His^{20}, Nle^{27}, D-Arg^{28}, Har^{29}]hGH-RH(1-29)NH_2, MIA-313 [$(Ac\text{-}Amc)^{0}$-Tyr^{1}, D-Arg^{2}, Cpa^{6}, Ala^{8}, Har^{9}, $Tyr(Me)^{10}$, His^{11}, Orn^{12}, Abu^{15}, His^{20}, Nle^{27}, D-Arg^{28}, Har^{29}, Agm^{30}]hGH-RH(1-30), MIA-459 [$(PhAc\text{-}Ada)^{0}$-Tyr^{1}, D-Arg^{2}, Cpa^{6}, Ala^{8}, Har^{9},Tyr (Me)^{10}, His^{11}, Orn^{12}, Abu^{15}, His^{20}, Orn^{21}, Nle^{27}, D-Arg^{28}, Har^{29}] hGH-RH(1-29)NH_2, and MZ-J-7-138 [CH_3-$(CH_2)_6$-CO-Tyr^{1},$DArg^{2}$, Cpa^{6},Ala^{8},His^{9}, $Tyr(Et)^{10}$,His^{11},Orn^{12},Abu^{15}, His^{20}, Orn^{21},Nle^{27}, D-Arg^{28}, Har^{29}]hGHRH(1–29)NH_2,where Abu is α-aminobutyryl, Ac is acetyl, Acm is 8-aminocaprylyl, Ada is 12-aminododecanoyl, Agm is agmatine (1-amino-4-guanidino-butane), Cpa is 4-chloro-Phe, Har is homoarginine, Nle is norleucine, Orn is ornithine, PhAc is phenylacetyl, Tyr(Et) is O-ethyltyrosine and Tyr(Me) is O-methyl-Tyr. JMR-132 and MIA-459 with amidated carboxy termini were prepared on p-methylbenzhydrylamine resin (0.5–0.9 mmol/g). For the synthesis of MIA-313 with C-terminal Agm, Boc-Agm-SPA-p-methylbenzhydrylamine resin (30 mmol/g; California Peptide Research) was used as the starting material. After completion of the synthesis and removal of the N-α-Boc–protecting group from Tyr^{1}, the resin-bound JMR-132, MIA-313, MIA-459, and MZ-J-7-138 peptides were acylated with PhAc, Ac-Amc, PhAc-Ada, and octanoic acid, respectively. Final deprotection and cleavage of the peptides from the resin with anhydrous hydrogen fluoride, as well as their purification and analysis by semipreparative and analytical HPLC and mass spectra, were done as described previously (120).

The LHRH antagonist Cetrorelix ([Ac-D-$Nal(2)^{1}$,D-$Phe(4Cl)^{2}$,D-$Pal(3)^{3}$,D-Cit^{6},D-Ala^{10}]-LHRH) originally synthesized in our laboratory by solid-phase methods (54) was made by Aeterna-Zentaris (Frankfurt-on-Main, Germany) as Cetrorelix acetate (D20761). For *in vitro* experiments, Cetrorelix acetate was dissolved in 0.1% DMSO and diluted in media. For *in vivo* experiments we used a depot formulation of Cetrorelix pamoate (D20762), also provided by Aeterna-Zentaris, containing Cetrorelix peptide-base and pamoic acid in a molar ratio of 2:1, respectively. For the injection, Cetrorelix pamoate was dissolved in distilled water at a final concentration of 15 mg/ml in 5% mannitol. This depot preparation can be injected every 21–30 days. Aliquots of this suspension (3mg/0.2ml) were injected s.c. giving an estimated daily release of 100μg/day of Cetrorelix for 30 days.

The peptides were lyophilized and stored in desiccator, and the stability and purity of the long stored compounds were checked by HPLC before the experiments.

In our rat BPH model, testosterone enanthate (TE) (Watson Pharmaceuticals), corn oil vehicle (Sigma-Aldrich), and 5α-reductase 2 (5AR2) inhibitor finasteride (Sigma-Aldrich) were used. For

daily injection, GHRH antagonists and finasteride were dissolved in 0.1% DMSO in 10% aqueous propylene glycol solution.

3.2 Animals

In our BPH studies adult male Wistar rats (Charles River Laboratories) weighing 250-400 g were used. Rats were allowed standard laboratory diet and tap water *ad libitum*. All rats remained healthy throughout the experiments.

For xenograft studies, approximately 5–6 weeks old male athymic (Ncr nu/nu) nude mice were obtained from the National Cancer Institute (Frederick Cancer Research and Develkopment Center, Frederick, MD), housed in sterile cages under laminar flow hoods and fed autoclaved chow and water *ad libitum*.

Rodents were housed in a climate-controlled (22 ± 2 °C, 50 ± 10% humidity), environment with a 12-h light/dark cycle (light on from 06-18 h). All experiments were conducted in accordance with the principles and procedures outlined in the National Institutes of Health Guide for the Care and Use of Laboratory Animals. The protocol of the animal experiments was reviewed and approved by the Institutional Animal Care and Use Committee (IACUC). Body weights were determined weekly.

3.3. In vivo experimental models

3.3.1. Testosterone-induced model of BPH

It is well known that enlargement of the prostate occurs in the presence of androgens (121) and that anabolic steroids increase prostatic volume and reduce urine flow, leading to increased urinary frequency (122). Maggi *et al.* described a model in male rats wherein BPH was produced by repeated injections of testosterone (51). The model described by Maggi *et al*. has been adapted for several studies (123-126). Given that the mechanism of prostate growth is complex and heterogeneous in different species and the testosterone-induced models of BPH show an epithelial hyperplasia (126,127), the androgen-induced models of BPH have limitations. These include the fact that inflammation was not described as a main characteristic, but rather was incidental (126).

Alonso-Magdalena's description of human BPH as predominantly of epithelial origin (17) and the fact that in our preliminary studies we found that our target receptors GHRH-R and LHRH-R are exclusively expressed in the rat prostatic epithelium supports the rationale for using a testosterone-induced model of BPH with predominant epithelial hyperplasia based on the reports of Maggi *et al.* (51) and Scolnik *et al.* (126).

In our in vivo experiments on BPH, after 7 days acclimatization, rats were randomly divided into experimental groups and one negative control group of ten animals each. BPH was induced in experimental groups by daily subcutaneous injection in the right flank of long acting testosterone enanthate (2mg/day), dissolved in corn oil from Day -28 to Day 0 (induction phase). Negative control animals received subcutaneous injections of corn oil alone on the same schedule. The dosage and duration of testosterone treatment were based on the reports by Maggi et al. (51) and Scolnik et al. (126).

3.3.1.A. Investigation of effects of LHRH antagonist Cetrorelix

Based on previous clinical (56,57) and experimental (59) reports, animals were administered subcutaneous injections of the LHRH antagonist Cetrorelix (0.625, 1.25, and 12.5mg/kg body weight) in the left flank on days 1 and 22 after BPH induction (day_28 to day 0). Experimental groups consisted of: (1) TE only, (2) TE/ Cetrorelix 0.625 mg/kg, (3) TE/Cetrorelix 1.25 mg/kg, and (4) TE/Cetrorelix 12.5mg/kg body weight. TE only positive control animals were injected with mannitol instead of Cetrorelix on the same schedule.

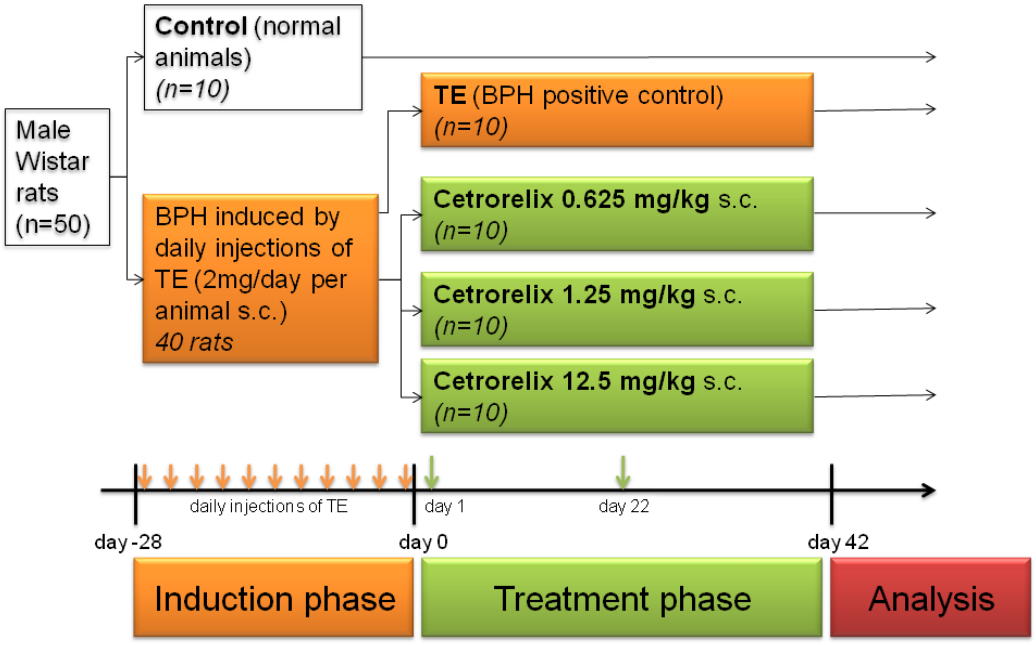

Figure 3. Scheme of the study. Induction phase included daily injections of 2mg TE s.c. per rat for 28 days. In the treatment phase, different doses of a depot preparation LHRH antagonist Cetrorelix pamoate (0.625,1.25, or12.5mg/kg) were administered s.c. on days 1 and 22. Study groups were as follows: Control, TE, Cetrorelix 0.625mg/ kg, Cetrorelix 1.25mg/ kg and Cetrorelix 12.5mg/kg. BPH, benign prostatic hyperplasia; LHRH, luteinizing hormone-releasing hormone; s.c., subcutaneous;TE, testosteroneSchematic figure is adapted from Rick et al. Prostate (2011) 71:736-47)

3.3.1.B. Investigation of effects of GHRH antagonist

One group of rats was administered daily s.c. injections of the 5AR2 inhibitor finasteride, 0.1 mg/kg, in the left flank from days 1–42 after BPH induction (Figure 3). This dosage of finasteride, an

approved drug for the treatment of BPH, is comparable to the human dosage (5mg/d). The other three groups of animals were given daily s.c. injections of the GHRH antagonists JMR-132, MIA-313, or MIA-459 (40, 20, and 20 µg/d, respectively). The dosage of GHRH antagonists was based on prior experimental oncological use (128). Experimental groups consisted of (i) TE only, (ii) TE/finasteride (0.1 $mg \cdot kg_{-1} \cdot d_{-1}$), (iii) TE/JMR-132, (iv) TE/MIA-313, and (v) TE/ MIA-459. TE-only positive control animals received 0.1% DMSO in 10% aqueous propylene glycol solution instead of finasteride or GHRH antagonists on the same schedule.

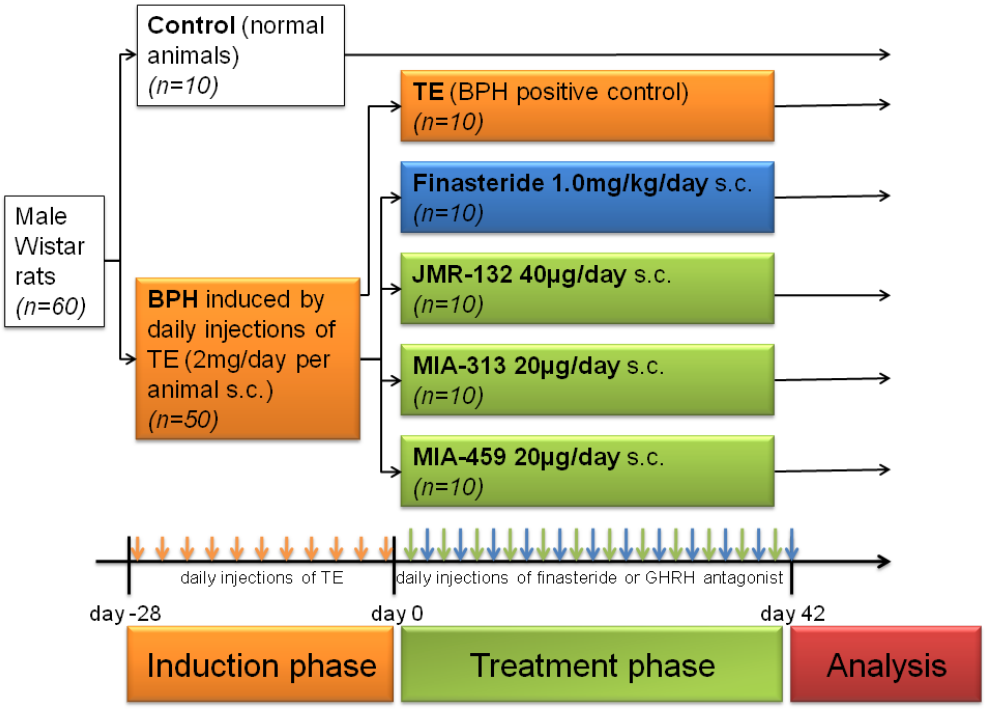

Figure 4. Scheme of the study. Induction phase included daily injections of 2mg TE s.c. per rat for 28 days. In the treatment phase, 5α-reductase inhibitor finasteride (0.1mg/kg/day), GHRH antagonist JMR-132 (40µg/day), MIA-313 (20µg/day) and MIA-459 (20µg/day) were administered s.c. daily.

3.3.1.C. Investigation of effects of combination of GHRH antagonist and LHRH antagonist

One group of rats was administered daily s.c. injections of the 5AR2 inhibitor finasteride 0.1 mg/kg in the left flank from days 1 to 42 after BPH induction. One group of animals was given daily s.c. injections of the GHRH antagonists JMR-132 (40 µg/day). Animals were administered subcutaneous injections of the LHRH antagonist Cetrorelix (0.625 mg/kg body weight) in the left flank on days 1 and 22 after BPH induction (day -28 to day 0). The combination group received daily s.c. injections of the GHRH antagonists JMR-132 (40 µg/day) and subcutaneous injections of the LHRH antagonist Cetrorelix (0.625 mg/kg body weight) in the left flank on days 1 and 22 after BPH induction. Experimental groups consisted of: (1) TE only, (2) TE/finasteride 0.1 mg/kg/day, (3) TE/JMR-132 40 µg/day, (4) TE/Cetrorelix 0.625 mg/kg and (5) TE/JMR-132 40 µg/day and

Cetrorelix 0.625 mg/kg. The dosage and duration of JMR-132 and Cetrorelix was chosen based on prior reports (117,129). TE-only positive control animals received 0.1% DMSO in 10% aqueous propylene glycol solution instead of finasteride or GHRH antagonists and mannitol instead of Cetrorelix on the same schedule.

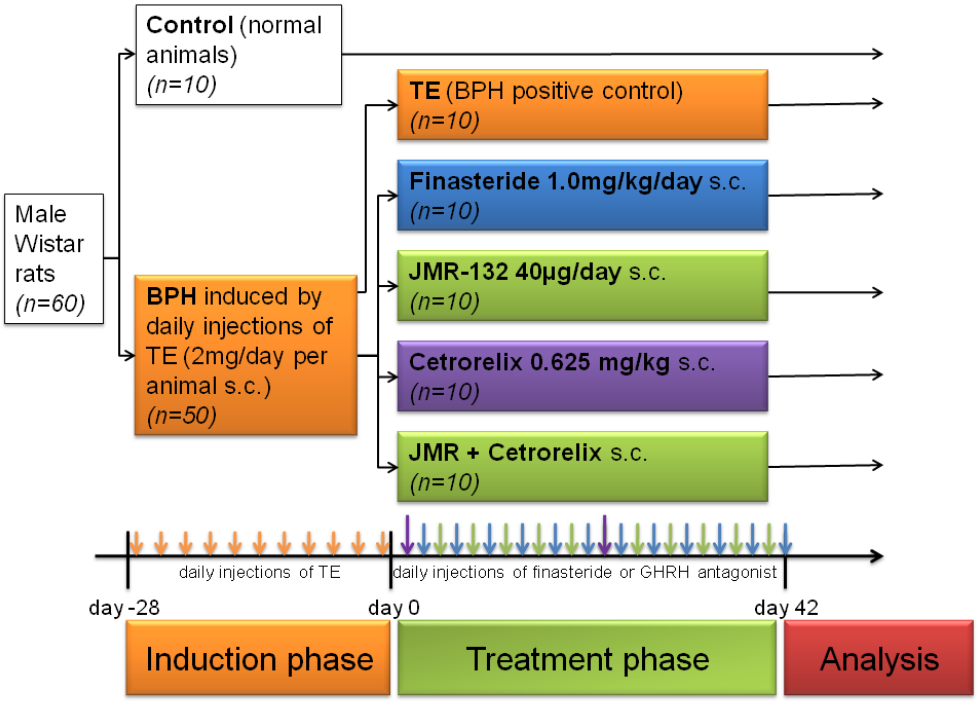

Figure 5. Scheme of the study. Induction phase included daily injections of 2mg TE s.c. per rat for 28 days. In the treatment phase, 5α-reductase inhibitor finasteride (0.1mg/kg/day), GHRH antagonist JMR-132 (40µg/day), depot preparation LHRH antagonist Cetrorelix pamoate (0.625mg/kg), and combination of JMR-132 and cetrorelix were administered s.c..

Venous blood samples were collected before the experiment and on the last day of the experiment (day 42). Serum was separated by centrifugation (10 min at 1000 rpm) and stored at -80°C. Rats were weighed and sacrificed under anesthesia on the morning of day 42; whole prostates were immediately removed, weighed and snap frozen. Alternate prostrate lobes were immersed in phosphate-buffered 10% formalin (pH 7.4) and embedded in paraffin for histological analysis.

3.3.2. Tumor models

3.3.2.A. Cell cultures

PC-3 and DU-145 human androgen-independent prostate cancer and cell lines were obtained from American Type Culture Collection (Manassas, VA) and cultured at 37 ◦C in a humidified 95% air/5% CO2 atmosphere, using their designated media supplemented with antibiotics/antimycotics and 10% FBS (Table X). The MDAPCa-2b human androgen sensitive prostate cancer cell line was

obtained from Dr. Nora Navone, University of Texas, MD. Anderson Cancer Center (Houston, TX) and maintained in culture as described (98).

3.3.2.B. Tumor xenograft model

In our in vivo tumor xenograft assays, 1.5 million of PC-3, DU-145 or MDA-PSa-2b cells were injected s.c. at each flank to three donor animals. Tumor tissue was harvested aseptically from donor animals. Nude mice were xenografted subcutaneously with 3 mm^3 pieces of respective tumor tissue using a trocar needle. When tumors had grown to a mean volume of approximately 30-75 mm_3, the animals were randomly assigned to treatment groups and control (n = 8 to 9, (74) and (130)).

Experiment 1:

PC-3 tumor tissue was harvested aseptically from donor animals. Male nude mice were xenografted subcutaneously with 3 mm^3 pieces of PC-3 tumor tissue using a trocar needle. When tumors had grown to a mean volume of approximately 56 mm3, the animals were randomly assigned two groups. One group received treatment with MZ-J-7-138 (5μg/day) (n=9) and control group (n=9) received vehicle solution. The experiment was ended on day 28.

Experiment 2:

Three mm^3 pieces of DU-145 tumor tissue, harvested from donor animals were xenografted s.c into male nude mice. When tumors had grown to approximately 30 mm^3 (exponential phase of growth), the animals were assigned to 2 experimental groups, each group containing 8 animals. Group 1 received GHRH antagonist MZ-J-7-138 at a dose of 5μg/day, group 2, controls was given vehicle solution. The experiment was ended on day 42.

Experiment 3:

Male nude mice were xenografted subcutaneously with 60 mg minced MDA-PCa-2b tumor tissue suspended in Matrigel as described (13). When tumors had grown to a mean volume of approximately 75 mm^3, the animals were assigned to 4 experimental groups. Group 1 (n=9) was injected daily with MZ-J-7-138 (5 μg/day); group 2 (n=9) was given s.c 30 day release preparation of LHRH antagonist Cetrorelix (100μg/day); group 3 (n=9) received a combination therapy of MZ-J-7-138 (5 μg/day) injected daily and Cetrorelix (100μg/day) depot formulation, group 4, controls (n=9) received vehicle solution. The experiment was ended on day 21.

Experiment 4:

Male nude mice were xenografted subcutaneously with 3 mm^3 pieces of PC-3 tumor tissue using a trocar needle. When tumors had grown to a mean volume of approximately 60 mm3, the animals were randomly assigned to treatment groups and control of nine animals each. The antagonist MZ-J-7-138 was injected s.c. daily at doses of 1.25, 2.5, 5, 10 μg/day and controls received the injection vehicle.

Tumor volumes (length x width x height x 0.5236) and body weights were recorded every week. At the end of the experiments, mice were anaesthetized with pentobarbital and sacrificed by cutting the abdominal aorta. Tumors were carefully excised, weighed, snap frozen and stored at -70 °C for further investigations. Blood was collected and a complete necropsy was performed of all animals. Liver, heart, lungs, kidneys, spleen, testicles, prostate and seminal vesicles were carefully removed and weighed.

Tumor doubling time (TDT) and tumor inhibition (TI) were calculated using the formula:

$$\mathbf{TDT = days\ of\ treatment * log\ 2/(log\ volume_{final} - log\ volume_{initial}),}$$

$$\mathbf{TI = 100\%*(\Delta volume_{control} - \Delta volume_{treated}) / (\Delta volume_{control}),}$$

where Δvolume = final volume – initial volume.

3.4. Histological procedures and morphological analyses

Serial 5 mm-thick sections from each fixed tissue specimen were prepared, mounted on glass slides, and stained with hematoxyline-eosin for morphological analysis. The sections were analyzed with a Nikon Eclipse 90i microscope with a built-in digital camera. The digitalized images of ventral prostatic lobes, obtained by using NIS-Elements BR 3.00 for Windows image analyzer software, were used for stereological-morphometric analysis. The mean epithelial height was determined from a total of 500 random interactive measurements with 40x objective at 10 different points on 10 different fields from five different individual ventral prostate sections. Measurements were taken from the intermediate to distal regions of the prostate lobe ducts, which represent the major portions of the prostatic lobes (131).

The mitotic and apoptotic cells in the ventral prostate from three animals in each group were counted in 10 random fields at 40x objective magnification from three different individual ventral prostate sections. Because the size of the glands and the height of epithelial cells vary, the counts were standardized as follows: (i) the area of epithelium in each field was determined by using a microscope ocular net, and the crossing points of the net that coincided with epithelial cells were counted; (ii) the ratio of these points to the number of all points represented the percentage area of epithelia in the fields; (iii) the numbers of mitotic and apoptotic cells in a theoretical microscopic view field composed entirely of epithelial cells were calculated.

3.5. Immunohistochemical staining

Serial 4-μm sections of rat prostates were used for immunoperoxidase staining following standard protocols. Briefly, the paraffin was melted at 37 °C overnight and cleared in a bath of xylene for 10 min. The slides then were rehydrated in decreasing grades of ethanol (10 min each) and washed in PBS. The antigen retrieval was performed in a pressure cooker with Dako Target Retrieval Solution (S1968; Dako) at 90°C for 15 min (pH 9.0). Antibodies to GHRH receptor in 1:1,000 dilution (sc28692; Santa Cruz Biotechnology), to LHRH-R in 1:5 dilution (sc8682, Santa Cruz), and to androgen receptor (AR) in 1:20 dilution (clone AR441; Dako) were added to the slides and incubated for 30 min at room temperature. Immunohistochemical analysis was performed using Dako Flex Detection System 1.0 (polymer-based). Diaminobenzidine was the chromogen in the presence of hydrogen peroxide. For AR, the slides were exposed briefly to cupric sulfate and counterstained with fast green. Positive reaction for GHRH-R and LHRH-R appeared as orange-brown granules, whereas nuclear localization of AR appeared black (117,132).

3.6. Total DNA Isolation.

To quantify the cellular content of rat prostates, total DNA was prepared from 20 mg of ventral prostate tissue for each sample using the DNeasy Blood and Tissue kit (Qiagen). Five prostate samples from each group were analyzed. The yield and purity of DNA was determined according to manufacturer's instructions.

3.7. Total RNA Isolation and cDNA sythesis.

Total RNA was isolated from 30 mg of prostate tissue for each sample using the NucleoSpin kit (Macherey-Nagel). Three prostate samples from each group were analyzed. The yield and quality of total RNA was determined spectrophotometrically using 260 nm and 260/280 nm ratio (A_{260}/A_{280}>1,8), respectively. Two micrograms of RNA with a final volume of 40 μl were reverse transcribed into cDNA with the QuantiTect Reverse Transcription Kit (Qiagen, Valencia, CA) using the Veriti 96-well Thermal Cycler (Applied Biosystems, Foster City, CA).

3.8. Quantitative real-time RT-PCR

We evaluated the mRNA expression of rat (Table 2) and human (Table 3) target genes using specific probes and primers (Table X). Specific primers were designed according to the following criteria: (1) a product-size range of 70-180 bases, (2) a primer size range of 18-24 bases, (3) a Tm difference of 3^{o}C, and (4) a GC content of 30-80%. The mRNA sequences used for the design of the primers were taken from the NCBI Reference Sequences. The primers were tested for sequence

similarity to other genes with NCBI BLAST (Basic Local Alignment Search Tool). The thermal cycling conditions for each set of primers comprised an initial denaturation step at 95°C for 3 min and then 35-40 cycles of two-step PCR including 95°C for 30 s and corresponding annealing tempreature for 1 min. Data were collected during the annealing step and were further analyzed by the iCycler™ iQ Optical system software (Bio-Rad). Real-time PCR melting curve analyses revealed a single product for each primer set.

All real-time PCR reactions were performed in the iCycler iQ Real-Time PCR Detection System (Bio- Rad Laboratories, Hercules, CA). All real-time PCR reactions were performed in the iCycler iQ Real-Time PCR Detection System (Bio-Rad Laboratories, Hercules, CA). All samples were run in triplicate and each well of PCR reaction contained 25 µl as final volume including 2 µl of cDNA, 200 nM of gene specific primers and 400 nM of probes. iQ SYBR Green Supermix (Bio-Rad Laboratories) for PCR reactions performed with primers only, and iQ Supermix (Bio-Rad Laboratories) was used in the PCR reactions for human pGHRH-R, GHRH and beta-actin. The efficiencies of all primers (Invitrogen Life Technologies, Carlsbad, CA) and probes (Integrated DNA Technologies, Coralville, IA) were tested prior to the experiments and they were all efficient in the range of 95–105%. Rat Gapdh, beta-actin and human beta-actin were used to normalize for differences in RNA input. Normal human and rat pituitary was used as positive control for pGHRH-R, SV1 and GHRH. Negative samples were run in each reaction consisting of no-RNA in reverse transcriptase reaction and no-cDNA in PCR reaction. The relative gene expression ratios were calculated using Pfaffl's method (133).

Table 2. Rat primers used in our studies

Gene	Accession number	Forward ('5 – 3')	Reverse ('5 – 3')	Annealing temp. (^{o}C)
GHRH	NM_031577	GGGTGTTCTTTGTGCTCCTC	TTTGTTCCTGGTTCCTCTCC	61
Ptgs2/Cox-2	NM_017232	CCCAAGGCACAAATATGATG	CTCGCTTCTGATCTGTCTT	59
Adra1a/α_{1A}-AR	NM_017191	ACTACTACATTGTCAACCT	TCAAAGATGGCAGAGAAG	59
Nf-κβ1	XM_342346	GAAATCTATCTTCTCTGTGA	ACCATTTTCTTCCTCTTC	58
Nf-κβ2	NM_001008349	ACTGCTCAATTTAATAATCTGG	GAGTTTCTGAATCATAATCTC	55
RelA	NM_199267	CCTTCCTGAAGCATGTAC	AGAGTGAGATATTGCTGATAA	55
Bcl-2	NM_016993	CCAAACAAATATGAAAAGGT	TGTGTGTGTTCTGCTTTA	55
Bax	NM_017059	AGATGAACTGGACAATAATATGGA	CGGAAGAAGACCTCTCGG	55
p53	NM_030989	GGATTCACAGTCGGATAT	CATCTGGAGGAAGAAGTT	55
Gapdh	NM_017008	ATTCTTCCACCTTTGATG	GCCATATTCATTGTCATAC	60
Hprt1	NM_012583	AGCGTCGTGATTAGTGAT	ATCTTCAGCATAATGATTAGGTA	55
IGF-1	NM_178866	GGCATTGTGGATGAGTGTTG	CGATAGGGGCTGGGACTT	61
IGF-2	NM_133519	CGCACCCACAGAGAAATAAAA	TCCGAGCACCTTCCTAACAC	61
TGF-α	NM_012671	GCCTTCTTGCTAACCCACAC	GATGTTTCCCCTTGTCCATTT	64
TGF-β1	NM_021578	CGCAATCTATGACAAAACCAAA	ACAGCCACTCAGGCGTATC	61
TGF-β2	NM_031131	CGCATCTCCTGCTAATGTTG	TTCGGGGTTTATGGTGTTGT	61
EGF	NM_012842	CCCGTGTTCTTCTGAGTTCC	TGTAACCGTGGCTTCCTTCT	61
FGF-2	NM_019305	CTGTCTCCCGCACCCTATC	CTTTCTCCCTTCCTGCCTTT	61
KGF/FGF-7	NM_022182	TCCACCTCGTCTGTCTTGTG	CCTTTCACTTTGCCTCGTTT	61
IL-1β	NM_031512	GTCACTCATTGTGGCTGTGG	GGGATTTTGTCGTTGCTTGT	61
IL-6	NM_012589	GCCAGAGTCATTCAGAGCAA	CATTGGAAGTTGGGGTAGGA	61
VEGF-A	NM_031836	GACACACCCACCCACATACA	ACATCCTCCTCCCAACTCAA	61
LHRH-R	NM_031038	GGGGCTGAGCATCTATAACACC	TGCTAACCTCTGGACAGGGATC	60
LHRH	NM_012767	GGCTTTCACATCCAAACAGAA	GCCTTCCAAACACACAGTCAA	61
AR	NM_012502	CAAAGGGTTGGAAGGTGAGA	GAGCGAGCGGAAAGTTGTAG	61
5α-reductase 2	NM_022711	GCAAAGTTTCTGTGGAGGA	AAGCAACTGGAATAACAAGAGA	59
β-actin	NM_031144	GGGTTACGCGCTCCCTCAT	GTCACGCACGATTTCCCTCTC	60

Table 3. Human primers used in our studies

Gene	Accession number	Forward (‘5 – 3’)	Reverse (‘5 – 3’)	Annealing temp. (^{o}C)
GHRHR	NM_000823	ATGGGCTGCTGTGCTGGCCAAC	TAAGGTGGAAAGGGCTCAGACC	65
GHRH	NM_021081	ATGCAGATGCCATCTTCACCAA	TGCTGTCTACCTGACGACCAA	60
SV1	AF282259.1	TGGGGAGAGGGAAGGAGTTGT	GCGAGAACCAGCCACCAGAA	60
SV2	AF282260.1	AGGAAGGCCCCATAGTGTGTC	GGCAGCCAGTGGAGAAGCT	60
SV3	AF282261.1	GCCCCATAGGGCTGTGAAAC	ACAGCTGGGTGTGGACGTAGT	58
SV4	AF282262.1	CTGAGGAGGGCTGCCCGT	GGCCCTTTGATGATCCACCAGT	65
β-actin	NM_001101	CTGGAACGGTGAAGGTGACA	AAGGGACTTCCTGTAACAATG	60

3.9. RT^2 Profiler PCR Array

Rat Growth Factor, Inflammatory Cytokines/Receptors, and Signal Transduction Real-Time PCR Arrays. Rat Growth Factor (PARN-041), Inflammatory Cytokines and Receptors (PARN-011), and Signal Transduction Pathway Finder (PARN-014) RT^2 Profiler Real-Time PCR arrays (SABiosciences) were used to examine the mRNA levels of 252 genes related to growth factors, inflammatory cytokines, and signal transduction. Total RNA extraction was as described. Quality control of RNA samples, synthesis of cDNA, and its amplification by real-time RT-PCR arrays were performed per the manufacturer’s instructions (SABiosciences). Fold-changes in gene expression were calculated using the ΔΔCt method. Normalization was performed using five housekeeping genes on the arrays.

3.10. Western-blot

Rat prostate tissue and tumor tissue were homogenized with Mikro-Dismembrator (Goettingen, Germany). Protein was isolated with NucleoSpin Kit (Macherey-Nagel) and sonicated with Branson Sonifier (Danbury, CT). Protein lysates were adjusted to equal concentrations (NanoDrop Technologies, Inc., Wilmington, DE), resuspended in 2× sample loading buffer containing 4% SDS, 20% glycerol, 120mM Tris and bromophenol blue, and boiled for 5min. Protein samples were subjected to SDS-polyacrylamide gel electrophoresis. Proteins on the gel were transferred onto nitrocellulose membranes that were blocked with 50–50% Odyssey buffer and phosphate buffered saline (PBS) for 1 h at room temperature. The membranes were incubated afterwards with corresponding primary antibody (Table X). After washing with PBS containing 0.1% Tween-20, the membranes were incubated with the appropriate secondary antibody. The immunoreactive bands were visualized with the Odyssey Infrared Imaging System and V.3.0 software was used (LI-COR Biosciences, Lincoln, NE). Immunoblot analyses were performed using the following primary antibodies following manufacturers’ instructions:

Table 4. Primary antibodies used for Western-blots

Primary antibody	Type of antibody	Catalogue number	Manufacturer
GHRH-R	Rabbit polyclonal	ab28692	Abcam
GHRH	Rabbit polyclonal	ab8911	Abcam
NF-κβ/p65	Rabbit polyclonal	ab7970	Abcam
NF-κβ/p50	Goat polyclonal	sc1191	Santa Cruz
phospho-NF-κβ/p50 (Ser337)	Rabbit polyclonal	sc33022	Santa Cruz
COX-2	Rabbit polyclonal	4842S	Cell Signaling
AR	Rabbit polyclonal	sc13062	Santa Cruz
5α-reductase 2	Rabbit polyclonal	sc20659	Santa Cruz
α_{1A}-adrenoreceptor	Mouse monoclonal	sc100291	Santa Cruz
IL-1β	Rabbit polyclonal	sc7884	Santa Cruz
PCNA	Mouse monoclonal	sc25280	Santa Cruz
β-actin	Mouse monoclonal	sc47778	Santa Cruz
LHRH-R	Rabbit polyclonal	sc13944	Santa Cruz
LHRH	Mouse monoclonal	sc55459	Santa Cruz
p53	Rabbit polyclonal	9282	Cell Signaling
phospho-p53 (Ser46)	Rabbit polyclonal	2521	Cell Signaling
p21	Mouse monoclonal	sc56335	Santa Cruz
α-tubulin	Mouse monoclonal	CP06	Calbiochem

3.11. Radioimmunoassay (RIA) and ELISA.

For our rat BPH studies, we used commercial immunoassay kits to determine GH, LH, DHT, IGF-1, and PSA levels in serum. Serum GH was determined by ELISA using the 32–5104 kit and serum LH by 29-AH-R002 RIA kit (Alpco Diagnostics, Salem, NH). Serum DHT was determined by RIA using DSL-9600 kit (Diagnostic Systems Laboratories, Webster, TX). For quantitative serum PSA and IGF-1 we used ELISA kits DSL-9700, DSL-10-2800. All immunoassays were done according to manufacturers' instructions.

For our human PC-3 prostatic cancer studies, human VEGF and IGF-II levels were determined by RIA in tumor tissue homogenates (88).VEGFand IGF-II were extracted from tumor tissue, using a modified acid-ethanol cryoprecipitation method (134). The total protein content was determined by using the Bio Rad protein assay kit (Bio-Rad Laboratories). The standard for VEGF was a recombinant human VEGF, 38.2 kDa, consisting of 165 amino acids. Antihuman VEGF was an affinity-purified, polyclonal antibody. Both VEGF and antihuman VEGF were purchased from PeproTech, Inc. (Rocky Hill, NJ). The standard was used in the range of 0.006 and 12.8 ng per tube. The antibody was used at a final dilution of 1:200,000.VEGF was iodinated by the lactoperoxidase method and purified by high-performance liquid chromatography, using a reverse-phase Vydac C4 column. The assay buffer for VEGF consisted of 0.01M sodium phosphate pH 7.6, 0.025 M EDTA,

0.14 M NaCl, and 1% BSA. The antibody and tracer were added simultaneously and incubated overnight at 48 ^{o}C. Bound and free fractions were separated by the polyethylene–glycol double antibody method. IGF-II concentration was measured by RIA using human recombinant IGF-II standard (Bachem, Torrance, CA) in the range of 2–2,000 pg per tube. IGF-II was iodinated by the lactoperoxidase method, and purified as described previously (91). Anti-rat IGF-II (10 mg/ml) monoclonal antibody (Amano International Enzyme, Troy, VA) was used at a final dilution of 1:12,500. This antibody crossreacts 100% with human IGF-II and rat IGF-II, and 10% with human IGF-I. The RIA results from all samples were evaluated in a computer-controlled gamma Counter (Packard Cobra System, Perkin Elmer Life&Analytical Science, Shelton, CT). The intraassay and the interassay coefficients of variation were less than 10% and 15%, respectively (74).

3.12. Ligand competition assays

Receptors for GHRH and LHRH on rat prostate tissues and receptors for GHRH on human prostate cancer xenograft tumor tissues from the experimental groups were characterized by the ligand competition assay. Preparation of membrane fractions for receptor studies was performed as described previously (135). Radioiodinated derivatives of GHRH antagonist JV-142 and [D-Trp^{6}]LHRH were prepared by the chloramine-T method and purified by reverse-phase HPLC in our laboratory (90,135). GHRH receptor binding assays were carried out as reported (90) using in vitro ligand competition assays based on binding of [^{125}I]JV-1-42 as radioligand to membrane fractions of rat prostate samples or human xenograft tumor tissues. LHRH receptor binding assays were carried out as reported (135) using in vitro ligand competition assays based on binding of [^{125}I][D-Trp^{6}]LHRH as radioligand to membrane fractions of rat prostate samples. The LIGAND-PC computerized curve-fitting program was used to determine the type of receptor binding, dissociation constant (K_d), and maximal binding capacity of the receptors (B_{max}).

3.13. Statistical Analysis.

For statistical evaluation, SigmaStat 3.0 software (Sytat Software) was used. Results are expressed as means ± SEM. One-way ANOVA followed by Bonferroni *t* test, Student–Newman–Keuls test, or a two-tailed Student's *t* test was used where appropriate, and significance was accepted at $P < 0.05$.

4. Results

4.1. Effects of LHRH antagonist cetrorelix on experimental benign prostatic hyperplasia (Study 1)

4.1.1. Effect of LHRH antagonist Cetrorelix on rat prostate weight

Body weights at sacrifice were not affected by Cetrorelix+TE compared to TE-only treated rats (Table 5). Corn oil-injected control prostates (negative control) weighed 264.8±9.6 mg/100 g rat (Figure 6); while in TE controls prostates were enlarged by 40.52% to 372.1±25.3 mg/100 g rat ($p<0.001$; Figure 6). Cetrorelix pamoate 0.625 mg/kg significantly lowered prostate weights by 17.88% ($p=0.02$). This decrease was similar to that obtained with 1.25 mg/kg Cetrorelix (18.65 % reduction [$p=0.01$]);further reduction occured but smaller than with 12.5 mg/kg Cetrorelix (35.17% reduction [$p<0.001$]).

Table 5. Effect of LHRH antagonist Cetrorelix at different doses on morphological parameters

	Body weight (g) □		Day 42□	
	Day -28	Day 42	Prostate weight (g)	Epithelial height (μm)
Control	255 ± 3	481 ± 9	1.27 ± 0.05	11.65 ± 0.11
TE	257 ± 7	445 ± 20	1.64 ± 0.10‡	20.43 ± 0.39□
TE/Cetrorelix 0.625 mg/kg	258 ± 4	446 ± 15	1.36 ± 0.06*	13.15 ± 0.14***
TE/Cetrorelix 1.25 mg/kg	258 ± 3	449 ± 10†	1.35 ± 0.04*	14.62 ± 0.17***
TE/Cetrorelix 12.5 mg/kg	254 ± 2	445 ± 12†	1.06 ± 0.05***	12.57 ± 0.15***

*† p<0.05, ‡ p<0.01 and □ p<0.001 as compared to Control, * p<0.05, ***p<0.01 as compared to TE. Statistical analysis was performed by one-way ANOVA, followed by Bonferroni t-test.*

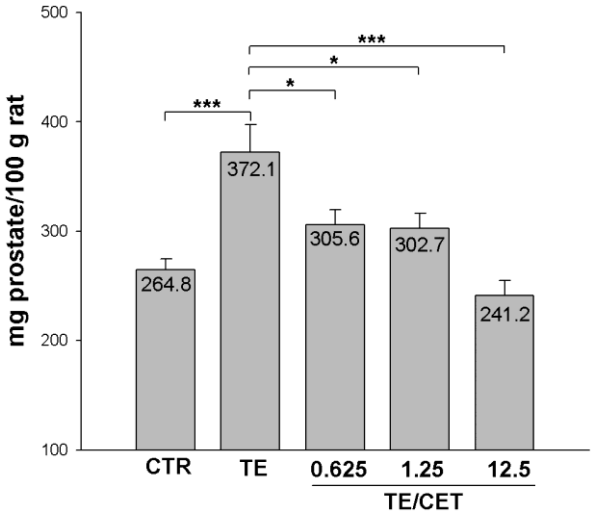

Figure 6. Effect of TE and treatment with LHRH antagonist Cetrorelix at doses of 0.625, 1.25 and 12.5 mg/kg on relative prostate weight, evaluated 42 days after the start of treatment with Cetrorelix. Statistical analysis was performed by one-way ANOVA, followed by Bonferroni *t*-test. Significant differences are marked by asterisks (*p<0.05 and ***p<0.001). CTR = negative control; CET = Cetrorelix; ANOVA = analysis of variance. Schematic figure is adapted from Rick et al. Prostate (2011) 71:736-47.

4.1.2. Morphology and morphometry

Macroscopically, no visible lesions were present in the prostates of Wistar rats in the different experimental groups, except for the obvious enlargement observed among TE-induced BPH rats.

In the ventral prostates of negative control rats, we noted normal histology (126) distinguished by monolayered low columnar epithelium with round-shaped nuclei adjacent to the intact basal membrane and regular acini surrounded by variable amounts of fibromuscular stroma. The acinar lumen contains only a small number of papillary folds (Figure 7 and Table 5).

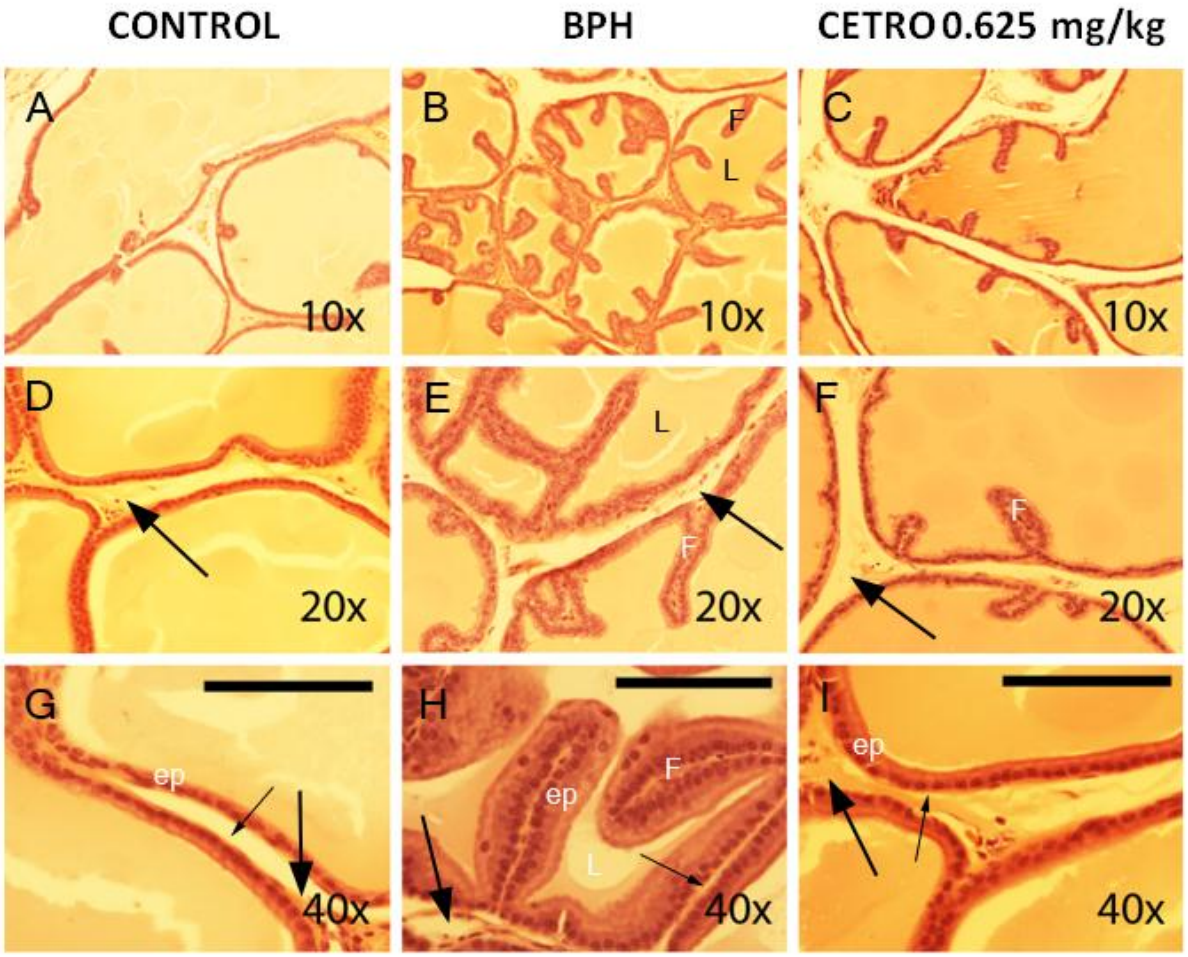

Figure 7. Morphological evaluation of ventral prostate sections from control rats (**A,D,G**), rats with testosterone-induced BPH (**B,E,H**) and rats treated with Cetrorelix 0.625 mg/kg (**C,F,I**). Compared to control, induction of BPH by testosterone decreased luminal area, promoted epithelial folds (F) and increased the epithelial height (ep). Treatment with Cetrorelix 0.625 mg/kg increased the luminal area of the ducts (L), diminished the epithelial folds and reduced epithelial height, as compared to TE-induced BPH animals. Bars indicate 100μm (G,H,I). Arrows indicate fibromuscular stroma, while fine arrows indicate intact basal membrane. Histomorphology is shown at x10 (A,B,C), x20 (D,E,F) and x40 (G,H,I) magnification (hematoxylin-eosin staining). Schematic figure is adapted from Rick et al. Prostate (2011) 71:736-47.

Induction of BPH by testosterone resulted in hyperplastic acinar morphology in the ventral prostates characterized by high columnar epithelial cells with round nuclei placed near to the intact basal membrane, secretory vacuoles at the apical zone, numerous intraluminal papillary folds and

variable amounts of stroma (Figure 7). These changes in acinar morphology after treatment with testosterone correspond to the observations of Scolnik *et al*. (126). We also found a 75% increase in the epithelial cell height compared to control (Table 5).

After treatment with Cetrorelix 0.625 mg/kg, the ventral prostatic acinar morphology showed characteristics similar to that of normal rats (Figure 7). The acini were lined with low columnar epithelium with round basal nuclei. The acinar lumina had only a small degree of infolding. Cetrorelix 0.625 mg/kg significantly decreased the epithelial height by 36% compared to TE-induced BPH controls (Table 5). The amount of fibromuscular stroma was seemingly not affected by treatment with Cetrorelix at a low dose.

Figure 8. Inflammatory infiltrate in ventral prostate of testosterone-induced BPH rats. In addition to the primary pathological lesions of the prostatic acini, we observed incidental inflammatory reactions in the stroma, including lymphocytes (fine arrowhead), mast cells (fine arrow), edema and blood congestion (arrow). This inflammatory infiltrate seemed to be present in the adjacent acinar lumen (arrowhead) as well. We noted inflammatory infiltrates in all experimental groups. Hematoxylin-eosin staining, x40 magnification. Schematic figure is adapted from Rick et al. Prostate (2011) 71:736-47.

In addition to the primary pathological lesions of the prostatic acini, incidental inflammatory reactions including lymphocyte and mast cell infiltration, edema and blood congestion, were also observed in all experimental groups (Figure 8). In some instances of TE-induced BPH, we found intraluminal infiltration as well (Figure 8). These inflammatory infiltrates in the ventral prostates of Wistar rats are consistent with the observations of inflammatory exudates that have been previously reported for this model (126).

4.1.3. Effect of TE and Cetrorelix 0.625 mg/ kg on expression of inflammatory cytokine/growth factor mRNA

Using real-time PCR arrays for rat inflammatory cytokines/receptors and growth factors on control, TE-induced BPH control and TE-induced BPH treated with Cetrorelix 0.625 mg/kg (= lowest dose), we identified important functional molecules affected by treatment with Cetrorelix and selected genes potentially related to prostate shrinkage. More than 30 genes were significantly altered after

treatment with TE and Cetrorelix ($p<0.05$; Table 6). Cytokines including IL-3, IL-5, IL-6, IL-13, IL-15, IL-17β and lymphotoxin-A (LTA) were upregulated by induction of BPH with TE, by 2.95-, 4.54-, 1.98-, 4.47-, 4.17-, 1.95-, and 4.62-fold, respectively. Treatment with Cetrorelix significantly downregulated cytokines IFN-γ, IL-1α, IL-3, IL-4, IL-5, IL-6, IL-13, IL-15, IL-17β and LTA by 2.35-, 3.96-, 4.06-, 4.14-, 2.03-, 2.73-, 4.09-, 2.68-, 5.35- and 3.78-fold, respectively. Among chemokines and chemokine receptors, expression of C5, CCL25, SPP1, CCR4, CCR9 and BLR-1/CXCR5 was significantly decreased by Cetrorelix by 3.07-, 4.06-, 2.33-, 3.76-, 12.30- and 2.87-fold, respectively. Levels of FGF-2, FGF-7, FGF-8 and FGF-14 were significantly reduced by Cetrorelix by 2.02-, 2.07-, 4.72- and 18.90-fold, respectively. Levels of mRNA for TGF-β superfamily members, TGF-β1 and BMP-7, showed 1.79- and 1.75-fold decrease after Cetrorelix. The level of VEGF-A was 1.83-fold lower after Cetrorelix.

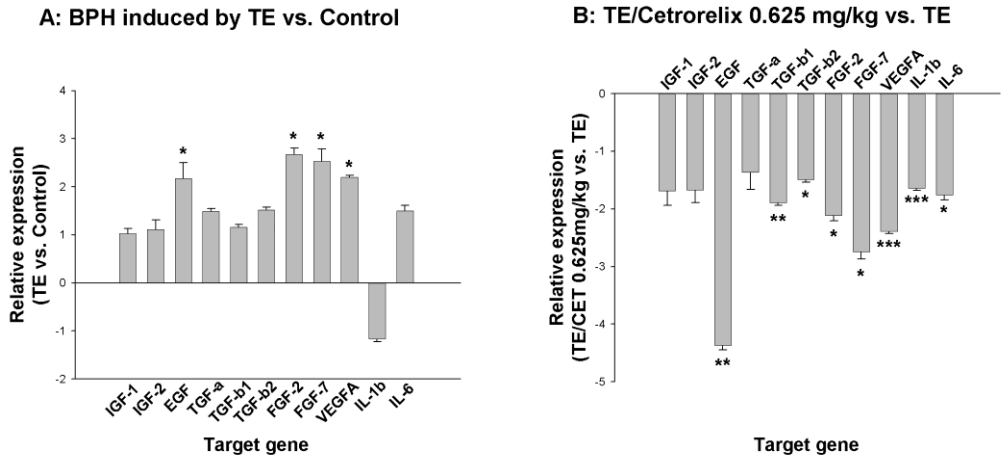

Figure 9. Real-time PCR quantification of various growth factors involved in prostatic growth and function. Bars represent fold differences of individual gene expression between prostate samples from **A:** TE and CTR (negative control) groups or **B:** Cetrorelix 0.625 mg/kg and TE groups. Positive values (>1.00) mark upregulation of individual genes, while negative values (<1.00) mark downregulation. Data are shown as mean±SE. Asterisks indicate a significant difference (*$p<0.05$; **$p<0.01$and ***$p<0.001$ Student's *t*-test). Schematic figure is adapted from Rick et al. Prostate (2011) 71:736-47.

Evaluating our PCR array data, we used real-time RT-PCR to analyze selected proinflammatory and growth factor genes (Figure 9). We found that levels of mRNA for EGF, FGF-2, FGF-7 and VEGF-A were significantly elevated in TE-induced BPH by 2.17-, 2.67-, 2.53- and 2.20-fold, respectively ($p<0.05$). Treatment with Cetrorelix 0.625 mg/kg significantly decreased expression of EGF (4.37-fold [$p<0.01$]), TGF-β1(1.89-fold [$p<0.01$]), TGF-β2 (1.46-fold [$p<0.05$]), FGF-2 (2.11-fold [$p<0.05$]), FGF-7 (2.75-fold [$p<0.05$]), VEGF-A (2.39-fold [$p<0.001$]), IL-1β (1.64-fold [$p<0.001$]) and IL-6 (1.76-fold [$p<0.05$]).

Table 6. Gene expression of rat inflammatory cytokines and receptors and growth factors in prostates harvested from TE treated and Cetrorelix 0.625 mg/kg treated rats 42 days after start of treatment with Cetrorelix.

	Gene	Fold change		Description
		TE vs. Control	TE/Cetrorelix 0.625 mg/kg vs TE	
Cytokine genes	IFN-γ	1.29	**-2.35**	Interferon gamma, induction of proliferation of BPH stromal cells[9]
	IL-1α	1.41	**-3.63**	Interleukin 1 alpha, stimulates the production of epithelial growth promoting FGF-7 in fibroblastic stromal cells
	IL-1β	1.56	-1.47	Interleukin 1 beta, important mediator of the inflammatory response
	IL-2	1.14	-1.27	Interleukin 2, stimulation of growth of stromal cell clones
	IL-3	**2.95**	**-4.06**	Interleukin 3, secreted by activated T cells to support growth and differentiation of T cells in an immune response
	IL-4	1.12	**-4.14**	Interleukin 4, inhibition of proliferation of slowly growing stromal cell clones, stimulation of growth of fibroblasts
	IL-5	**4.54**	**-2.03**	Interleukin 5, produced by T helper-2 cells and mast cells, stimulates B cell growth and increase immunoglobulin secretion
	IL-6	**1.98**	**-2.73**	Interleukin 6, stimulates epithelial cell growth
	IL-f6	**4.49**	**-4.02**	Interleukin 1 family, member6, function unknown
	IL-13	**4.47**	**-4.09**	Interleukin 13, a central mediator of the physiologic changes induced by allergic inflammation in many tissues
	IL-15	**4.17**	**-2.68**	Interleukin 15, a growth factor for BPH memory T cells
	IL-17β	**1.95**	**-5.35**	Interleukin 17B, a potent inductor of IL-6 and IL-8 production by prostate epithelial and stromal cells
	LTA	**4.62**	**-3.78**	Lymphotoxin A, produced by lymphocytes, mediates a large variety of inflammatory, immunostimulatory, and antiviral responses
Cytokine receptors	IL-5Rα	**4.51**	**-4.15**	Interleukin 5 receptor alpha, receptor for IL-5
Chemokines	C5	1.04	**-3.07**	Complement component 5, a protein involved in the complement system
	CCL25	**4.42**	**-4.06**	Chemokine (C-C motif) ligand 25, chemotactic for macrophages
	CXCL2	**3.89**	-1.43	Chemokine (C-X-C motif) ligand 2, chemotactic for polymorphonuclear leukocytes [42,43]
	SPP1	**2.75**	**-2.33**	Secreted phosphoprotein 1 or osteopontin (OPN), immunmodulator and adhesion protein, involed in chemotaxis and wound healing
Chemokine Receptors	CCR4	1.04	**-3.76**	Chemokine (C-C motif) receptor 4, a receptor for certain CC chemokines
	CCR9	1.20	**-12.30**	Chemokine (C-C motif) receptor 9, the specific ligand of this receptor is CCL25
	BLR-1/CXCR5	**2.08**	**-2.87**	Chemokine (C-X-C motif) receptor 5, plays an essential role in B cell migration
Growth factors	EGF	**3.93**	**-2.47**	Epidermal growth factor, potent mitogenic growth factor for prostatic epithelial cells
	IGF-1	1.52	-1.45	Insulin-like growth factor 1, a mitogen for prostatic epithelial cells
	IGF-2	-1.15	1.12	Insulin-like growth factor 2, the predominant mitogenic IGF produced chiefly by prostatic stromal cells
	FGF-2	**2.64**	**-2.02**	Fibroblast growth factor 2, a potent growth factor for prostatic epithelial and stromal cells
	FGF-7	1.41	**-2.07**	Fibroblast growth factor 7, a potent mitogen for prostatic epithelial cells
	FGF-8	**8.07**	**-4.72**	Fibroblast growth factor 8, a FGF family member possessing broad mitogenic and cell survival activities
	FGF-9	1.32	-1.25	Fibroblast growth factor 9, a potent mitogen for both prostatic epithelial and stromal cells
	FGF-14	**24.25**	**-18.90**	Fibroblast growth factor 14 , involved in cell growth, morphogenesis, tissue repair, tumor growth and invasion
TGF-β superfamily	BMP5	**4.29**	-1.36	Bone morphogenetic protein 5, function unknown in the prostate
	BMP7	**4.00**	**-1.75**	Bone morphogenetic protein 7, function unknown in the prostate
	TGF-β1	1.23	**-1.79**	Transforming growth factor beta 1, inhibition of stromal cell growth by induction of differentiation and angiogenesis
	TGF-β2	1.16	-1.41	Transforming growth factor beta 2, inhibition of stromal cell growth by induction of differentation and angiogenesis
Angiogenic factors	VEGF-A	**1.75**	**-1.83**	Vascular endothelial growth factor A, angiogenesis
	VEGF-B	**-2.64**	-1.27	Vascular endothelial growth factor B, angiogenesis
	VEGF-C	-1.07	-1.03	Vascular endothelial growth factor C, angiogenesis

Multiple genes related to inflammatory response and growth factors were evaluated for expression using real-time PCR via RT^2 Profiler™ PCR Array system. The table lists the genes of interest evaluated and their fold increase or decrease in prostates obtained from TE treated and TE/Cetrorelix 0.625 mg/kg treated rats 42 days after the start of treatment with Cetrorelix. Data represent fold differences of individual gene expression between study groups TE and control prostate or TE/Cetrorelix 0.625 mg/kg and TE. Positive values mark upregulation of individual genes, while negative values mark downregulation. Three experiments were run for each study group. The data were evaluated by two-tailed Student's t-test. Boldface depicts significant changes ($p<0.05$).Table adapted from Rick et al. Prostate (2011) 71:736-47.

4.1.4. Effect of Cetrorelix 0.625 mg/kg on expression of LHRH-R, LHRH, AR and 5α-reductase 2 in rat prostate

mRNA for LHRH-R and LHRH-R protein and its LHRH ligand were detected in rat prostate (Figure 10.1 and 2). There were no significant changes in the mRNA and the protein levels of LHRH-R in TE-induced BPH and also after treatment with Cetrorelix (Figure 10.1., A and B). Expression of LHRH was elevated after Cetrorelix; this is significant compared to control (Figure 10.2 B). There were no significant changes in the expression of prostatic androgen receptor (AR) in TE-induced BPH, while Cetrorelix significantly downregulated mRNA for AR and AR protein levels (Figure 10.3 A and B [$p<0.001$ and $p<0.05$, respectively]). Prostatic 5α-reductase 2 protein increased after TE treatment compared to control ($p<0.01$); Cetrorelix significantly lowered 5α-reductase 2 mRNA and protein levels (Figure 10.4 A and B [$p<0.01$ and $p<0.05$, respectively]).

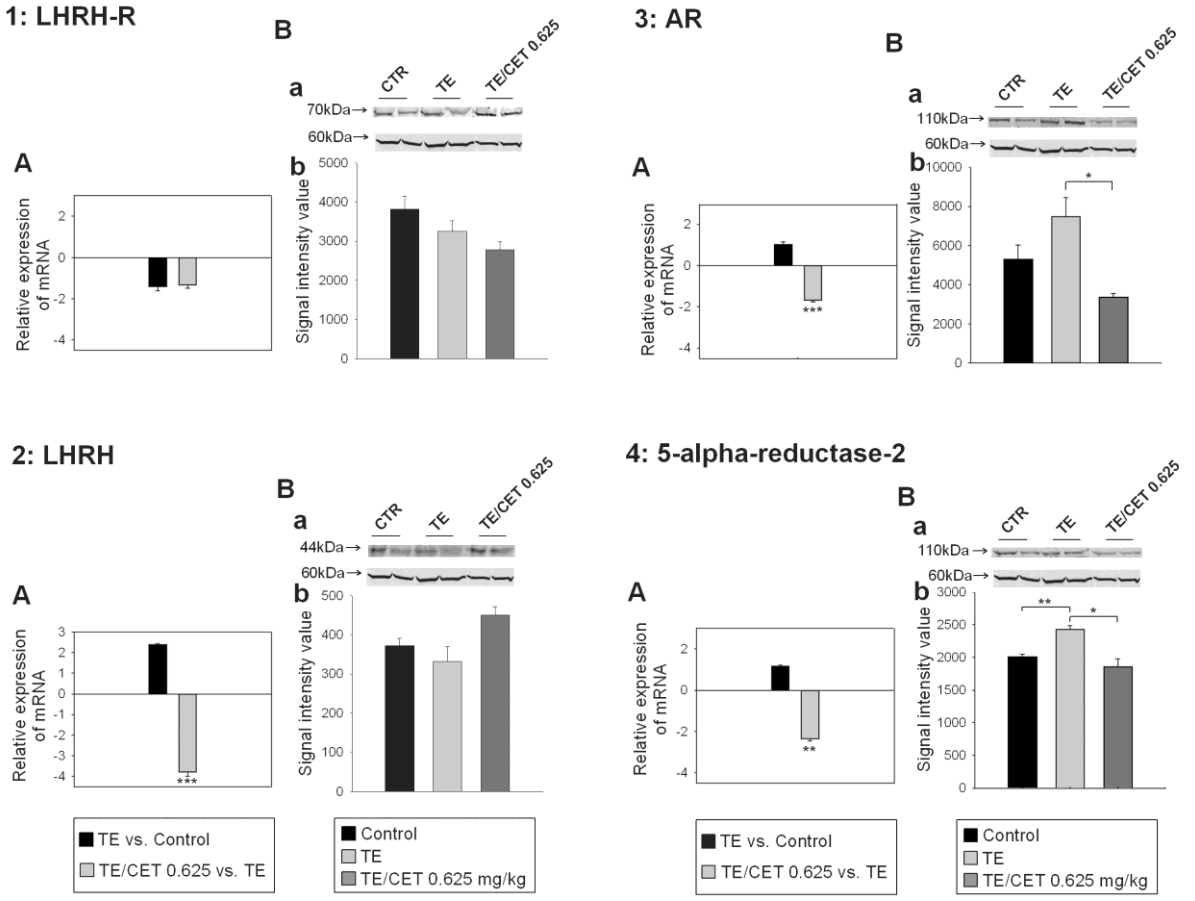

Figure 10. A: Real-time PCR and **B:** Western blot analysis of LHRH-R **(1)**, LHRH **(2)**, AR **(3)** and 5-alpha-reductase 2 **(4)** in rat prostate after induction of BPH with TE and treatment with Cetrorelix at low doses of 0.625 mg/kg. **A:** Real-time PCR analysis of individual genes. Bars represent fold differences of individual gene expression between prostate samples from TE and control groups or Cetrorelix 0.625 mg/kg and TE groups. Positive values (>1.00) mark upregulation of individual genes, while negative values (<1.00) mark downregulation. Data are shown as mean±SE. Asterisks indicate a significant difference (*$p<0.05$; **$p<0.01$ and ***$p<0.001$ by Student's *t*-test). **B:** Western blot analysis of individual proteins showing immunoblot images **(a)** and corresponding signal intensity values **(b)**. Representative blots are presented and include 60kDa internal standard α-tubulin. Molecular masses are shown. Data are presented as mean of scaled signal intensity values ± SE. Asterisks indicate a significant difference (*$p<0.05$ and **$p<0.01$ by Student's *t*-test). Schematic figure is adapted from Rick et al. Prostate (2011) 71:736-47.

4.1.5. Binding assay for LHRH receptors in rat prostate

Receptor analyses revealed a single class of high affinity binding sites for LHRH in rat prostate with dissociation constant [K_d] of 0.82±0.12 nM) and a mean B_{max} (maximal receptor binding capacity) value of 143.0±3.81 fmol/mg membrane protein. Non- significant changes were found in K_d or B_{max} values in TE-induced BPH. Bmax for LHRH was significantly ($p<0.01$) reduced to 68.9±8.28 fmol/mg membrane protein after Cetrorelix (12.5 mg/kg), compared with control; but Kd remained unchanged.

4.1.6. Effect of Cetrorelix on serum DHT, LH, IGF-1 and PSA

In TE-induced BPH there was a 10-fold increase in the serum DHT as compared to control at day 42 (328.52±44.51 pg/ml [$p<0.001$]), while serum DHT was lowered after all doses of Cetrorelix. A significant reduction in DHT was observed with 1.25 and 12.5 mg/kg doses of Cetrorelix only (146.97±28.24 and 134.06±21.73 pg/ml, respectively [$p<0.05$]), but not with 0.625 mg/kg. TE markedly decreased serum LH as compared to control (0.22±0.02 ng/ml [$p<0.001$]). Cetrorelix caused an additional decrease in serum LH, however, significant changes were only seen with the highest dose (0.15±0.01 ng/ml [$p<0.05$]). Serum PSA and IGF-1 changes were not significant (Table 6).

Table 6. Effect of Treatment with Cetrorelix on serum levels of DHT, LH, PSA and IGF-1

	DHT (pg/ml) □		LH (ng/ml) □		PSA (ng/ml) □		IGF-1 (ng/ml) □	
	Day -28	Day 42	Day -28	Day 42	Day -28	Day 42	Day -28	Day 42
Control	39.75±5.61	36.11±7.84	0.36±0.02	0.35±0.02	0.62±0.21	0.55±0.35	3.35±0.53	4.40±0.22
TE	39.89±2.03	328.52±44.51†	0.35±0.01	0.22±0.02†	0.53±0.30	0.50±0.23	4.21±0.25	4.84±0.77
TE/Cetrorelix 0.625 mg/kg	35.74±6.40	227.37±41.63	0.34±0.03	0.18±0.01	0.48±0.18	0.34±0.06	3.67±0.27	5.05±0.49
TE/Cetrorelix 1.25 mg/kg	40.44±7.52	146.97±28.24*	0.36±0.02	0.16±0.01	0.46±0.25	0.30±0.14	5.58±0.25	3.75±0.33
TE/Cetrorelix 12.5 mg/kg	38.62±4.72	134.06±21.73*	0.32±0.05	0.15±0.01*	0.51±0.11	0.29±0.05	4.93±1.13	4.06±0.50

*$^{\dagger}p<0.001$ as compared to Control; *$p<0.05$ as compared to TE. The data were evaluated by two-tailed Student's t-test. Table adapted from Rick et al. Prostate (2011) 71:736-47.*

4.2. Effects of GHRH antagonists on experimental benign prostatic hyperplasia (Study 2)

4.2.1. Expression of GHRH receptor, SV1 and GHRH.

Protein and mRNA for GHRH-R and for GHRH, as well as the protein of splice variant SV1 of GHRH-R were detected in rat prostate (Figure 11A and 11B). Levels of prostatic GHRH-R protein were significantly increased after testosterone-enanthate (TE) treatment compared to control ($P<0.01$; protein signal intensity values are shown in Figure 12); GHRH antagonist JMR-132 and finasteride significantly elevated GHRH-R protein levels compared to TE (testosterone-enanthate) controls ($P < 0.05$ and $P < 0.01$, respectively; Figure 11B and Figure 12). Radioligand binding assays revealed a single class of high affinity binding sites for GHRH in rat prostate with dissociation constant (K_d) of 4.13±0.09 nM and a mean maximal receptor binding capacity (B_{max}) of 313.0±25.9 fmol/mg membrane protein. The number of receptors for GHRH in rat BPH tissues induced by TE was significantly ($P<0.01$) increased to 540.7±50.1 fmol/mg membrane protein; receptor K_d was unchanged (4.02±0.20 nM). No significant changes were found in K_d or B_{max} values in rat BPH tissues after treatment with finasteride or GHRH antagonists JMR-132, MIA-313, and MIA-459, compared with TE-induced rat BPH tissues. Further, protein expression of GHRH-R encoded by SV1 was quantified in rat prostates by Western blot (Figure 11B and Figure 12). Expression of GHRH mRNA and protein was elevated after treatment with TE, while GHRH antagonists and finasteride significantly suppressed expression of prostatic GHRH mRNA and protein levels compared to TE-induced BPH (Figure 11A and 11B and Figure 12).

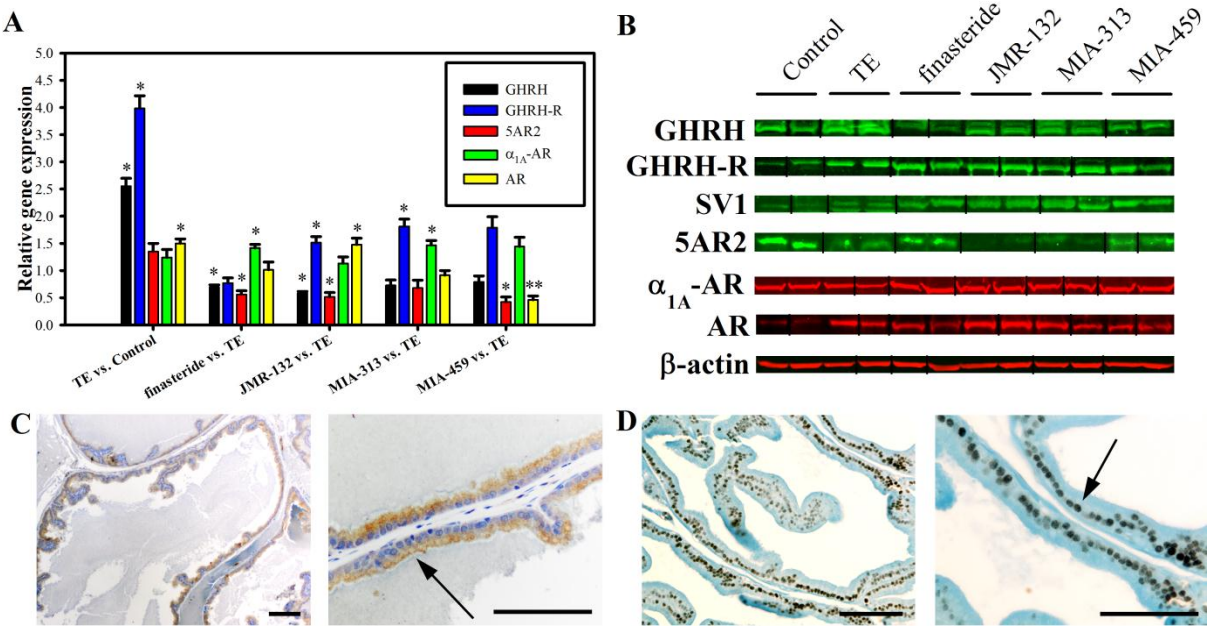

Figure 11. Effect of GHRH antagonists JMR-132, MIA-313 and MIA-459 on the expression of GHRH, GHRH-R, SV1, 5AR2, α_{1A}-AR, and AR (A and B). Bar graph (A) showing real-time RT-PCR analysis of GHRH, GHRH-R, 5AR2, α_{1A}-AR, and AR. Bars represent relative expression of individual genes between prostate samples (n=3) from TE and control groups or between finasteride, JMR-132, MIA-313 or MIA-459 and TE groups. Values > 1.00 mark upregulation of individual genes, while values < 1.00 mark downregulation. Data are shown as means ± SEM. Asterisks indicate a significant difference (*$P < 0.05$ and **$P < 0.01$ by Student's *t*-test). Western blot analysis (B) of of

GHRH, GHRH-R, SV1, 5AR2, α_{1A}-AR, and AR. Representative blots of three independent experiments are presented and include internal standard β-actin; corresponding signal intensity values are shown in Fig. S1A. Grouping of representative bands for each experimental group was digitally performed. Expression of GHRH receptors(C) in representative ventral prostate of control rats was confined to the cytoplasm and luminal membrane of prostatic acinar cells (Arrow). Localization of GHRH receptors are shown in 10X (Left) and 40X (Right) magnification (Scale bars: 50µm). Androgen receptors (D) in representative ventral prostates of control rats were localized in the in the nuclei of prostatic acinar cells (Arrow), as shown by 20X (Left) and 40X (Right) magnification (Scale bars: 50µm). Schematic figure is adapted from Rick et al. Proc Natl Acad Sci USA (2011) 108:3755-60.

4.2.2. Immunohistochemical confirmation of the expression of GHRH receptor protein.

Immunohistochemical analyses revealed that expression of GHRH-R is confined to the cytoplasm and luminal membrane of prostatic acinar cells in rat (Figure 11C).

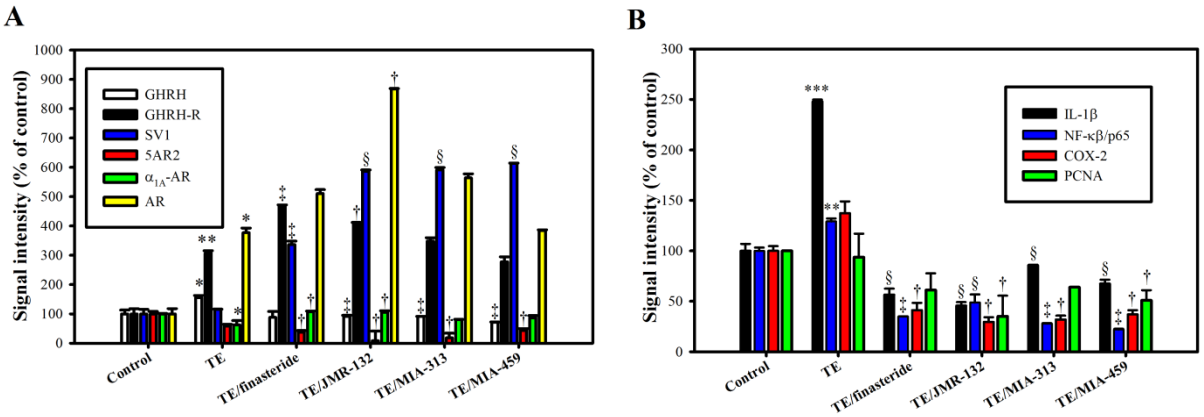

Figure 12. Protein expression of GHRH, GHRH-R, SV1, 5AR2, α_{1A}-AR and AR (A) and IL-1β, NF-κβ/p65, COX-2 and PCNA (B) in rat prostates (n=3 in each study group) obtained by Western blotting. Signal intensity values are compared to control (* $P < 0.05$, ** $P < 0.01$ and ***$P < 0.01$ as compared to TE; $^{\dagger}P < 0.05$, $^{\ddagger}P < 0.01$ and $^{\S}P < 0.001$ as compared to control by Student's *t*-test). Schematic figure is adapted from Rick et al. Proc Natl Acad Sci USA (2011) 108:3755-60.

4.2.3. Reduction of prostate size by GHRH antagonists.

Body weights of rats at sacrifice were not affected by any GHRH antagonist+TE- or by treatment with finasteride+TE compared to TE-only (Table 7). Corn oil-injected control prostates weighed 234.9±16.7 mg/100 g rat; while in TE controls prostates were enlarged by 55.5% to 365.4±20.3 mg/100 g rat ($P<0.001$; Table 7). GHRH antagonists JMR-132 at 40µg/day, MIA-313 at 20µg/day, and MIA-459 at 20µg/day significantly lowered prostate weights by 17.8%, 17.0% and 21.4%, respectively compared to TE controls($P<0.05$; Table 7). These reductions in prostate weight were superior to that obtained with finasteride 0.1 mg/kg/day (nonsignificant 14.43 % reduction; Table 7). In addition, GHRH antagonists significantly decreased prostatic DNA content as well (Table 7). Testicular weights did not change after treatment with GHRH antagonists (Table 7).

Table 7. Effect of GHRH antagonists JMR-132, MIA-313 and MIA-459 on morphological parameters

	Body weight (g)		Relative prostate weight (mg/100g rat BW)	Prostatic DNA content (ng DNA/mg tissue)	Relative testicle weight (mg/100g rat BW)
	Day -28	Day 42	Day 42	Day 42	Day 42
Control	400.9 ± 9.9	551.6 ± 13.3	234.9 ±16.7	224.8 ± 8.6	617.6 ± 22.2
TE	392.8 ± 6.8	482.6 ± 7.1†	365.4 ± 20.3§	266.8 ± 5.9	565.5 ± 25.7
TE/finasteride 0.1mg/kg/day	396.0 ± 8.8	476.0 ± 12.7†	337.6 ± 26.0	214.1 ± 9.4*	507.2 ± 30.6†
TE/JMR-132 40 µg/day	409.2 ± 10.2	517.4 ± 20.2	300.4 ± 18.1*	216.1 ± 8.7*	522.2 ± 28.5
TE/MIA-313 20 µg/day	403.7 ± 8.4	499.0 ± 14.2	303.4 ± 17.3*	186.0 ± 8.3***	541.6 ± 10.4
TE/ MIA-459 20 µg/day	410.4 ± 8.8	510.1 ± 15.2	287.0 ± 16.3*	214.6 ± 7.8*	525.4 ± 19.1

*† P<0.05, ‡ P<0.01 and § P<0.001 as compared to control; * P<0.05 and ***P<0.01 as compared to TE. Statistical analysis was performed by one-way ANOVA, followed by Bonferroni t-test. Table is adapted from Rick et al. Proc Natl Acad Sci USA (2011) 108:3755-60.*

4.2.4. Effect of GHRH antagonists on 5AR2, α1A-AR and AR.

There were no significant changes in levels of prostatic 5AR2 protein in TE-induced BPH. GHRH antagonists JMR-132, MIA-313, and MIA-459 as well as finasteride significantly lowered protein levels of 5AR2 (P<0.05 for all; Figure 11B and protein signal intensity values are shown in Figure 12). While finasteride and JMR-132 significantly elevated the α_{1A}-AR protein levels (P<0.05 for both, Figure 11B and Figure 12), MIA-313 and MIA-459 caused a nonsignificant increase in α_{1A}-AR protein levels. Levels of prostatic AR protein was significantly elevated in TE-induced BPH (P<0.05); only treatment with JMR-132 resulted in significant change in AR protein level (2.30 fold upregulation and P<0.05; Figure 11B and Figure 12). AR was localized to localized to the nuclei of prostatic acinar cells by immunohistochemical staining (Figure 11D).

4.2.5. GHRH antagonists suppress proinflammatory IL-1β, NF-κβ and COX-2.

Prostatic IL-1β protein was significantly increased after TE treatment compared to control (P<0.001), while GHRH antagonists JMR-132, MIA-313, and MIA-459 and finasteride significantly reduced IL-1β levels (P<0.001 for all; Figure 13B and signal intensity values are shown in Figure 12). Expression of NF-κβ/p65 (RelA) protein was significantly elevated after treatment with TE (P<0.01). GHRH antagonists JMR-132, MIA-313 and MIA-459 and finasteride significantly decreased prostatic NF-κβ/p65 protein levels compared to TE-induced BPH (P<0.001, P<0.01, P<0.01 and P<0.01, respectively; Figure 13B and Figure 12). Prostatic COX-2 protein was elevated after TE treatment, but not significantly. All three GHRH antagonists and finasteride significantly lowered prostatic

COX-2 protein levels (P<0.05 for all; Figure 13B and Figure 12). There was a suppression of NF-κβ2 and RelA genes after treatment with all three GHRH antagonists and finasteride (P<0.01for all; Figure 13A), while COX-2 gene was significantly downregulated after MIA-313, MIA-459, or finasteride (P<0.05, P<0.01 and P<0.01, respectively; Figure 13A).

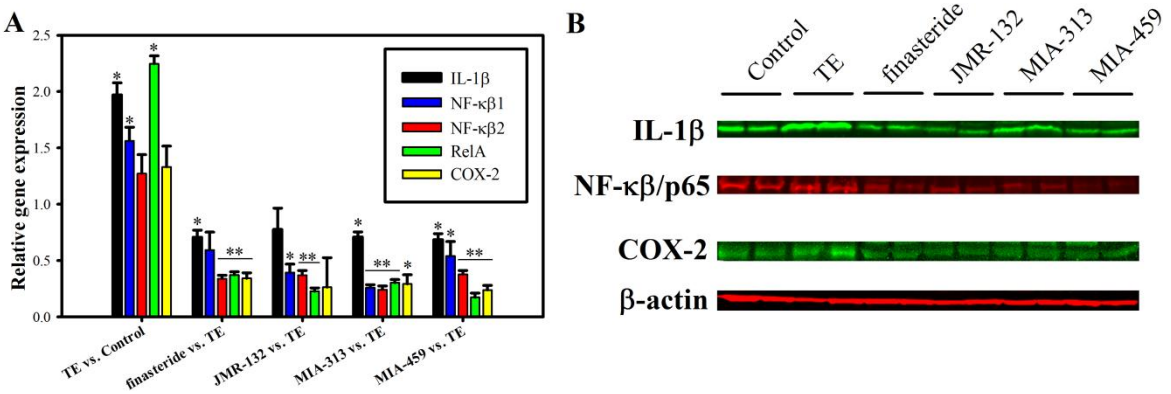

Figure 13. GHRH antagonists suppress expression of IL-1β, NF-κβ and COX-2 in rat prostates. Bar graph (A) showing real-time RT-PCR analysis of IL-1b, NF-κβ1, NF-κβ2, RelA and COX-2. Bars represent relative expression of individual genes between prostate samples (n=3) from TE and control groups or between finasteride, JMR-132, MIA-313 or MIA-459 and TE groups. Values > 1.00 mark upregulation of individual genes, while values < 1.00 mark downregulation. Data are shown as means ± SEM. Asterisks indicate a significant difference (*P <0 .05 and **P < 0.01 by Student's *t*-test). Western blot analysis (B) of IL-1β, NF-κβ/p65, and COX-2. Representative blots of three independent experiments are presented and include internal standard β-actin; corresponding signal intensity values are shown in Fig. 12B. Schematic figure is adapted from Rick et al. Proc Natl Acad Sci USA (2011) 108:3755-60.

4.2.6. GHRH antagonists inhibit cell division and induce apoptosis.

Morphologic evaluation on H&E slides revealed that sizes of average epithelial areas in the ventral prostate did not differ among the study groups. Mitoses were significantly fewer in all groups compared to TE treated BPH controls. Apoptotic cell numbers were higher in the groups treated with GHRH antagonists MIA-313, MIA-459, and finasteride, but the differences from TE treated controls were not statistically significant (Table 8). Representative apoptotic cells among epithelial cells in ventral prostates of rats treated with MIA-459 are displayed in Figure 14F.

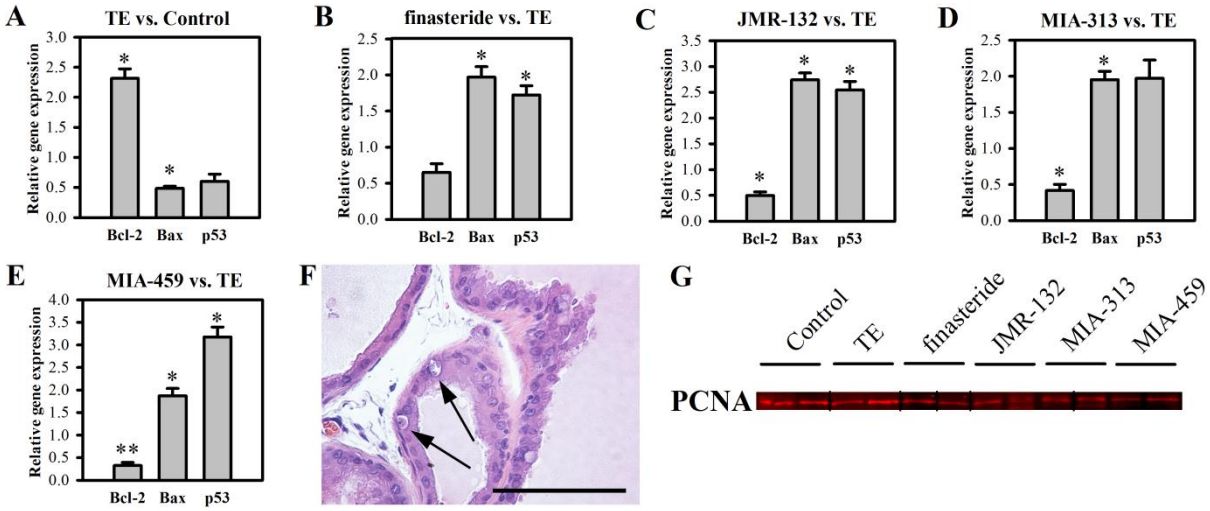

Figure 14. GHRH antagonists induce apoptosis and inhibit proliferation of prostatic epithelial cells in rats. Bar graphs (A-E) showing real-time RT-PCR analysis of Bcl-2, Bax and p53. Bars represent relative expression of individual genes between prostate samples (n=3) from

TE and control groups (A) or between finasteride (B), JMR-132 (C), MIA-313 (D) or MIA-459 (E) and TE groups. Values > 1.00 mark upregulation of individual genes, while values < 1.00 mark downregulation. Data are shown as means ± SEM. Asterisks indicate a significant difference (*P < 0.05 by Student's *t*-test). Representative apoptotic cells (Arrows) among prostatic acinar epithelial cells of a MIA-459 treated rats are shown (F) in H&E stained slide (40X; scale bar: 50μm). Western blot analysis (G) of PCNA. Representative blots of three independent experiments are presented; corresponding signal intensity values are shown in Fig. 12B. Grouping of representative bands for each experimental group was digitally performed. Schematic figure is adapted from Rick et al. Proc Natl Acad Sci USA (2011) 108:3755-60.

We found transcriptional upregulation of Bcl-2 and downregulation of Bax after TE treatment (P<0.05 for both; Figure 14A). The expression of mRNA for Bax was elevated after treatment with all three GHRH antagonists or finasteride (P<0.05 for all; Figure 14B-E), while that of Bcl-2 was decreased after treatment with JMR-132, MIA-313 and MIA-459 (P<0.05, P<0.05 and P<0.01, respectively; Figure 14C-E). No significant change in prostatic PCNA (proliferating cell nuclear antigen) protein levels occurred after TE treatment; GHRH antagonists JMR-132 and MIA-459 significantly reduced PCNA protein (P<0.05 for all; Figure 14G).

Table 8. Effect of GHRH antagonists on cell proliferation and apoptosis in rat prostatic epithelium

	Mean epithelial area in view fields (%)	Number of mitoses in one theoretical field composed entirely of epithelial cells	Number of apoptotic cells in one theoretical field composed entirely of epithelial cells
Control	14.3 ± 1.6	1.93 ± 1.32	3.40 ± 0.43
TE	17.1 ± 2.3	5.86 ± 1.81†	3.12 ± 0.69
TE/finasteride 0.1mg/kg/day	15.9 ± 2.6	0.69 ± 0.35 *	6.42 ± 2.30
TE/JMR-132 40μg/day	15.0 ± 0.4	0.87 ± 0.43 *	3.55 ± 0.16
TE/MIA-313 20μg/day	14.7 ± 1.3	1.73 ± 0.47 *	5.18 ± 1.10
TE/MIA-459 20μg/day	16.0 ± 2.3	0.00 ± 0.00 *	5.69 ± 1.47

*†P<0.05 as compared to control; *P<0.05 as compared to TE. The data were evaluated by one way ANOVA, followed by Student-Newman-Keuls method. Table is adapted from Rick et al. Proc Natl Acad Sci USA (2011) 108:3755-60.*

4.2.7. GHRH antagonists cause transcriptional downregulation of multiple genes involved in growth, inflammatory response and signaling.

Growth factors, inflammatory cytokines and receptors and signal transduction factors were evaluated for control, TE-induced BPH control and TE-induced BPH treated with GHRH antagonists JMR-132, MIA-313, and MIA-459 by real-time RT-PCR arrays for rat. We identified important functional molecules affected by treatment with GHRH antagonists and selected genes potentially related to prostate shrinkage. More than 80 genes were significantly altered after treatment with TE and GHRH antagonists (p<0.05; Table 9-11).

Transcriptional levels of several growth factors including Bmp1, Bmp2, Bmp3, Bmp8a, Egf, Fgf1, Fgf2, Fgf11, Fgf12, Fgf14, Igf22, Igf2, Ntf4, Pdgfa, Spp1, Tgfa, Tgfb1, Tgfb2, Tgfb3 and Vegfa were significantly lowered by GHRH antagonists (P<0.05; Table 9).

Expression of inflammatory cytokines including IL-1α, IL-1β, IL-13, IL-15, IL-17β, Spp1 and Cd40lg were decreased by GHRH antagonists (P<0.05; Table 10). Among chemokines and their

receptors, expression of Ccl 6, Ccl7, Ccl12, Ccr1, Ccr6, Cxcr3 and Gpr2 was significantly decreased by GHRH antagonists (P<0.05; Table 10).

From PCR array for signal transduction (Table 11), we identified putative downstream pathways responsible for GHRH antagonist effects in this model. We found mRNAs for Egr1, Fos, Jun and Nab2 mitogenic pathway genes significantly downregulated after treatment with GHRH antagonists (P<0.05). Expression of Hedgehog pathway target genes (Bmp2, Bmp4, Hhip, Ptch1, Wnt1 and Wnt2) was significantly affected by GHRH antagonists (P<0.05). Levels of PI3K/AKT pathway-related genes such as Bcl2, Fn1, Jun and Mmp7 decreased after GHRH antagonists (P<0.05). Expression of genes involved in phospholipase C pathway, such as Bcl-2, Egr1, Fos, Icam1, Jun, Junb and Vcam1 was significantly lowered by GHRH.

Table 9. Gene expression of growth factors after treatment with TE and GHRH antagonists JMR-132, MIA-313 and MIA-459 in rat prostates

		Fold change			
Gene	Accession no.	TE vs. Control	TE/JMR-132 40µg/day vs. TE	TE/MIA-313 20µg/day vs. TE	TE/MIA-459 20µg/day vs. TE
Artn	NM_053397	1.38	**-1.84**	**-2.50**	**-3.37**
Bmp1	XM_573814	**1.45**	**-1.91**	**-2.33**	**-2.22**
Bmp2	NM_017178	**1.82**	**-1.43**	**-3.26**	**-2.93**
Bmp3	NM_017105	-1.02	**-1.61**	**-1.90**	**-2.08**
Bmp8a	XM_001059507	**15.28**	**-21.86**	**-9.13**	**-28.91**
Egf	NM_012842	**1.85**	**-2.41**	**-1.94**	**-4.25**
Fgf1	NM_012846	1.07	**-2.43**	**-1.90**	**-3.15**
Fgf2	NM_019305	**1.57**	-1.57	**1.88**	**-2.12**
Fgf11	NM_130816	**1.62**	**-2.05**	**-2.26**	**-2.16**
Fgf13	NM_053428	-1.02	**-2.30**	**-3.01**	**-2.80**
Fgf14	NM_022223	1.27	**-1.53**	-1.24	**-2.23**
Fgf22	NM_130751	1.06	**-2.02**	**-2.39**	**-2.74**
Gdf5	XM_001066344	-1.08	**-1.53**	**-1.81**	**-2.17**
Igf1	NM_178866	**1.42**	-1.33	1.00	1.16
Igf2	NM_031511	**1.85**	**-2.41**	**-1.58**	**-2.27**
Inha	NM_012590	-1.23	**-1.89**	**-1.94**	**-2.74**
Inhbb	XM_344130	-1.12	**-2.12**	**-2.59**	**-2.22**
Lep	NM_013076	**2.70**	**-3.14**	**-3.34**	**-6.44**
Ntf4	NM_013184	1.26	-1.62	**-2.62**	**-2.61**
Pdgfa	NM_012801	**1.95**	**-2.00**	**-2.13**	**-2.68**
Pgf	NM_053595	1.41	-1.48	**-2.08**	**-1.50**
Rabep1	NM_019124	1.07	**-2.00**	**-2.06**	**-2.56**
S100a6	NM_053485	1.26	**-1.68**	**-2.45**	**-2.08**
Spp1	NM_012881	**-2.00**	**-2.38**	**-1.61**	**-6.90**
Tgfα	NM_012671	**1.68**	**-1.87**	**-2.06**	**-2.50**
Tgfβ1	NM_021578	**4.81**	**-1.82**	**-2.01**	**-1.85**
Tgfβ2	NM_031131	1.23	**-2.14**	**-2.62**	**-1.54**
Tgfβ3	NM_013174	1.12	**-1.80**	**-1.92**	-1.37
Vegfa	NM_031836	**1.59**	**-1.87**	**-1.92**	**-2.44**
Vegfb	NM_053549	1.05	**-1.93**	**-1.51**	**-2.50**

Table S1. *Multiple genes related to growth were evaluated for expression using real-time PCR via RT^2 Profiler™ PCR Array system. The table lists the genes of interest evaluated and their fold increase or decrease in prostates obtained from TE treated and TE/JMR-132, TE/MIA-313 and TE/MIA-459 treated rats 42 days after the start of treatment with GHRH antagonists. Data represent fold differences of individual gene expression between study groups TE and control prostate or TE/JMR-132, TE/MIA-313, TE/MIA-459 and TE. Positive values mark upregulation of individual genes, while negative values mark downregulation. Three experiments were run for each study group. The data were evaluated by two-tailed Student's t-test. Boldface depicts significant changes (P<0.05). Table is adapted from Rick et al. Proc Natl Acad Sci USA (2011) 108:3755-60.*

We used real-time RT-PCR to verify changes in the expression of selected proinflammatory and growth factor genes (Figure 15). Levels of mRNA for IGF-1, IGF-2, TGF-α, TGF-β2, EGF and FGF-2 were significantly elevated in TE-induced BPH by 1.36-, 1.64-, 1.89-,1.98-, 2.21- and 1.83-fold, respectively (P<0.05 for all; Figure 15A). Finasteride 0.1 mg/kg significantly decreased the expression of mRNA for IGF-2 and IL-6 by 1.97- and 2.21-fold, respectively (P<0.05 for all; Figure 15B). Antagonist JMR-132 significantly lowered the expression of IGF-2, TGF-β1, TGF-β2, EGF, VEGF-A and IL-6 by 1.36-, 1.96-, 1.59-, 1.61-, 1.51- and1.65-fold, respectively (P<0.05 for all; Figure 15C). Treatment with MIA-313 significantly decreased the expression of TGF-α, TGF-β2, EGF, FGF-7, VEGF-A and IL-6 by 1.49-, 1.47-, 1.53-, 1.72-, 1.63-, and 1.52-fold, respectively (P<0.05 for all; Figure 15D). GHRH antagonist MIA-459 exerted the greatest downregulation at the transcriptional level: IGF-2 (2.35-fold [P<0.01]), TGF-α (4.98-fold [P<0.01]), TGF-β1 (1.63-fold [P<0.05]), TGF-β2 (1.45-fold [p<0.05]), EGF (2.75-fold [P<0.01]), FGF-2 (2.10-fold [P<0.05]) and FGF-7 (1.87-fold [P<0.05]) (Figure 15E).

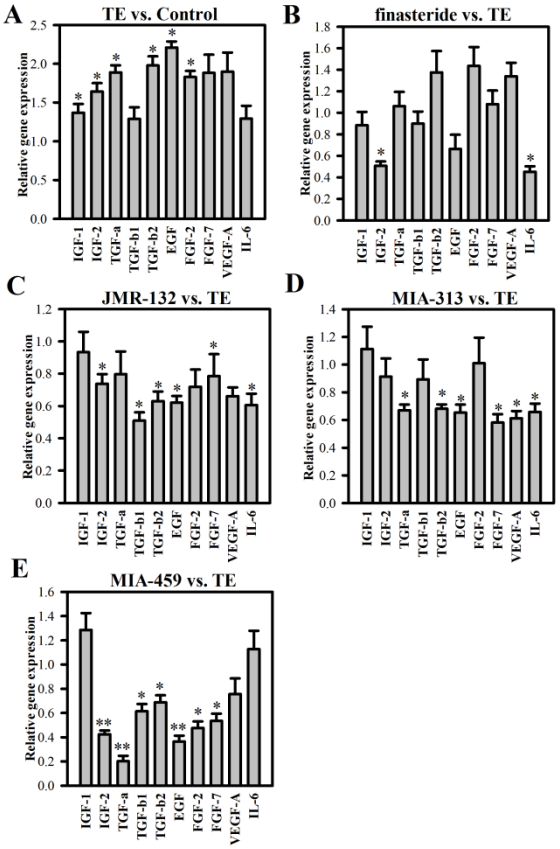

Figure 15. Real-time RT-PCR quantification of various growth factors and inflammatory cytokines involved in prostatic growth and function. Bars represent fold differences of individual gene expression between prostate samples from TE and control (A) groups; finasteride 0.1 mg/kg/day and TE groups (B); JMR-132 40 µg/day and TE groups (C); MIA-313 20 µg/day and TE groups (D) or MIA-459 20 µg/day and TE groups (E). Values > 1.00 mark upregulation of individual genes, while values < 1.00 mark downregulation. Data are shown as means ± SEM. Asterisks indicate a significant difference (*P < 0.05 and **P < 0.01 by Student's *t*-test). Schematic figure is adapted from Rick et al. Proc Natl Acad Sci USA (2011) 108:3755-60.

4.2.8. Effect of GHRH antagonists on serum GH, IGF-1, DHT and PSA.

TE markedly increased serum GH (104.8±13.4 ng/ml [p<0.01]) as compared to control (49.4 ± 3.9 ng/ml). GHRH antagonists and finasteride did not cause a significant decrease in serum GH levels (Table 12). Serum IGF-1 was significantly elevated after TE (4.9±0.6 ng/ml [p<0.05]) while GHRH

antagonists did not significantly lower serum IGF-1 levels. In TE-induced BPH rats there was an approximately 10-fold increase in the serum DHT as compared to control at day 42 (337.4±53.5 pg/ml [P<0.001]), however, no significant differences in serum DHT levels were observed after treatment of GHRH antagonists. A significant 60%reduction in DHT was observed after treatment with finasteride 0.1mg/day(P<0.05). Serum PSA changes were not significant. Values for serum markers: see Table 12.

Table 10. Expression of genes involved in inflammatory response after treatment with TE and GHRH antagonists JMR-132, MIA-313 and MIA-459 in rat prostates

		Fold change			
Gene	Accession no.	TE vs. Control	TE/JMR-132 40µg/day vs. TE	TE/MIA-313 20µg/day vs. TE	TE/MIA-459 20µg/day vs. TE
Bcl6	XM_221333	**1.69**	**-3.12**	**-5.06**	**-4.53**
RGD1561905/	XM_345342	**2.23**	**-2.36**	**2.57**	**-3.43**
Ccl12	XM_213425	**1.36**	**-1.78**	**-1.36**	-1.21
Ccl24	NM_001013045	1.12	-1.10	**-1.45**	-1.13
Ccl6	NM_001004202	**2.20**	1.12	**-1.47**	**-1.39**
Ccl7	NM_001007612	**-1.67**	**-2.91**	**-3.34**	**-1.43**
Ccr1	NM_020542	**-1.67**	**-2.20**	-1.18	**-1.50**
Ccr6	NM_001013145	**2.08**	**-1.37**	**-1.45**	-1.30
Cxcl4	NM_001007729	**1.58**	1.20	**-1.56**	1.09
Cxcr3	NM_053415	1.12	**-1.69**	1.10	**-1.39**
Gpr2	XM_343968	**2.23**	**-1.56**	-1.36	**-1.98**
Il13	NM_053828	**3.39**	-1.36	**-1.55**	**-1.97**
Il15	NM_013129	**2.57**	**-1.44**	-1.03	**-1.63**
Il17b	XM_341621	**2.08**	1.24	**-1.67**	**-1.54**
Il1α	NM_017019	**1.69**	**-1.95**	1.28	**-3.06**
Il1β	NM_031512	**1.66**	**-1.58**	**-2.23**	**-2.17**
Spp1	NM_012881	**4.17**	1.12	-1.03	**-2.79**
Tnfrsf1a	NM_013091	1.38	**-1.45**	**-1.67**	**-2.26 :**
Cd40lg	NM_053353	**2.57**	1.04	**-2.06**	**-1.38**
Tollip	XM_341961	1.28	-1.27	**-1.45**	**-2.11**
Tnf	NM_012675	**2.57**	1.31	-1.24	1.07

Multiple genes related to inflammatory response were evaluated for expression using real-time PCR via RT^2 Profiler™ PCR Array system. The table lists the genes of interest evaluated and their fold increase or decrease in prostates obtained from TE treated and TE/JMR-132, TE/MIA-313 and TE/MIA-459 treated rats 42 days after the start of treatment with GHRH antagonists. Data represent fold differences of individual gene expression between study groups TE and control prostate or TE/JMR-132, TE/MIA-313, TE/MIA-459 and TE. Positive values mark upregulation of individual genes, while negative values mark downregulation. Three experiments were run for each study group. The data were evaluated by two-tailed Student's t-test. Boldface depicts significant changes (P<0.05). Table is adapted from Rick et al. Proc Natl Acad Sci USA (2011) 108:3755-60.

Table 11. Expression of genes involved in signal transduction after treatment with TE and GHRH antagonists JMR-132, MIA-313 and MIA-459 in rat prostates

		Fold change			
Gene	Accession no.	TE vs. Control	TE/JMR-132 40µg/day vs. TE	TE/MIA-313 20µg/day vs. TE	TE/MIA-459 20µg/day vs. TE
Bax	NM_017059	**-1.69**	**1.65**	**2.20**	1.47
Bcl2	NM_016993	**1.45**	**-1.49**	**-1.78**	-1.20
Bmp2	NM_017178	-1.04	**-2.33**	**-3.12**	**-6.32**
Bmp4	NM_012827	-1.28	**-2.87**	**-3.84**	**-2.95**
Brca1	NM_012514	1.18	**-2.68**	**-3.58**	**-1.95**
Cdh1	NM_031334	1.27	-1.01	-1.10	**-1.69**
Cdk2	NM_199501	1.10	1.06	**-1.28**	**-1.47**
Cdkn1a	NM_080782	-1.20	-1.09	1.27	**1.40**
Cdkn1b	NM_031762	-1.28	**1.34**	1.06	**2.23**
Csf2	XM_340799	**-3.39**	1.30	**-1.45**	**-2.95**
Cxcl9	NM_145672	**-1.95**	**2.11**	**2.23**	**2.91**
Egr1	NM_012551	**2.20**	**-1.35**	**-1.79**	1.03
Fas	NM_139194	-1.20	**-1.43**	**-1.67**	**-1.95**
Fn1	NM_019143	**-1.82**	**-2.33**	**-2.06**	**-1.58**
Fos	NM_012743	-1.04	**-1.89**	**-2.20**	1.27
Hoxa1	NM_013075	**1.67**	**3.20**	**4.17**	**2.51**
Icam1	NM_012967	-1.28	**-1.54**	-1.10	**-1.69**
Igfbp3	NM_012588	**-1.82**	**-2.33**	-1.67	**-2.39**
Ikbkb	NM_053355	**1.79**	1.13	-1.10	-1.28
Il4ra	NM_133380	-1.04	-1.43	**-1.68**	**-1.67**
Irf1	NM_012591	**-1.69**	**-1.54**	**-1.67**	-1.47
Jun	NM_021835	**1.92**	-1.09	**-1.79**	**-1.69**
Junb	NM_021836	**1.45**	**-2.03**	**-1.92**	**-3.16**
Hhip	XM_238042	**-1.69**	**-2.05**	**-2.53**	-1.47
Mmp7	NM_012864	-1.38	**-3.78**	**-2.53**	**-6.77**
Nab2	XM_235224	**-1.58**	**-2.03**	**-1.92**	**-2.75**
Nfkβ1	XM_342346	**2.20**	-1.34	-1.18	**-1.95**
Pparg	NM_013124	1.10	**-4.66**	**-3.34**	**-2.39**
Ptch1	XM_345570	-1.47	**4.23**	**3.63**	**2.36**
Selp	NM_013114	**-3.89**	**-24.59**	**-17.63**	**-33.36**
Tcf7	XM_343891	1.36	1.60	**2.23**	**1.92**
Tp53	NM_030989	**-1.56**	**1.39**	**-1.10**	**1.27**
Vcam1	NM_012889	**-1.58**	**-2.17**	**-1.79**	**-2.04**
Wisp1	NM_031716	**-3.16**	**-2.03**	-2.53	**-2.08**
Wnt1	XM_235639	1.27	**-1.65**	1.15	**-1.46**
Wnt2	XM_575397	1.36	**-2.33**	-1.18	**-2.23**

Multiple genes involved in signal transduction were evaluated for expression using real-time PCR via RT^2 Profiler™ PCR Array system. The table lists the genes of interest evaluated and their fold increase or decrease in prostates obtained from TE treated and TE/JMR-132, TE/MIA-313 and TE/MIA-459 treated rats 42 days after the start of treatment with GHRH antagonists. Data represent fold differences of individual gene expression between study groups TE and control prostate or TE/JMR-132, TE/MIA-313, TE/MIA-459 and TE. Positive values mark upregulation of individual genes, while negative values mark downregulation. Three experiments were run for each study group. The data were evaluated by two-tailed Student's t-test. Boldface depicts significant changes (P<0.05). Table is adapted from Rick et al. Proc Natl Acad Sci USA (2011) 108:3755-60.

Table 12. Effect of treatment with GHRH antagonists on serum levels of GH, IGF-1, DHT and PSA in rat

	GH (ng/ml)		IGF-1 (ng/ml)		DHT (pg/ml)		PSA (ng/ml)	
	Day -28	Day 42	Day -28	Day 42	Day -28	Day 42	Day -28	Day 42
Control	43.4 ± 4.1	49.4 ± 3.9	2.9 ± 0.4	3.6 ± 0.3	39.1 ± 6.7	34.2 ± 3.9	2.1 ± 0.5	1.6 ± 0.4
TE	43.8 ± 3.9	104.8 ± 13.4‡	3.3 ± 0.5	4.9 ± 0.6†	32.1 ± 2.6	337.4 ± 53.5§	1.5 ± 0.4	2.6 ± 0.5
TE/finasteride	45.1 ± 4.3	90.4 ± 12.1	3.3 ± 0.4	5.2 ± 0.5	29.9 ± 3.2	134.1 ± 15.4**	2.9 ± 0.7	3.0 ± 0.6
TE/JMR-132	38.5 ± 3.7	76.9 ± 11.7	3.9 ± 0.4	4.4 ± 0.4	38.1 ± 5.1	225.0 ± 34.5	1.47 ± 0.4	1.8 ± 0.3
TE/MIA-313	40.5 ± 3.5	85.1 ± 9.8	3.7 ± 0.3	4.8 ± 0.5	36.1 ± 5.0	238.3 ± 29.7	1.7 ± 0.3	2.3 ± 0.7
TE/MIA-459	39.0 ± 3.6	79.2 ± 10.4	2.9 ± 0.3	3.9 ± 0.3	37.5 ± 4.6	249.8 ± 28.4	2.3 ± 0.2	4.2 ± 0.3

*†P<0.05, ‡P<0.01 and §P<0.001 as compared to Control; **P<0.01 as compared to TE. The data were evaluated by two-tailed Student's t-test. Table is adapted from Rick et al. Proc Natl Acad Sci USA (2011) 108:3755-60.*

4.3. Effects of combination of antagonist of LHRH with antagonist of GHRH on experimental benign prostatic hyperplasia (Study 3).

4.3.1. Expression of GHRH-R, LHRH-R and their ligands

Protein for GHRH, GHRH-R, and protein of SV1 of GHRH-R were shown in rat prostate (Figure 16A, Table 13). Combinations of GHRH and LHRH antagonists significantly suppressed the expression of GHRH protein by 53% ($P<0.05$). The expression of LHRH-R protein and LHRH protein was also detected. GHRH antagonist JMR-132, LHRH antagonist cetrorelix and the combination significantly lowered the expression of LHRH protein by 25%, 24% and 22%, respectively ($P<0.05$ for all, Figure 16A, Table 13).

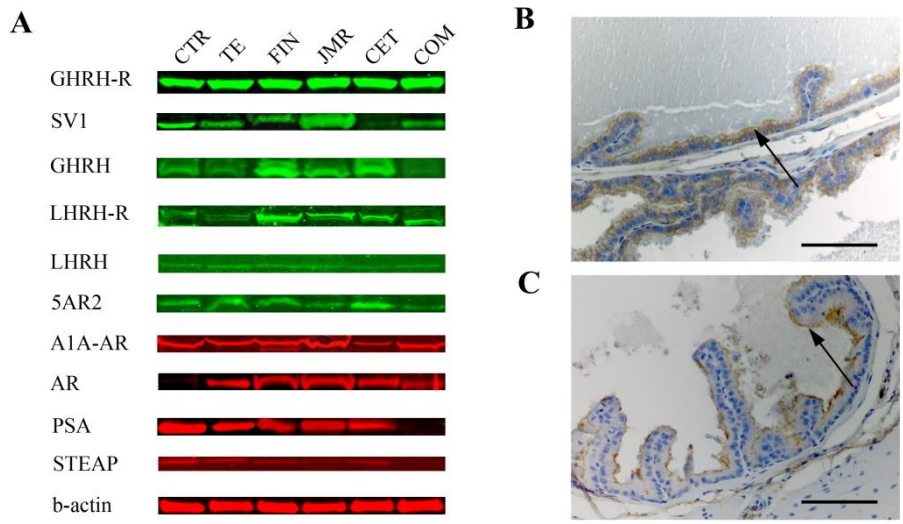

Figure 16. Effect of growth hormone-releasing hormone (GHRH) antagonist JMR-132, LHRH antagonist cetrorelix (0.625 mg/kg) and their combination on the protein expression of GHRH receptor (GHRH-R), its splice variant 1 (SV1), GHRH, luteinizing hormone-releasing hormone receptor (LHRH-R), LHRH, 5α-reductase 2 (5AR2), α1A-adrenoreceptor (α_{1A}-AR), androgen receptor (AR), prostate specific antigen (PSA) and six-transmembrane epithelial antigen of the prostate (STEAP) by Western blot analysis (A). Representative blots of three independent experiments are presented and include internal standard β-actin; corresponding signal intensity values are shown in Table 1. Grouping of representative bands for each experimental group was digitally performed. Expression of GHRH receptors (B) and LHRH receptors (C) in representative ventral prostate of control rats was confined to the cytoplasm and luminal membrane of prostatic acinar cells (Arrows). Localization of GHRH and LHRH receptors are shown in 20X magnification (scale bars: 50μm). CTR, negative control; TE, testosterone enanthate; FIN, finasteride; JMR, JMR-132; CET, cetrorelix; COM, combination of JMR-132 and cetrorelix.

4.3.2. Immunohistochemical confirmation of the expression of GHRH-R and LHRH-R protein.

Immunohistochemical analyses revealed that expression of both GHRH-R (Figure 16B) and LHRH-R (Figure 16C) is limited to the cytoplasm and luminal membrane of rat prostatic acinar cells.

Table 13. The effect of GHRH antagonist JMR-132, LHRH antagonist cetrorelix and their combination on the expression of various prostatic proteins in androgen-induced model of BPH

	Protein expression as % of TE					
	Control	TE	TE/finasteride 0.1 mg/day	TE/JMR-132 40 µg/day	TE/cetrorelix 0.625 mg	TE/JMR-132 and cetrorelix
GHRH-R	54.2 ± 53.2	100.0 ± 34.0	172.9 ± 25.0	152.1 ± 26.6	132.6 ± 41.0	82.6 ± 6.9
SV1	121.2 ± 29.0	100.0 ± 25.1	251.3 ± 9.1	267.0 ± 9.0	99.2 ± 24.6	108.4 ± 10.3
GHRH	85.1 ± 18.7	100.0 ± 14.8	105.7 ± 61.0	86.7 ± 24.7	147.4 ± 21.1	47.3 ± 11.3*
LHRH-R	178.9 ± 28.8	100.0 ± 25.8	123.0 ±31.0	100.2 ± 16.9	83.5 ± 21.8	133.4 ± 32.1
LHRH	74.5 ±35.7	100.0 ±5.3	82.1 ± 17.8	74.9 ± 10.1*	74.0 ± 15.5*	72.7 ± 7.4*
5AR2	84.3 ± 42.1	100.0 ± 9.2	64.3 ± 8.5	34.9 ± 20.2	105.9 ± 34.0	46.6 ± 25.4
A1A-AR	88.9 ± 1.1	100.0 ± 16.8	83.5 ± 14.8	105.1 ± 11.2	12.0 ± 22.2*	86.9 ± 7.5
AR	26.6 ± 19.1	100.0 ± 16.9†	168.9 ± 19.4	248.2 ± 3.3*	57.8 ± 11.9	70.4 ± 11.2
PSA	249.4 ± 2.9	100.0 ± 23.4‡	95.3 ± 26.5	106.0 ± 35.8	66.7 ± 29.7	16.6 ± 15.8*
STEAP	100.9 ± 31.1	100.0 ± 6.0	79.6 ± 28.3	26.5 ± 33.0*	60.5 ± 44.4	3.8 ± 17.9*
IL-1b	87.3 ± 59.8	100.0 ± 5.7	156.7 ± 60.2	61.7 ± 19.3	83.8 ± 17.4	43.2 ± 25.0*
NF-kb/p65	78.1 ± 9.4	100.0 ± 10.1	32.9 ± 10.1**	52.4 ± 21.9*	63.2 ± 10.6*	45.6 ± 8.7**
NF-kb/p50	63.7 ± 23.7	100.0 ± 9.4	432.6 ± 17.5*	203.5 ± 14.0	89.9 ± 36.5	170.2 ± 9.3
pNF-kb/p50	97.6 ± 33.5	100.0 ± 6.2	130.2 ± 2.7*	212.3 ± 15.6*	82.5 ± 79.6	59.6 ± 15.3
COX-2	72.9 ± 11.4	100.0 ± 16.4	30.0 ± 13.0*	21.4 ± 6.6*	69.4 ± 5.0	2.6 ± 12.0**
PCNA	78.0 ± 36.9	100.0 ± 33.0	65.2 ± 23.4	52.5 ±32.3	76.2 ± 24.2	42.2 ± 10.2*

*†P<0.05 and ‡P<0.01 as compared to Control; *P<0.05 and **P<0.01 as compared to TE. The data were evaluated by two-tailed Student's t-test.*

4.3.3. Reduction of prostate size by GHRH antagonist JMR-132, LHRH antagonist cetrorelix and their combination.

Control prostates weighed 248.0±10.7 mg/100 g rat BW; while in TE controls prostates were enlarged by 48.2% to 367.5±15.9 mg/100 g rat BW (P<0.001; Figure 17). GHRH antagonist JMR-132 at 40µg/day, LHRH antagonist cetrorelix at 0.625 mg/kg, and their combination significantly lowered prostate weights by 18.6% (P<0.05), 21.3% (P<0.05) and 30.3% (P<0.01), respectively compared to TE controls (Fig. 2). This reduction of prostate weight was superior to that obtained with finasteride 0.1 mg/kg/day (nonsignificant 13.8 % reduction; Figure 17). In addition, JMR-132, cetrorelix and combinations decreased prostatic DNA content by 18.3% (P<0.05), 14.9% (P<0.05) and 34.5% (P<0.01), respectively (Table 14).

Table 14. Effect of GHRH antagonist JMR-132, LHRH antagonist cetrorelix and their combination on morphological parameters

	Body weight (g)		Prostatic DNA content (ng DNA / mg tissue)	Relative testicle weight (mg / 100g rat BW)
	Day -28	Day 42	Day 42	Day 42
Control	389.5 ± 8.3	548.4 ± 14.8	221.0 ± 10.9	634.9 ± 24.1
TE	393.7 ± 9.5	476.8 ± 12.6†	271.9 ± 7.5	570.2 ± 23.6
TE/finasteride 0.1 mg/kg/day	408.1 ± 9.3	475.2 ± 11.9†	218.2 ± 8.3*	509.7 ± 28.2†
TE/JMR-132 40 µg/day	398.4 ± 8.8	520.3 ± 16.4	222.2 ± 5.1*	538.3 ± 26.3
TE/Cetrorelix 0.625 mg/kg	411.5 ± 10.3	523.7 ± 18.2	231.4 ± 12.5*	521.8 ± 28.9
TE/ Combination	403.2 ± 7.9	537.0 ± 18.5	178.1 ± 7.1**	524.3 ± 21.6

*†P<0.05 as compared to Control; *P<0.05 and **P<0.01 as compared to TE. Statistical analysis was performed by one-way ANOVA, followed by Bonferroni t-test.*

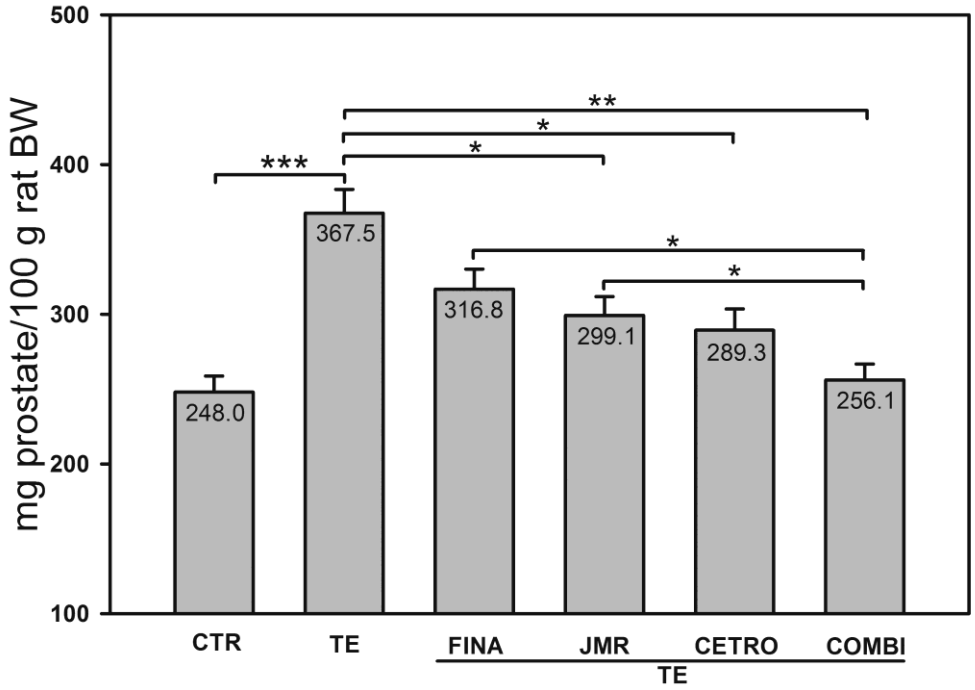

Figure 17. Effect of TE and treatment with GHRH antagonist JMR-132 (40 µg/day), LHRH antagonist cetrorelix (0.625 mg/kg) and combination of JMR-132 and cetrorelix on relative prostate weight, evaluated 42 days after the start of treatments. Statistical analysis was performed by one-way ANOVA, followed by Bonferroni *t*-test. Significant differences are marked by asterisks (*P<0.05, **P<0.01 and ***P<0.001). CTR, negative control; TE, testosterone enanthate; FINA, finasteride; JMR, JMR-132; CETRO, cetrorelix; COMBI, combination of JMR-132 and cetrorelix; ANOVA, analysis of variance.

4.3.4. Effect of GHRH antagonist JMR-132, LHRH antagonist cetrorelix and their combination on 5AR2, α1A-AR, AR, PSA and STEAP.

GHRH antagonist JMR-132 lowered protein levels of 5AR2 (P<0.05, Figure16A). LHRH antagonist cetrorelix caused a decrease in α_{1A}-AR protein levels (P<0.05). Protein levels of prostatic AR were significantly increased in TE-induced BPH (P<0.05); among treatments only JMR-132 alone resulted in a significant increase in AR protein (P<0.01, Fig1A). Prostatic PSA protein was lowered significantly after TE treatment by 62% compared with control (P<0.01), whereas combination of GHRH/LHRH antagonists significantly reduced PSA levels by 83% (P<0.05, Figure 16A). Prostatic STEAP protein expression was significantly decreased by JMR-132 and combination therapy by 74% (P<0.05) and 96%, (P<0.01), respectively (Figure 16A).

4.3.5. Combination of GHRH and LHRH antagonists suppresses IL-1β, NF-κβ and COX-2

The expression prostatic IL-1β protein was significantly decreased by the combination by 57% (P<0.05, Figure 18A). JMR-132, cetrorelix and combination treatment also significantly lowered prostatic NF-κβ/p65 protein levels by 48% (P<0.05), 37% (P<0.05) and 54% (P<0.01), respectively (Figure 18A). Prostatic COX-2 protein was significantly lowered after JMR-132 and combination treatment by 79% (P<0.05) and 97 % (P<0.01), respectively (Figure 18A).

Relative expression of pNF-κβ/p50 markedly decreased after finasteride and combination treatment (RI 0.06 and 0.07, respectively vs. RI of 0.20 in TE, Figure18B).

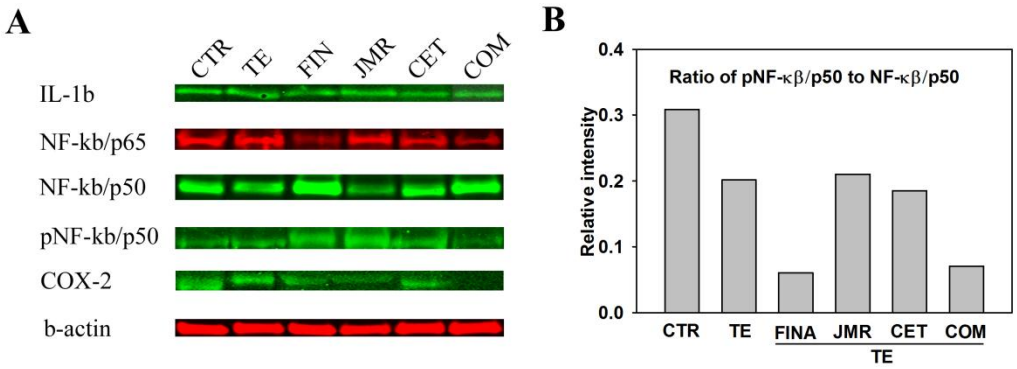

Figure 18. Combination of GHRH antagonist JMR-132 and LHRH antagonist cetrorelix suppresses expression of IL-1β, NF-κβ and COX-2 in rat prostates. Western blot analysis (A) of IL-1β, NF-κβ/p65, NF-κβ/p50, phosphorylated NF-κβ/p50 (p NF-κβ/p50) and COX-2. Representative blots of three independent experiments are presented and include internal standard β-actin; corresponding signal intensity values are shown in Table 1. Grouping of representative bands for each experimental group was digitally performed. Bar graph (B) showing relative expression of phosphorylated NF-κβ/p50. Bars represent average relative intensity values of p NF-κβ/p50. CTR, negative control; TE, testosterone enanthate; FIN, finasteride; JMR, JMR-132; CET, cetrorelix; COM, combination of JMR-132 and cetrorelix.

4.3.6. GHRH antagonists inhibit cell division and induce apoptosis.

Morphologic evaluation on H&E slides revealed that JMR-132, cetrorelix, their combination and finasteride significantly decreased the sizes of average epithelial areas in the ventral prostate by 51.4% (P<0.05), 43.8% (P<0.01), 42.2% (P<0.01), and 48.6% (P<0.05) respectively (Table 15). The number of mitoses was significantly reduced in all groups compared to TE treated BPH controls. Apoptotic cell numbers were higher in the groups treated with JMR-132, cetrorelix and their combination and finasteride, but the differences from TE treated controls were not statistically significant. Representative apoptotic cell is displayed in Figure 19F.

Table 15. Effect of JMR-132, cetrorelix and their combination on cell proliferation and apoptosis in rat prostatic epithelium

Group	Mean epithelial area in view fields (%)	Number of mitoses in one theoretical field composed entirely of epithelial cells	Number of apoptotic cells in one theoretical field composed entirely of epithelial cells
Control	21.8 ± 1.7	1.35 ± 0.35	0.89 ± 0.39
TE	31.3 ± 0.6†	1.76 ± 0.13	0.95 ± 0.31
TE/finasteride 0.1mg/kg/day	16.1 ± 2.5*	0.48. ± 0.1*	1.68 ± 0.62
TE/JMR-132 40µg/day	15.2 ± 2.4*	0.29 ± 0.29*	2.14 ± 0.99
TE/Cetrorelix 0.625 mg/kg	17.6 ± 2.3**	0.26 ± 0.15**	2.00 ± 0.58
TE/Combination	18.1 ± 1.8**	0.85 ± 0.18*	2.83 ± 0.86

*†P<0.05 as compared to Control; *P<0.05 and **P<0.01 as compared to TE. The data were evaluated by one-way ANOVA followed by Student-Newman-Keuls test.*

No significant changes in prostatic PCNA protein levels occurred after TE treatment. The combination of GHRH and LHRH antagonists reduced PCNA protein by 58% (P<0.05, Figure 19G). We observed transcriptional downregulation of Bcl-2 after treatment with JMR-132, cetrorelix, and

combination (P<0.05, P<0.05, and P<0.01, respectively, Figure 19 C-E). Bax mRNA expression was elevated after treatment with finasteride and combination (P<0.05 for all, Figure 19B,E). Transcriptional suppression of p53 was found after treatment with finasteride, JMR-132, cetrorelix and combination (P<0.05 for all, Figure 19B-E).

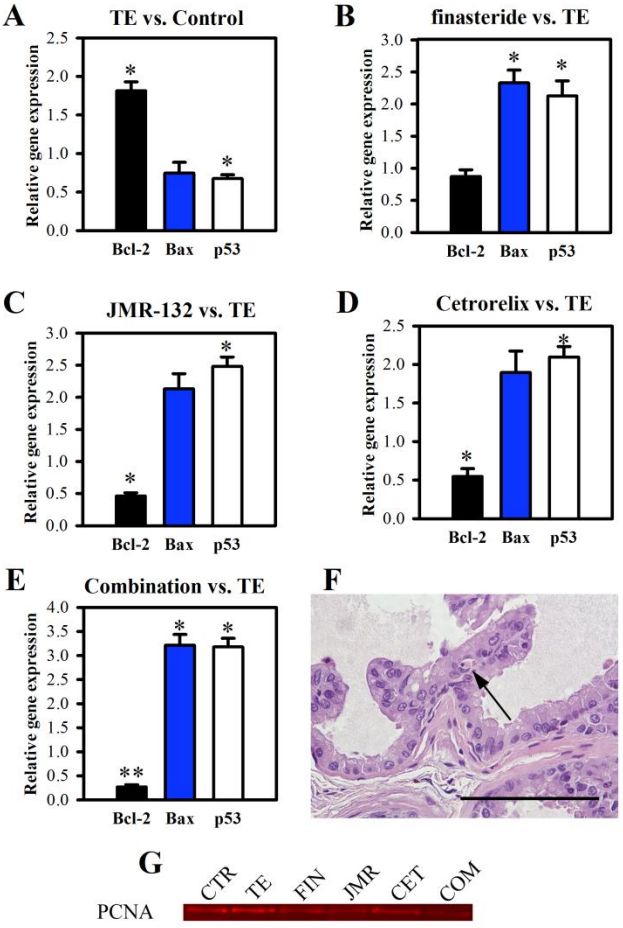

Figure 19. Combination of GHRH antagonist JMR-132 and LHRH antagonist cetrorelix induces apoptosis and inhibit proliferation of prostatic epithelial cells in rats. Bar graphs (A-E) showing real-time RT-PCR analysis of Bcl-2, Bax and p53. Bars represent relative expression of individual genes between prostate samples (n=3) from TE and control groups (A) or between finasteride (B), JMR-132 (C), cetrorelix (D) or combination (E) and TE groups. Values > 1.00 mark upregulation of individual genes, while values < 1.00 mark downregulation. Asterisks indicate a significant difference (*P < 0.05 and **P<0.01 by Student's *t*-test). Representative apoptotic cell (Arrow) among prostatic acinar epithelial cells of rat prostate treated with combination treatment is shown (F) in H&E stained slide (40X; scale bar: 50µm). Western blot analysis (G) of PCNA. Representative blots of three independent experiments are presented; corresponding signal intensity values are shown in Table 1. Grouping of representative bands for each experimental group was digitally performed. CTR, negative control; TE, testosterone enanthate; FIN, finasteride; JMR, JMR-132; CET, cetrorelix; COM, combination of JMR-132 and cetrorelix.

4.3.7. Effect of JMR-132, cetrorelix and their combination on serum GH, LH, IGF-1, DHT and PSA.

TE increased serum GH by 65% compared to control (P<0.05); while JMR-132, cetrorelix and their combination caused no significant changes in GH levels as compared to TE (Table 16). No significant changes in serum IGF-1 levels were observed. In TE-induced BPH rats there was an approximately 8-fold increase in serum DHT compared to control at day 42 (242.7±41.3 pg/ml [P<0.001]), however, no significant differences in serum DHT levels were observed after treatment of JMR-132, cetrorelix and their combination. A significant 57%reduction in DHT was observed after treatment with finasteride 0.07 mg/day(P<0.05). Combination treatment decreased serum PSA levels by 41% (P<0.05). Values for serum markers: see Table 16.

Table 16. Effect of treatment with JMR-132, cetrorelix and their combination on serum levels of GH, LH, IGF-1, DHT and PSA in rats

	GH (ng/ml)		LH (ng/ml)		IGF-1 (ng/ml)		DHT (pg/ml)		PSA (ng/ml)	
	Day -28	Day 42	Day -28	Day 42	Day -28	Day 42	Day -28	Day 42	Day -28	Day 42
Control	28.5±4.7	34.5±4.8	0.32±0.02	0.34±0.03	3.1±0.3	2.9±0.4	32.2±3.8	29.9±3.2	0.39±0.03	0.54±0.07
TE	33.7±3.8	57.1±8.3†	0.34±0.02	0.21±0.02	2.8±0.4	4.3±0.7	34.4±4.2	242.7±41.3§	0.51±0.08	0.49±0.11
TE/finasteride 0.1 mg/kg/day	30.5±4.1	50.1±6.7	0.34±0.03	0.23±0.02	3.2±0.2	4.0±0.6	29.5±3.1	103.2±13.8*	0.46±0.04	0.53±0.05
TE/JMR-132 40µg/day	35.1±6.6	45.4±7.1	0.31±0.01	0.27±0.04	3.0±0.4	3.6±0.4	36.1±2.9	179.4±21.4	0.63±0.15	0.47±0.12
TE/Cetrorelix 0.625 mg/kg	31.3±4.8	54.7±5.2	0.36±0.04	0.17±0.02	3.3±0.4	4.1±0.3	39.1±4.8	161.9±22.3	0.55±0.09	0.35±0.06
TE/Combination	36.8±5.3	52.7±6.9	0.33±0.02	0.21±0.03	2.7±0.2	3.8±0.3	33.4±3.7	158.5±24.7	0.48±0.06	0.29±0.04*

*$^{\dagger}P<0.05$ and $^{\S}P<0.001$ as compared to Control; *$P<0.05$ as compared to TE. The data were evaluated by two-tailed Student's t-test.*

4.4 Dose-dependent growth inhibition in vivo of PC-3 prostate cancer with a reduction in tumoral growth factors after therapy with GHRH antagonist MZ-J-7-138 (Study 4)

4.4.1. Effect of GHRH antagonist MZ-J-7-138 on the growth of PC-3 human androgen independent prostate cancer in nude mice

As shown in Figure 20 and Table 17, MZ-J-7-138 at the dose of 1.25 μg/day did not produce any inhibition of tumor growth compared to the control group. The lowest dose which caused a significant growth suppression of 52% by the end of the fourth week was 2.5 μg/day. MZ-J-7-138 at the dose of 5 μg/day led to a significant decrease in tumor growth of 65%. The highest dose of MZ-J-7-138, 10 μg/day significantly suppressed PC-3 tumor growth exerting a final tumor inhibition of 78%. Already after the first week, the groups receiving 5 and 10 μg/day MZ-J-7-138, showed a better growth inhibition than the 1.25 μg/day group. After the fourth week significant differences were observed between the treatment groups of 10 μg/day versus 2.5 mg/day and 1.25 μg/day. The tumor doubling time increased from 6.2 days in control group to 12.4 days by the treatment with 10 μg/day. No significant differences were found in the body and organ weights of animals receiving various treatments versus controls, indicating the lack of toxicity of GHRH antagonist.

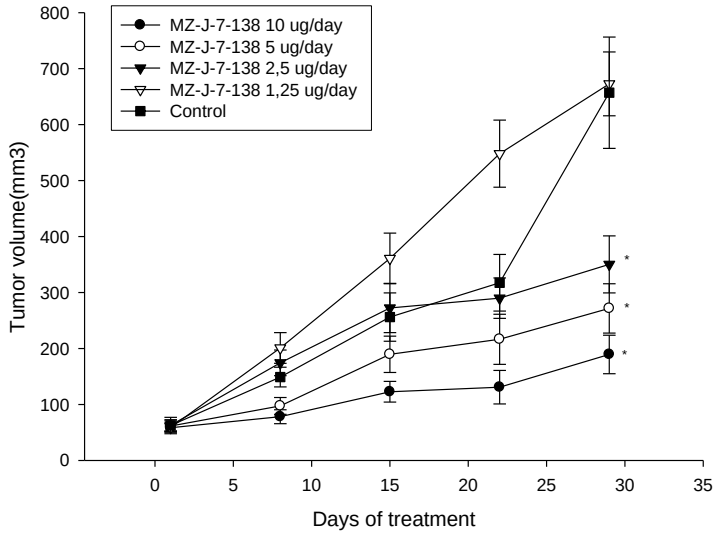

Figure 20. Growth of PC-3 tumors, treated with different doses of the GHRH antagonist MZ-J-7-138. Significant differences from the control are marked by asterisks (P<0.001). Schematic figure is adapted from Heinrich et al. Prostate (2008) 68:1763-72.

Table 17. Effect of GHRH antagonist MZ-J-7-138 on the Growth of Human PC-3 Androgen Independent Prostate Cancers in Nude Mice.

	Tumor volume (mm^3)		Tumor volume doubling time (days)	Tumor weight (mg)
Treatment	Initial	Final (%inhibition)		
Control	62.44±14.63	657.02±99.39	6.18	762.22±271.71
MZ-J-7-138 (1.25 µg/day)	58.78±7.74	672.84±57.07 (0.35%)	6.05	737.50±298.89
MZ-J-7-138 (2.5 µg/day)	62.85±10.07	350.25±26.60 (52%)*†	8.47	710.00±204.95
MZ-J-7-138 (5 µg/day)	61.46±9.42	271,67±44.07 (65%)*†	9.79	592.50±70.59 *
MZ-J-7-138 (10 µg/day)	58.47±7.96	189.37±34.33 (78%)*†	12.39	385.71±53.14 *

**p=<0.001 vs controls; †p=<0.05 vs lower dose step.*

4.4.2. Effect of GHRH antagonist MZ-J-7-138 on the expression of IGF-II and VEGF

The treatment with GHRH antagonist MZ-J-7-138 decreased the expression of tumoral proteins of VEGF and IGF-II (Figs. 21 and 22). Administration of 10 mg/day induced a significant reduction to 47.3% for IGF-II and to 55% for VEGF versus the control groups ($P<0.05$ in both cases). Lower doses of the antagonist caused a smaller reduction in both proteins (Figs. 21 and 22). VEGF protein levels were reduced to 75% of the control group by 5 µg/day ($P<0.05$), to 80% by 2.5 µg/day (NS) and to 82% by 1.25 µg/day (NS). Treatment with 1.25, 2.5, and 5 mg/day of MZ-J-7-138 reduced tumoral IGF-II protein to 66.8%, 64%, and 57.2% respectively of the control group (NS). Significant differences between the different doses (10 µg/day vs. 2.5 µg/day and 1.25 µg/day) were seen in the VEGF expression.

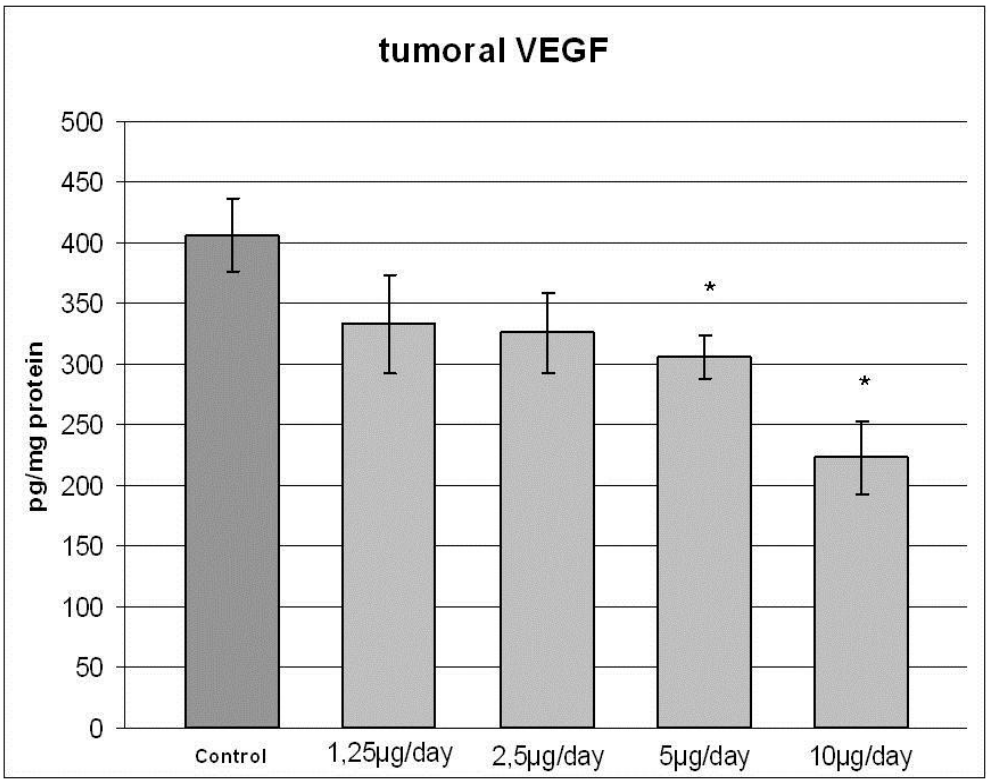

Figure 21. Effect of GHRH antagonist MZ-J-7-138 at different doses on the protein levels of tumoral VEGF after 4 weeks of daily treatment. Significant differences from the control are marked by asterisks ($p<0.05$). Schematic figure is adapted from Heinrich et al. Prostate (2008) 68:1763-72.

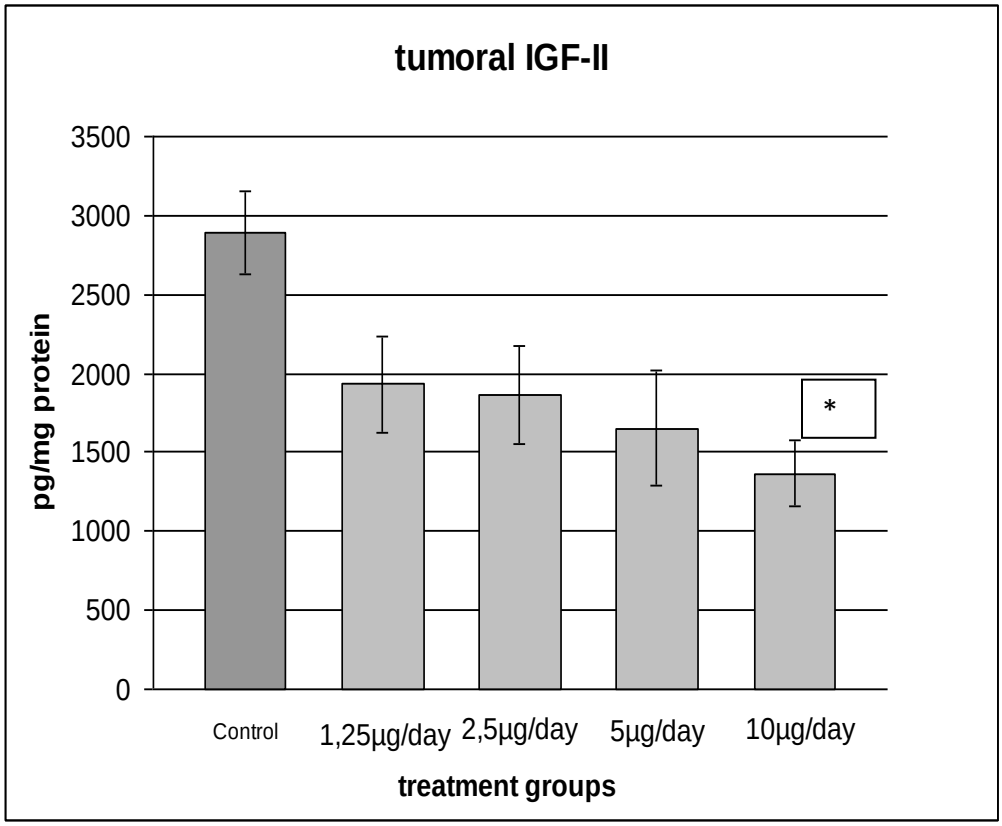

Figure 22. Effect of GHRH antagonist MZ-J-7-138 at different doses on the protein levels of tumoral IGF-II after 4 weeks of daily treatment. Significant differences from the control are marked by asterisks ($p<0.05$). Schematic figure is adapted from Heinrich et al. Prostate (2008) 68:1763-72.

4.4.3. Effect of GHRH antagonist MZ-J-7-138 on the mRNA expression for pGHRH-R, SV1 and GHRH

The presence of mRNA for the SV1 of the GHRH receptor and GHRH ligand in PC-3 tumors was reported previously (136). In this study, using real-time PCR we demonstrated the presence of mRNA for pituitary type of GHRH receptor pGHRH-R. The reaction efficiencies for the probes of pGHRH-R, GHRH, and beta-actin were 103.7%, 101.3% and 97.4% respectively. The relative expression of pGHRH-R in PC-3 tumors treated with MZ-J-7-138 was significantly elevated, being 2.75-fold higher than the control group. Moreover, real-time PCR also revealed a non-significant downregulation of SV1 receptor and significant downregulation of GHRH after treatment withGHRH antagonist, the ratios being 0.63 and 0.25, respectively. The results are shown in Table 18.

Table 18. Real-time PCR values of the relative expression of mRNA for pGHRH-R, SV1, and GHRH in PC-3 tumors after treatment with GHRH antagonist MZ-J-7-138

	Control	MZ-J-7-138	
	C_T values, mean ± SEM	C_T values, mean ± SEM	Ratio
pGHRH-R	38.18±0.37	36.86±0.25	2.75*
SV1	33.87±0.46	34.66±0.42	0.63
GHRH	36.94±0.30	39.09±0.71	0.25*
β-actin	19.74±0.09	19.88±0.03	-

*The ratio represents the gene expression level in the treatment group as compared to the control group. *P<0.05 vs. controls. Table is adapted from Heinrich et al. Prostate (2008) 68:1763-72.*

4.4.4. Binding assays for GHRH receptors in PC-3 tumors

The presence of GHRH receptors was assessed by radioligand binding assays in control tumors. Binding studies demonstrated the presence of a single class of specific, high affinity (dissociation constant, K_d = 0.63 ± 0.08 nM) binding sites for GHRH antagonist JV-1-42 in the membrane preparation of PC-3 tumors with a mean maximal binding capacity (B_{max}) of 178.5 ± 24.7 fmol/mg membrane protein. In competition displacement experiments on subcutaneously grown PC-3 tumors from the control group, GHRH antagonist MZ-J-7-138 was able to displace the [^{125}I]JV-1-42 radioligand with an IC_{50} = 0.32 nM. This IC_{50} value indicates a high affinity binding of MZ-J-7-138 to GHRH receptors expressed on PC-3 tumors.

4.5. Inhibitory effects of antagonists of growth hormone releasing hormone on experimental prostate cancers are associated with upregulation of wild-type p53 and decrease in p21 and mutant p53 proteins (Study 5)

4.5.1. Experiment 1: Effect of GHRH antagonist MZ-J-7-138 on the growth of PC-3 human androgen independent prostate cancers in nude mice

As shown in Table 19 and Figure 23, treatment with MZ-J-7-138 significantly inhibited PC-3 tumor growth after four weeks of treatment. The final tumor inhibition was 77%, as compared to controls ($p<0.01$). This antiproliferative effect is also reflected by final tumor weights (Table 19 indicating a 66% inhibition). The tumor volume doubling time was similarly significantly ($p<0.01$) extended by MZ-J-7-138 compared to controls. No significant differences were observed in the body and organ weights of treated animals versus controls (not shown), indicating that the GHRH antagonist was not toxic.

Table 19. The effect of GHRH antagonist MZ-J-7-138 on growth of PC-3 and DU-145 androgen independent prostate cancers xenografted subcutaneously into nude mice

Treatment	Tumor volume (mm^3)		Tumor volume doubling time (days)	Tumor weight (mg) (% inhibition)
	Initial	final (% inhibition)		
Experiment 1: (PC-3)				
Control	56.31±10.76	1136.50±351.06	7.3±0.5	1450.9±342.5
MZ-J-7-138 (5µg/day)	56.21±13.34	300.82±65.22** (77%)	11.0±0.9**	489.5±114.1**(66%)
Experiment 2: (DU-145)				
Control	32.78±9.08	604.28±145.34	10.6±0.5	727.4±182.2
MZ-J-7-138 (5µg/day)	23.55±4.07	218.58±48.10** (66%)	25.2±4,0	279.4±69.1** (62%)

***p<0.01 vs. Control.*

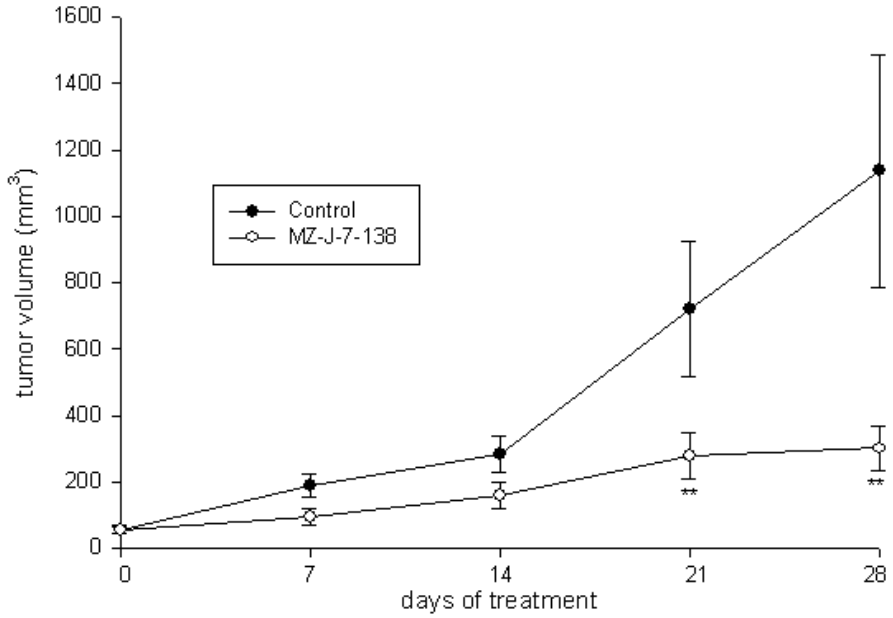

Figure 23. Effect of GHRH antagonist MZ-J-7-138 (5µg/day) on growth of subcutaneous PC-3 human androgen independent prostate cancer xenografted into nude mice. Treatment was started when tumors had grown to about 56mm^3 and lasted for 28 days. Bars ± SE. **p<0.01 vs. controls.

4.5.2. Experiment 2: Effects of GHRH antagonist MZ-J-7-138 on the growth of DU-145 human androgen independent prostate cancers in nude mice

MZ-J-7-138 significantly suppressed the proliferation of s.c. implanted DU-145 xenografts after 6 weeks of treatment and led to a 66% inhibition of tumor volume (Table 19, Figure 24). This tumor inhibition is also reflected by tumor weights, which were lower by 62% ($p<0.01$) in animals treated with GHRH antagonist MZ-J-7-138 compared to controls. Tumor volume doubling time was extended from 10.6 to 25.2 days, but that did not reach statistical significance. No significant differences were observed in the body and organ weights of animals receiving treatment versus controls, indicating that the GHRH antagonist was not toxic.

4.5.3. Experiment 3: Effects of GHRH antagonist MZ-J-7-138 and LHRH antagonist Cetrorelix on the growth of MDA-PCa-2b human androgen sensitive prostate cancer in nude mice

An even greater inhibition of tumor growth than in PC-3 and DU-145 tumors was observed in mice bearing MDA-PCa-2b cancers that received a combination therapy of MZ-J-7-138 and Cetrorelix. The inhibition of tumor volume became significant after the first week of treatment ($p<0.05$) (not shown) and remained significant until the end of the experiment on day 21. At this point in time, significant tumor inhibition was found in all treated groups and combined therapy with MZ-J-

7-138 and Cetrorelix caused the greatest inhibition ($p<0.001$) (Figure 25). Final tumor weights of all treated groups, were also significantly smaller as compared to controls, the combination of MZ-J-7-138 and Cetrorelix causing the greatest inhibition (not shown). Tumor volume doubling time (TDT) was also significantly extended in animals treated with Cetrorelix alone ($p<0.05$) and with combination of GHRH antagonist and Cetrorelix ($p<0.01$) as compared to controls (not shown).

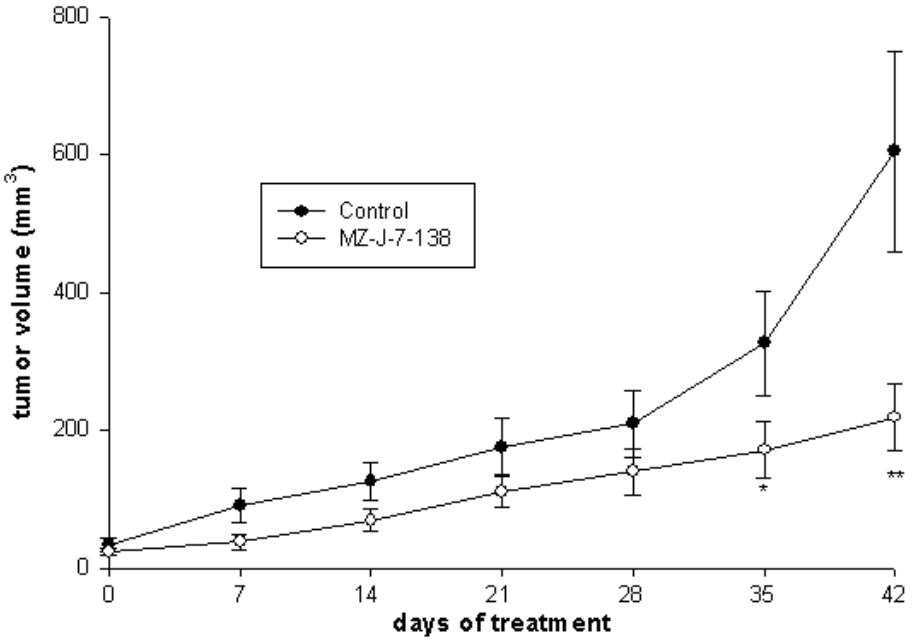

Figure 24: Effect of GHRH antagonist MZ-J-7-138 (5µg/day) on growth of subcutaneous DU-145 human androgen independent prostate cancer xenografted into nude mice. Treatment was started when tumors had grown about 28mm^3 and lasted for 42 days. Bars ± SE. *p<0.05 vs controls, **p<0.01 vs. controls.

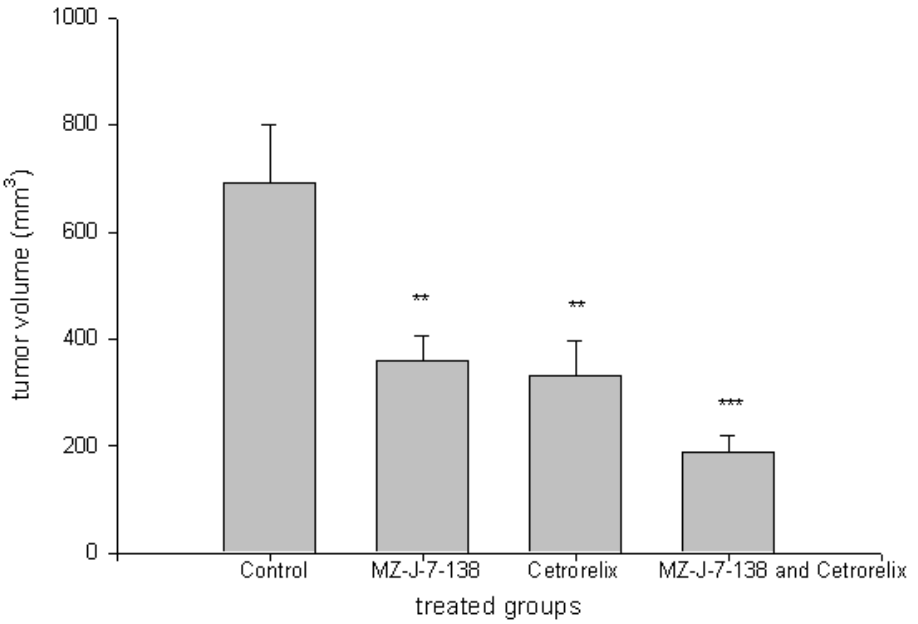

Figure 25: Effect of GHRH antagonist MZ-J-7-138 (5μg/day) s.c , Cetrorelix (100μg/day) and the combination of MZ-J-7-138 (5μg/day) and Cetrorelix (100μg/day) on the growth of subcutaneous MDA-Pca-2b human androgen sensitive prostate cancers in nude mice. Treatment was started when tumors had grown about 76mm^3 and lasted for 21 days. Bars ± SE. **p<0.01 vs. controls. ***p<0.001 vs controls.

Weights of prostates, seminal vesicles and testicles of animals that received Cetrorelix were significantly lower compared to contols, indicating the androgen deprivation effect of Cetrorelix. No significant differences were observed in the body weights or other organ weights of animals receiving various treatments compared to controls, indicating that none of our compounds was toxic.

4.5.4. GHRH Receptor-binding studies

The presence of GHRH receptors was assessed by radioligand binding assays in control tumors. Binding studies demonstrated the presence of a single class of specific, high-affinity binding sites for GHRH antagonist JV-1-42 in all 3 human prostate cancer models investigated. The binding data are shown in Table 20.

Table 20. Binding characteristics of GHRH receptors on membranes of experimental human prostate cancers

Tumor	K_d(nM)	B_{max}(fmol/mg membrane protein)
PC-3	1.25±0.18	305.4±14.6
DU-145	3.52±0.05	420.0±30.0
MDA-PCa-2b	6.08±0.14	498.9±6.61

The data are means ± SE. Two-three binding experiments were performed in duplicate or triplicate. K_d, Dissociation constant; B_{max}, maximal binding capacity

4.5.5. Effects of GHRH antagonist MZ-J-7-138 and LHRH antagonist Cetrorelix on the expression of p53 tumor suppressor protein

To further investigate the signaling mechanisms involved in the antitumor action of GHRH antagonist MZ-J-7-138, we investigated the expression of p53 protein by Western blotting assays. PC-3, DU-145 and MDA-PCa-2b tumor tissue samples presented a band of 53 kDA corresponding to p53 protein (Figure 26, 27 and 28). Mutant p53 in PC-3 and DU-145 was significantly decreased by treatment with GHRH antagonist to 17.9±6.0% and 31.6±10.7% respectively (Table III, Figure 4 and 5). Wild type p53 in MDA-PCa-2b tumors was significantly up regulated by treatment with Cetrorelix ($p<0.01$) and a non significant increase of wt-p53 was observed in MDA-PCa-2b tumors after treatment with MZ-J-7-138 and the combination of MZ-J-7-138 and Cetrorelix (Table 21, Figure 28).

4.5.6. Effects of GHRH antagonist MZ-J-7-138 and LHRH antagonist Cetrorelix on p21 protein expression

Treatment of PC-3 and DU-145 prostate cancers with GHRH antagonist MZ-J-7-138 significantly inhibited the expression of p21 protein levels (Table III, Figure 4 and 5). In

MDA-PCa-2b tumors treated with the same GHRH antagonist or Cetrorelix, the decrease in p21 protein expression did not reach statistical significance as compared to controls due to the high standard error (Table 21, Figure 28b).

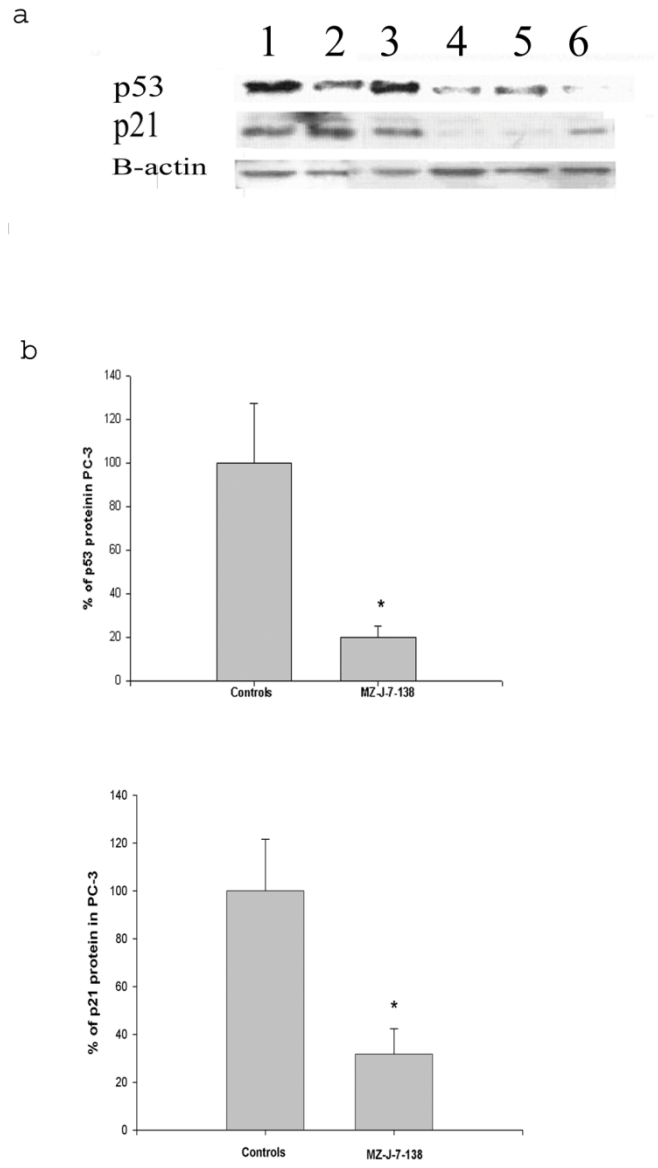

Figure 26. Effect of GHRH antagonist MZ-J-7-138 (5μg/day) s.c on the expression of mutant p53 and p21 protein expression in PC-3 tumors grown in nude mice. a) Western blot representative samples are shown lane 1-3, controls; lane 4-6, samples treated with MZ-J-7-138; b) bar chart for p53 mutant protein and p21 protein expression: Bars ± SE. *p<0.05 vs controls, ***p<0.001 vs. controls.

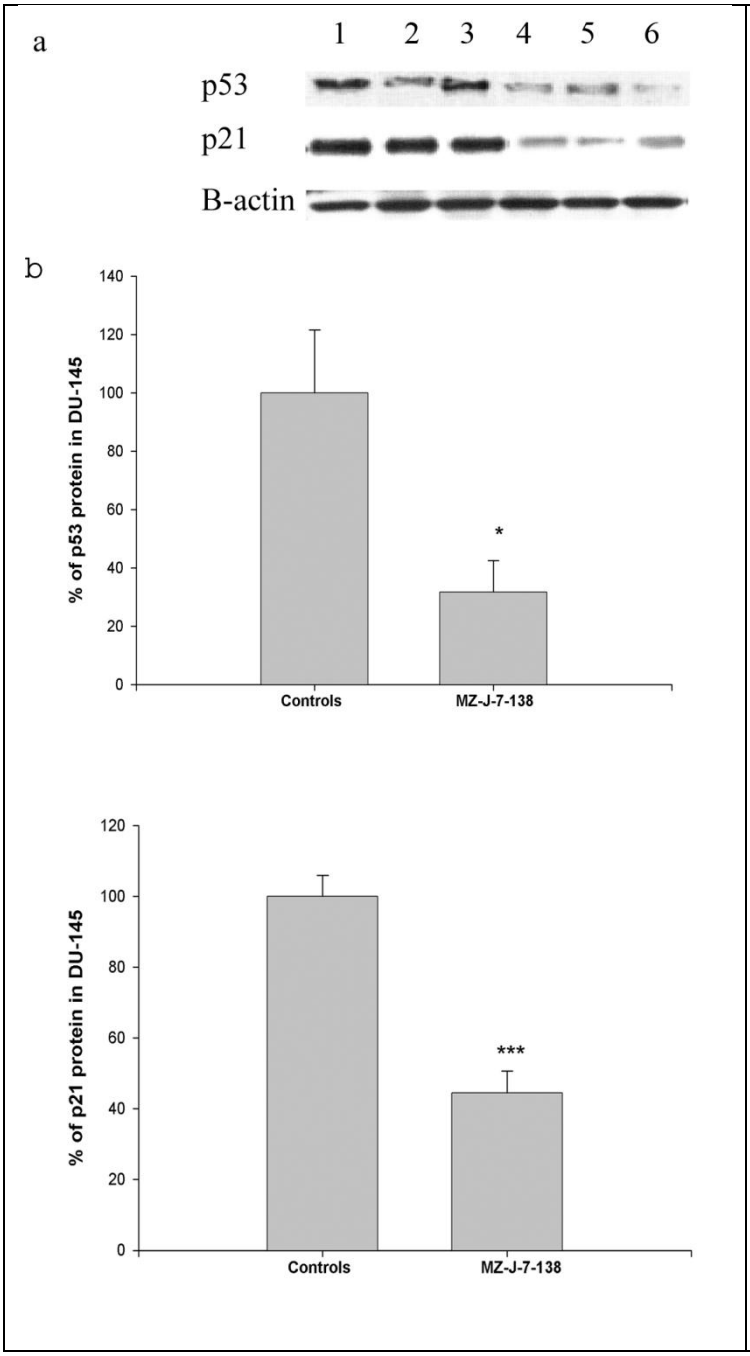

Figure 27. Effect of GHRH antagonist MZ-J-7-138 (5μg/day) s.c on the expression of mutant p53 and p21 protein in DU-145 tumors. a) Western blot: lane 1-3, controls; lane 4-6, samples treated with MZ-J-7-138, ; b) bar chart for p53 mutant protein and p21 protein expression. Bars ± SE. **p<0.01 vs. controls, ***p<0.001 vs controls.

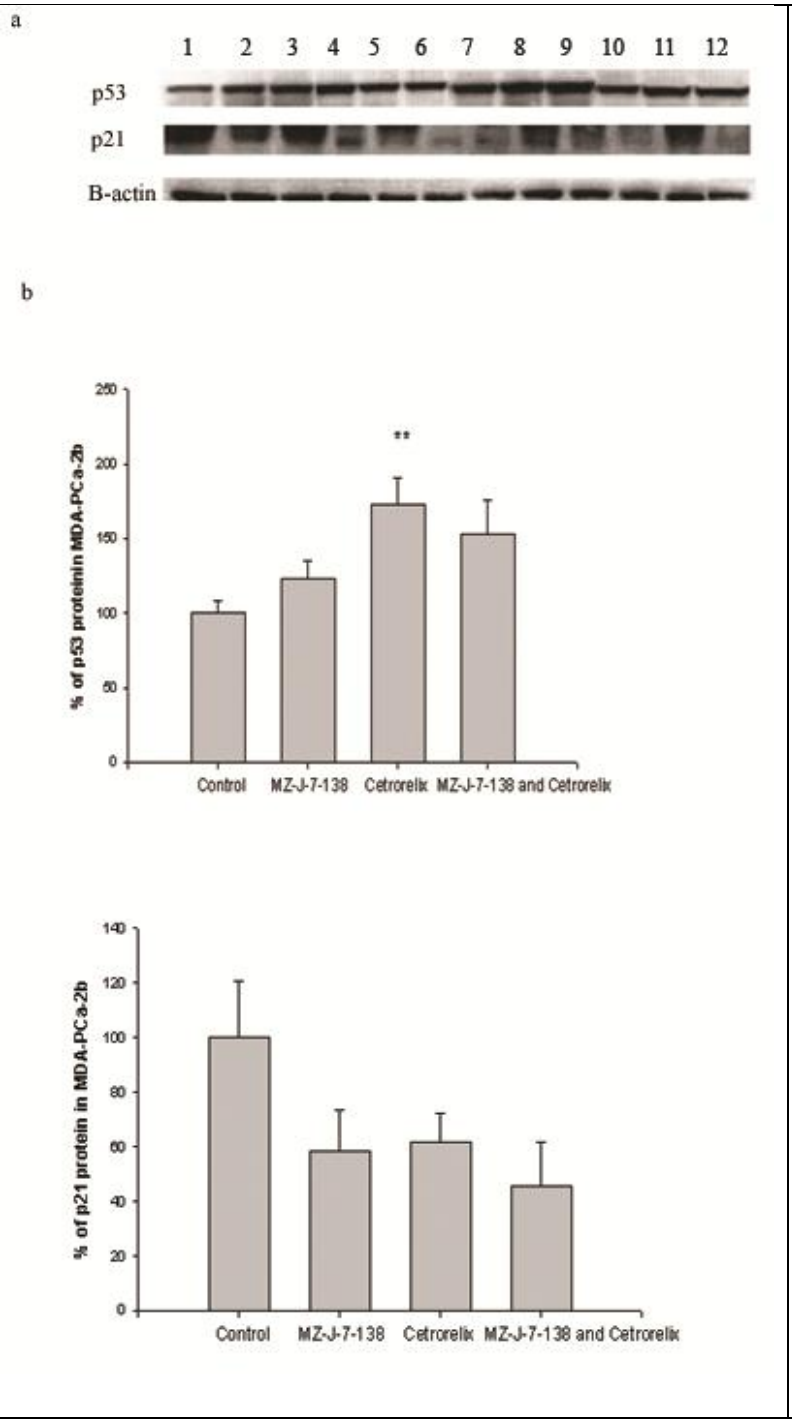

Figure 28. Effect of GHRH antagonist MZ-J-7-138 (5μg/day) s.c , Cetrorelix (100μg/day) and the combination of MZ-J-7-138 (5μg/day) and Cetrorelix (100μg/day) on the protein expression of wt p53 and p21 in MDA-PCa-2b human androgen independent prostate cancer grown in nude mice.

a) Western blot: lanes 1-3 controls, lane 4-6 samples treated with Cetrorelix, lanes 7-9 samples treated with MZ-J-7-138, lane 10-12 samples treated with a combination of Cetrorelix and MZ-J-7-138. *p<0.05, **p<0.01. b) Bar chart for p53 mutant protein and p21 protein expression: Bars ± SE. **p<0.01 vs. controls.

Table 21. The effect of GHRH antagonist MZ-J-7-138, Cetrorelix and their combination on the protein expression of p53 and p21 in PC-3, DU-145 androgen independent and MDA-PCa-2b androgen sensitive prostate cancers xenografted into nude mice

	PC-3 protein expression in % of controls	**DU-145** protein expression in % of controls	**MDA-PCa-2b** protein expression in % of controls
p53			
Control:	100.0±27.1	100.0±21.6	100.0±8.6
MZ-J-7-138:	(mt) 17.9±6.0*	(mt) 31.6±10.7*	(wt) 123.0±11.8
Cetrorelix:	n.i.	n.i.	(wt) 172.9±17.8**
	n.i.	n.i.	(wt) 152.9±23.3
MZ-J-7-138 and Cetrorelix			
p21			
Control:	100.0±16.0	100.0±5.9	100.0±20.6
MZ-J-7-138:	37.9±17.3*	44.4±6,2***	61.9±10.3
Cetrorelix:	n.i.	n.i.	58.2±15.2
MZ-J-7-138 and Cetrorelix	n.i.	n.i.	45.8±15.7

**P<0.05, **P<0.01 and ***P<0.001 vs controls; n.i.-not investigated*

5. Discussion

5.1. Effects of LHRH antagonist cetrorelix on experimental benign prostatic hyperplasia (Study 1)

Clinical data have demonstrated that therapy with LHRH antagonist Cetrorelix resulted in long-lasting improvement in LUTS (55,56,58). This improvement, including reduction in prostate volume and increase in urinary peak flow rate, appears to be superior to that produced by α-blockers or 5α-reductase inhibitors(57). Low doses of Cetrorelix used in recent clinical trials cause only a partial suppression of pituitary-gonadal axis and testosterone levels.

In the present study, we have shown that Cetrorelix significantly reduced prostate weights by 18% in non-castrating doses of 0.625 mg/kg (59). Histological observations in our rat model of BPH revealed marked hyperplastic morphological changes in the prostates of testosterone-treated BPH animals, while treatment with a low dose of Cetrorelix (0.625 mg/kg) caused an involution of these hyperplastic changes resulting in a morphology similar to that of normal animals. Although inflammation is not a main characteristic of the BPH model used in this study, we also observed incidental inflammatory infiltrates in all experimental groups.

The presence of LHRH and LHRH-R in rat prostate was demonstrated by real-time PCR and Western blot. Furthermore, ligand competition assay detected specific high affinity receptors for LHRH in rat prostate. Cetrorelix 0.625 mg/kg significantly lowered prostatic AR and 5α-reductase 2 levels, however, serum DHT and LH were only slightly decreased. Changes in serum PSA were not significant after treatment with Cetrorelix at 0.625 mg/kg. Moreover, the expression of LHRH and LHRH-R and direct antiproliferative effects of LHRH and its analogs have been demonstrated in many malignant human tumors (61,62,137). Recently we showed that Cetrorelix inhibits the proliferation of human prostate epithelial BPH-1 cell line *in vitro* (66). These findings suggest that low doses of Cetrorelix did not impair gonadal function in rats as was also shown by experimental (59) and clinical findings (55-58). Prostate shrinkage is a result of direct inhibitory effects of Cetrorelix exerted through prostatic LHRH receptors, implies the presence of an LHRH-based autocrine regulatory system.

Herein, we used real-time PCR arrays to investigate the beneficial molecular mechanisms of Cetrorelix in a BPH-model. The analyses showed several proinflammatory pathways and growth factors were upregulated in control animals with induced BPH and markedly downregulated in Cetrorelix-treated animals. Verifying PCR array results and more precisely determining changes in gene expression, we studied the expression of selected proinflammatory and growth factor encoding genes by real-time RT-PCR. Of the 11 genes analyzed, nine (IGF-1, EGF, TGF-β1 and-β2, FGF-2, FGF-7, VEGF-A, IL-1β and IL-6) showed the same change pattern as in the PCR arrays, i.e.

upregulation after TE treatment and downregulation after Cetrorelix. These insulin-like, transforming and fibroblast growth factors and downstream effector molecules as well as a variety of interleukins, can lead to abnormal stromal and epithelial prostate cell growth (21,37,40).

Our observation of the transcriptional activation of inflammatory chemokine ligands (e.g., C5, CCL25 and CXCL2) and interleukins (e.g., IL-3, IL-5, IL-6, IL-13, IL-15 and IL-17) in the prostate of rats with induced BPH is consistent with clinical findings (138) and with experimental findings in rats (139). Chemokines promote neutrophil recruitment and T-lymphocyte infiltration and the subsequent progression of the inflammation associated with BPH. We found that Cetrorelix significantly lowered transcriptional expression of several chemokines including C5 and CCL25.

Low doses of Cetrorelix caused a marked reduction in cytokine mRNA levels for IFN-γ, IL-1α, IL-3, IL-4, IL-5, IL-6, IL-13, IL-15 and IL-17. These cytokines are part of an inflammatory network in BPH including several growth factors (20,38,140). IFN-γ,produced by infiltrating T-cells, is a natural antagonist of growth inhibiting TGF-β; FGF-2 stimulates growth (37). IFN-γ also stimulates IL-15, thereby augmenting increased influx of T-lymphocytes (41). These T-cells further produce lymphokines such as IL-4 and IL-13, facilitating formation of active androgens and estrogens by inducing 3β-hydroxydehydrogenase/isomerase. T-cell derived IL-17 fine tunes immune response, stimulating IL-6, IL-8 and IL-1α and β (38,40-42).

In summary, our wide-range analysis of gene expression in the prostate of rats with testosterone-induced BPH revealed the transcriptional activation of several genes including those for proinflammatory interleukins, chemokines and prostatic growth factors. The expression of these genes was suppressed in Cetrorelix-treated animals. These findings suggest that Cetrorelix exerts its beneficial effects on BPH by suppressing proinflammatory cytokines and growth factors at the transcriptional level.

The results of this study indicate that the reduction in prostate volume could be due to direct inhibitory effects of Cetrorelix exerted through prostatic LHRH receptors as well as transcriptional suppression of proinflammatory cytokines and growth factors. These findings shed light on the mechanism of action of LHRH antagonists in BPH and also suggest a role for LHRH as a locally acting growth factor in BPH. It is possible that LHRH antagonists could be clinically used for therapy of BPH in combination with other agents.

5.2. Effects of GHRH antagonists on experimental benign prostatic hyperplasia (Study 2)

The main finding of our study is that GHRH antagonists JMR-132, MIA-313 and MIA-459 reduce prostate size in an experimental model of BPH. In addition to prostate shrinkage in rats,

multiple factors related to growth and inflammation, which are crucial in the pathogenesis and progression of BPH (21), were markedly reduced by treatment with GHRH antagonists. The expression of GHRH, GHRH-R and its splice variant SV1 in rat prostate was demonstrated by Western blot. The antibody used to detect GHRH receptors identifies both pituitary type GHRH-R and its splice variant SV1 (141). Furthermore, ligand competition assay detected specific high affinity receptors for GHRH in rat prostate and immunohistochemical analyses revealed that this expression of GHRH-R is confined to luminal epithelial cells of the rat prostate. Changes in serum GH, IGF-1, DHT, and PSA were not significant after treatment with GHRH antagonists. Recently we showed that GHRH antagonists inhibit the proliferation of human prostate epithelial BPH-1 cell line *in vitro* (76).These findings strongly suggest that prostate shrinkage is a result of direct inhibitory effects of GHRH antagonists exerted through prostatic GHRH receptors, not involving the GH/IGF-1 axis. The demonstration of the co-expression of GHRH and its receptors in rat prostate supports the hypothesis that GHRH produced locally in the prostate could act in an autocrine/paracrine manner through an interaction with the GHRH receptors (72). The presence of this pathway, which is disrupted by GHRH antagonists, provides a mechanistic explanation for the antiproliferative effects of such antagonists in prostate cell growth in culture (76) and in nude mice xenograft models of prostate cancer (67,73,74). Our data also imply that GHRH could be involved in the pathogenesis of BPH.

Herein, we used real-time PCR arrays to investigate the beneficial molecular mechanisms of GHRH antagonists in a BPH-model. The analyses showed that several growth factors were upregulated in TE-induced BPH control rats and markedly downregulated in animals treated with GHRH antagonists. Growth factors are regulatory peptides that govern the response of cells to injury and mediate the highly coordinated processes of cell growth, differentiation, and apoptosis. Among them there are many polypeptides which use autocrine or paracrine pathways to signal stromal and epithelial cells in the microenvironment (21). Verifying PCR array results and more precisely determining changes in gene expression, we studied the expression of selected growth factor and proinflammatory encoding genes by real-time RT-PCR. We confirmed that GHRH antagonists suppress transcriptional expression of IGF-2, TGF-α, TGF-β1 and-β2, EGF, FGF-2, VEGF-A and IL-1β. Several of these growth factors were reported to be involved in the pathogenesis of BPH: EGF and TGF-α (EGF family); FGF-2, FGF-7and FGF-9 (FGF family); IGF-1and IGF-2 (IGF family); TGF-β1and TGF-β2 (TGF-β family) and VEGF (VEGF family) (21).

Our observation of the transcriptional activation of inflammatory cytokines (e.g. Ccl6, Ccl12, IL-1α, IL-1β, IL-13, IL-15 and IL-17β) in the prostate of rats with induced BPH is consistent with clinical findings (138) and with experimental findings in rats (139). We found that GHRH antagonists significantly lowered transcriptional expression of several cytokines including IL-1α, IL-1β, IL-13, IL-15 and IL-17β. These cytokines are part of an inflammatory network in BPH including several

growth factors (20); they promote T-lymphocyte infiltration and the subsequent inflammation progression associated with BPH (42).

We showed that treatment with TE results in elevated levels of IL-1β, NF-κβ and COX-2 protein in the rat prostate, while GHRH antagonists JMR-132, MIA-313, and MIA-459 caused a pronounced comparative decrease in IL-1β, NF-κβ and COX-2 protein levels. Vykhovanets *et al* recently demonstrated that IL-1β, an inflammatory cytokine, causes NF-κβ activation in the mouse prostate (142). The NF- κβ family proteins, like NF-κβ/p65 (RelA) are inducible transcription factors that regulate the expression of hundreds of genes in immune response, angiogenesis, cell adhesion, proliferation, differentiation, and apoptosis. The activation of NF-κβ is one of the earliest events in chronic inflammation (143). COX-2, an inducible isoform of cyclooxygenase enzyme, is an early response gene upregulated by specific stimuli such as mitogens, growth factors, and a variety of cytokines including IL-1 (144). Expression of COX-2, and COX-2-dependent prostanoid production induced by proinflammatory mediators are predominantly regulated by NF- κβ dependent gene transcription (145), suggesting a causal relationship between the lowered NF- κβ/p65 levels, inhibition of COX-2 upregulation and decreased IL-1β production caused by GHRH antagonists. Overexpression of COX-2 in human BPH samples was reported (146), while GHRH antagonists were shown to lower levels of COX-2 in experimental lung cancer (147) and prostate cancer (75).COX-2 was also shown to upregulate anti-apoptotic Bcl-2 with an associated decrease in apoptosis in prostate tissue (148).

All three GHRH antagonists were demonstrated to inhibit cell proliferation, elevate tumor suppressor p53, and lower PCNA levels in rat prostatic epithelium. We observed an increased expression of anti-apoptotic Bcl-2 in TE-induced BPH prostates. This overexpression of Bcl-2 corresponds to observations of Alonso-Magdalena *et al* (17) in human BPH samples, which suggest that BPH is not a proliferative disease, but rather an accumulation of cells resistant to death. Our work shows that treatment with GHRH antagonists causes significant translational upregulation of proapoptotic Bax and suppression of anti-apoptotic Bcl-2 in rat prostates. The number of apoptotic cells in prostatic epithelium after GHRH antagonists was also decreased, although this decrease was not statistically significant. These propapoptotic effects of GHRH antagonists might be due to the significant suppression of prostatic COX-2 or to inhibition of both intrinsic and extrinsic pathways of p53 mediated apoptosis (149).

Analyzing transcriptional changes in signal transduction pathways with quantitative PCR arrays, we observed the involvement of the mitogenic, hedgehog, PI3/AKT and phospholipase C pathways and their downstream effectors.These may be responsible for transmitting beneficial effects

of GHRH antagonists in experimental BPH. GHRH antagonists can strongly inhibit the proliferation rate of cancer cells through the inhibition of the MAPKs pathway (150).

Therapeutic effects of GHRH antagonists were superior to that of finasteride in many aspects of our study including prostatic shrinkage, suppression of growth factors and proinflammatory COX-2, as well as antiproliferative and proapoptotic effects. The adverse effects of finasteride may inculpate GHRH antagonists as an alternative medical therapy of BPH.

In summary, herein we demonstrated that GHRH antagonists JMR-132, MIA-313, and MIA-459 reduce prostate volume in an experimental BPH model. Our data suggest that this reduction in prostate volume is due to direct inhibitory effects of GHRH antagonists exerted through prostatic GHRH receptors as well as through transcriptional suppression of enumerated growth factors and proinflammatory cytokines. We also showed strong inhibition of proinflammatory IL-1β, NF-κβ, and COX-2. Antiapoptotic effects of these GHRH antagonists have also been demonstrated. These findings suggest mechanisms of action of GHRH antagonists in BPH and also indicate a role for GHRH as a locally acting growth factor in BPH. It is possible that GHRH antagonists could be clinically useful for therapy of BPH alone or in combination with other agents.

5.3. Effects of combination of antagonist of LHRH with antagonist of GHRH on experimental benign prostatic hyperplasia (Study 3).

Our study shows that the combination of GHRH antagonist JMR-132 with LHRH antagonist cetrorelix augments prostate shrinkage and reduction in cellular content in experimental BPH. Similarly, multiple functional molecules potentially related to pathogenesis and progression of BPH, were markedly reduced by treatment with GHRH antagonist.

Immunohistochemical analyses revealed that this expression of GHRH-R and LHRH-R is confined to luminal epithelial cells. The expression of GHRH, LHRH and their receptors in rat prostate was demonstrated by Western blot. Previously, we reported that ligand competition assay detected specific high-affinity receptors for GHRH and LHRH in rat prostate (117,129). Serum GH, LH, IGF1, and DHT were not significantly affected by treatment with combination of GHRH and LHRH antagonist. Prostatic and serum PSA, a well-known tumor marker markedly declined after combination treatment. Levels of STEAP, a cell surface antigen expressed predominantly in prostate cancer (151) and a potential target for immunotherapy in various solid tumors (152), were radically lowered after combination treatment.

Recently we showed that antagonists of GHRH and LHRH inhibit the proliferation of the human prostate epithelial BPH-1 cell line in vitro (66,76). These findings strongly suggest that prostate shrinkage is a result of direct inhibitory effects of GHRH and LHRH antagonists exerted

through their prostatic receptors, not involving the hypothalamic-pituitary axis. The demonstration of co-expression of GHRH-R or LHRH-R and their ligands in rat prostate supports the view that prostatic GHRH and LHRH could act in an autocrine/paracrine manner through interaction these receptors (72). This pathway, which is disrupted by antagonists of GHRH and LHRH, provides a mechanistic explanation for the antiproliferative effects of these antagonists on prostate cell growth in culture and in nude mouse xenograft models (67,74,153). Our data also imply that GHRH and LHRH could be involved in the pathogenesis of BPH.

We demonstrated that combination of JMR-132 and cetrorelix caused a pronounced decrease in IL-1β, NF-κβ/p65, and COX-2 protein levels and decreased phosphorylation of NF-κβ/p50. A recent report confirmed that IL-1β, an inflammatory cytokine, causes NF-κβ activation in mouse prostate (142). The NF-κβ family proteins are inducible transcription factors that control the expression of multiple genes of immune response, angiogenesis, cell adhesion, proliferation, differentiation, and apoptosis. The activation of NF-κβ is one of the initial events in chronic inflammation (143). COX-2, an inducible isoform of the cyclooxygenase enzyme, is an early-response gene, up-regulated by specific stimuli such as mitogens, growth factors, and many cytokines including IL-1 (144). Expression of COX-2 and COX-2–dependent prostanoid production induced by proinflammatory mediators is regulated predominantly by NF-κβ–dependent gene transcription (145), indicating an underlying relationship between the lowered NF-κβ levels, inhibition of COX-2 up-regulation, and decreased IL-1β production caused by combination of GHRH and LHRH antagonists. Overexpression of COX-2 in human BPH samples was reported (146); GHRH antagonists were shown to lower levels of COX-2 in experimental lung cancer (147) and prostate cancer (75). COX-2 was also shown to upregulate antiapoptotic Bcl-2 with an associated decrease in prostatic apoptosis (148).

Our study showed that combination treatment markedly decreases the sizes of average epithelial areas in ventral prostate, prostatic DNA content and protein levels of proliferation marker PCNA. Significant transcriptional downregulation of anti-apoptotic Bcl-2, and upregulation of pro-apoptotic Bax were observed.

The therapeutic effects of JMR-132 and cetrorelix combination were superior to those of finasteride on prostatic shrinkage and suppression of PSA, STEAP, IL-1β and COX-2 and so were its antiproliferative and proapoptotic effects. The adverse effects of finasteride may support the use of combination of GHRH and LHRH antagonists as an alternative medical therapy for BPH.

This study shows that combination of GHRH antagonist with LHRH antagonist potentiates reduction in prostate volume in an experimental BPH model. Our data indicate that shrinkage of prostate is induced by direct inhibitory action of GHRH and LHRH antagonists exerted through

prostatic receptors as well as by strong suppression of PSA, STEAP, IL-1β, NF-κβ, and COX-2. Proapoptotic and antiproliferative effects of combination therapy were also demonstrated. Our findings shed light on the mechanisms of action of combinations of GHRH plus LHRH antagonists and also imply that GHRH and LHRH may serve as a local growth factor in BPH. Our study suggests that GHRH antagonists should be considered for further development of a therapy for BPH, possibly in combination with LHRH antagonists.

5.4. Dose-dependent growth inhibition in vivo of PC-3 prostate cancer with a reduction in tumoral growth factors after therapy with GHRH antagonist MZ-J-7-138 (Study 4)

Treatment of relapsed androgen-independent prostate cancer remains a major challenge (77,78,80,82). New therapeutic modalities are being developed based on antagonists of LHRH, GHRH and targeted cytotoxic peptide analogs (61,67,154). Polypeptide growth factors such as GHRH, gastrin-releasing peptide, IGF-I and -II, VEGF, bFGF, EGF, and their receptors are widely expressed in prostate cancer (67,72,77,90,134,136,155-159). Some of these growth factors aberrantly stimulate the androgen receptor pathway (80,157,160) and contribute to the androgen-independent growth of prostate cancer cells. The involvement of GHRH in the growth of various human neoplasms prompted the development of GHRH antagonists for the endocrine therapy of these cancers (67,77,82,84). GHRH antagonists can inhibit the growth of various human experimental prostate cancers indirectly by reducing pituitary GH and hepatic IGF-I secretion and directly by blocking tumoral GHRH receptors and decreasing tumoral IGF-I and –II (67,73,84,136,154).

The PC-3 tumor model represents an advanced stage androgen independent prostate cancer and has been extensively utilized in our previous investigations for the assessment of antitumor effects of less potent GHRH antagonists such as MZ-4-71, MZ-5-156, JV-1- 38, MZ-J-7-118 (77,86-88,92,93,161). In the present study we used the latest and most potent GHRH antagonist MZ-J-7-138 developed very recently. Our results indicate that the minimum effective dose of GHRH antagonist MZ-J-7-138 is 2.5 μg/day for the inhibition of PC-3 cancers in nude mice, and a clear relationship of dose-dependent tumor inhibition is observed in the dose range of 2.5–10 μg/day. This pattern of dose–response relationship where greater inhibition of tumor growth is observed with higher doses of GHRH antagonist represents an advantage compared to some of the other peptide hormones used in cancer treatment. By comparison, several studies found that the response of cells to exposure of somatostatin analog octreotide produces a biphasic dose–response curve, implying that overdosing or underdosing of somatostatin analogs may result in suboptimal antitumor activity (162). The present study and previous work also indicates that MZ-J-7-138 and otherGHRHantagonists are devoidof toxic side-effects and have an extremely broad therapeutic window(67). Thus, here we obtained significant inhibition of PC-3 tumor growth with 2.5 μg/day of MZ-J-7-138, but in other studies in

nude mice, this antagonist was used at a 32-fold higher dose level of 2 x 40 μg/day, without any visible side-effects or toxicity (163).

Table 3. Comparative effects of various GHRH antagonists on the growth of human PC-3 and DU-145 androgen independent and MDA-PCa-2b androgen-sensitive prostate cancers in nude mice.

PC-3 tumors xenografted s.c. into nude mice			
GHRH antagonist (Reference No.)	**Dose**	**Inhibition of tumor volume**	**Other human prostate cancers xenografted s.c. into nude mice**
MZ-4-71 (92)	2 x 20 μg/day	70% **	DU-145 (92): MZ-4-71 (2x20 μg/day) significantly inhibited tumor volumes by 81% (**).
MZ-5-156[a] (86)	20 μg/day[a] (Exp. 1)	53% n.s.[a]	DU-145 (91): MZ-5-156 (2x20 μg/day) significantly inhibited tumor volumes by 57% (*).
JV-1-38 (86)	20 μg/day[a] (Exp. 1)	65% *[a]	DU-145 (73): JV-1-38 (20 μg/day) significantly inhibited tumor volumes by 57% (*).
	20 μg/day (Exp. 2)	65% *	MDA-PCa-2b (73) : JV-1-38 (20 μg/day) did not inhibit tumor volumes.
JV-1-38 (87)	20 μg/day	49% **	MDA-PCa-2b (164): In two separate experiments JV-1-38 (20 μg/day) did not significantly affect tumor volumes.
JV-1-38[b] (93)	10 μg/day[b]	0% n.s.[b]	
MZ-J-7-114[b] (93)	5 μg/day[b]	43% *[b]	
MZ-J-7-118 (161)	5 μg/day	56% *	DU-145 (88): MZ-J-7-118, at 2.5 μg/day and 5 μg/day, inhibited tumor volumes by 67% (*) and 82% (*), respectively.
MZ-J-7-118 (88)	5 μg/day	65% *	MDA-PCa-2b (153): MZ-J-7-118 (5 μg/day) slightly inhibited tumor volumes by 24% (n.s.).
MZ-J-7-138 (present study)	2.5 μg/day 5 μg/day 10 μg/day	52% *** 65% *** 78% ***	MDA-PCa-2b (153): MZ-J-7-138 (5 μg/day) significantly inhibited tumor volumes by 50% (**).

*[a]GHRH antagonists MZ-5-156 and JV-1-38 directly compared in the same experiment. [b]JV-1-38 and MZ-J-7-114 directly compared in the same experiment. Accurate comparisons of the potencies of GHRH antagonists are only possible when they are used in the same experiment. Nevertheless, inhibitory results obtained in different experiments are helpful for a rough estimation of the order of potencies and effective doses of various antagonists. *p<0.05 vs. controls; **p<0.01 vs. controls; ***p<0.001 vs. controls; n.s., not significant. Table is adapted from Heinrich et al. Prostate (2008) 68:1763-72.*

A comparison between the effects of MZ-J-7-138 and older antagonists on the growth of various human prostate cancers in nude mice is given in Table 22. Collectively, the data presented in Table 22 indicate that potent such as MZ-J-7-118 and MZ-J-7- 138 are effective against androgen-independent prostate cancers PC-3 and DU-145 at doses 8- to 16-fold lower than early GHRH antagonists MZ-4-71 and MZ-5-156 that had to be used at doses of up to 2 x 20 μg/day to inhibit tumor growth. In addition, MZ-J-7-138 is the first GHRH antagonist that was effective alone as a therapeutic agent for the treatment of MDA-PCa-2b human androgen-sensitive prostate cancers in nude mice (153). Thus, MZ-J-7-138 at a dose of 5 μg/day inhibited the growth of MDA-PCa-2b tumors to a similar degree as LHRH antagonist Cetrorelix at a dose of 100 μg/day (153). Earlier antagonists such as JV-1-38 or MZ-J-7-118 were not effective when used alone against MDA-PCa-2b cancers, although in combination with androgen deprivation therapies such as LHRH antagonist Cetrorelix they enhanced the antitumor effects of the latter agents (73,153,164). Recently, we also

performed experiments to directly compare the effects of MZ-J-7-138 with other highly potent GHRH antagonists including MZ-J-7-118. In these studies, we found that MZ-J-7-138 more potently inhibited the growth of PC-3 cancers in vivo and showed an increased binding affinity to the GHRH receptors on PC-3 tumor membranes, as compared to other antagonists tested (Zarandi M, Schally AV, Varga JL et al., unpublished data).

The present data allow an extrapolation from the doses effective in nude mice to the doses recommended for clinical trials, based on extensive preclinical (nude mice) and clinical data available with other classes of peptide drugs for cancer, such as somatostatin analogs, and agonists and antagonists of LHRH. In the nude mouse model, GHRH antagonist MZ-J-7-138 is effective at much lower doses (2.5–5 μg/day) against androgen-independent PC-3 and androgen-sensitive MDA-PCa-2b prostate cancers than other types of peptide drugs that are already in clinical use or showed efficacy in clinical trials. Thus, somatostatin analog RC-160 (Vapreotide) inhibited the growth of PC-3 prostate cancers in nude mice at 100 μg/day, but was ineffective at the lower dose of 50 μg/day (87,165). Likewise,LHRH agonist triptorelin (Decapeptyl), and LHRH antagonist SB-75 (cetrotide, Cetrorelix) need to be used in a dose range of 50–100 μg/day for a significant inhibitory effect on the growth of MDA-PCa-2b androgensensitive tumors in nude mice (153,164). Thus, GHRH antagonist MZ-J-7-138 is effective against prostate cancers in nude mice at dose levels that are 10–40 times lower than those of the mentioned somatostatin and LHRH analogs. For the clinical therapy of prostate cancer, Decapeptyl is used at a dose of 0.125 mg/day (3.75 mg/month), Cetrorelix showed clinical efficacy at a dose of 2 x 0.5 mg/day, and Vapreotide produced clinical responses in patients with advanced prostate cancer at a dose of 3 x 1 mg/day (55,61,62,166,167). Thus, supposing that GHRH antagonists will be active in human cancer therapy at dose levels 10–40 times lower than these analogs of somatostatin and LHRH, the clinically effective doses of GHRH antagonists would fall into the range of 0.0125–0.3 mg/day. A clinical therapy based on sub-milligram daily doses of GHRH antagonist would be feasible both from a pharmaceutical technological and economical standpoint, as it would permit the use of depot formulations containing full monthly dose of peptide. The cost of the pharmaceutical preparation at such low doses would also be reasonable.

The present studydemonstrates the dose-dependent inhibitory effect of GHRHantagonist MZ-J-7-138 on the tumoral growth factors VEGF and IGF-II in PC-3 prostate cancer. In the past few years, different GHRH antagonists have been tested at various doses in studies on growth inhibition of prostate cancer xenografts in vivo (67,73,77,82,84,86-88,91-93,153,161).

The effects of previous GHRH antagonists on tumor inhibition and expression of tumoral growth factors have been discussed (62,67,82,84). GHRH antagonists used in the earlier studies by our group were administered at doses as high as 20–40 μg/day, because of their lower tumor

inhibitory potency and at these doses they significantly affected the expression of tumoral growth factors. With more potent GHRH antagonists such as MZ-J-7-118, effective tumor inhibition was demonstrated at lower doses like 5 μg/day, with a decrease in VEGF, but not in the levels of IGF-II (88). In this study, with the one of the most potent GHRH antagonist, MZ-J-7-138 developed so far in our laboratory, we were able to clearly demonstrate dose-dependent effects on both tumor inhibition and growth factor suppression. We observed significant ($P<0.05$) decrease in VEGF protein levels at the doses of 5 μg and 10 μg/day. IGF-II was also significantly decreased by the highest dose of 10 μg/day, but 5 mg/day caused a non-significant reduction ($P<0.07$). The inhibition of tumoral VEGF and IGF-II is in agreement with the data obtained previously in our laboratory, where a reduction of growth factors was detected with high doses of GHRH antagonists. However, the present study shows that the tumor inhibition obtained with a low dose of GHRH antagonist is not associated with a significant decrease of tumoral growth factors, and it may be chiefly due to the direct inhibitory effect of this antagonist on the tumoral GHRH receptors.

In previous studies (136), we could not detect the expression ofmRNAfor the pituitaryGHRH-R in PC-3 cell line using conventional RT-PCR. Moreover,GHRH binding sites could not be detected with [His^1,Nle^{27}]hGHRH(1–32)NH_2 ligand which binds with high affinity to the pituitary isoform of GHRH-R. Thus, it was concluded that PC-3 cell line does not express pituitary GHRH-R. However, in the present investigation using the more sensitive real-time PCR method, we detected the expression of mRNA for pituitary GHRHR. Based on the low expression of mRNA for pituitary GHRH-R, it is likely that the corresponding receptor protein is expressed only at minimal levels in PC-3 cells, which would explain the negative results obtained in previous receptor binding studies. Specific high affinity binding sites forGHRHwere found on PC-3 tumor membranes using ligand competition assays with ^{125}I-labeled GHRH antagonist JV-1-42 which detects both SV-1 and the pituitary type of GHRH receptors. In competition assays GHRH antagonist MZ-J-7-138 displaced the [^{125}I]JV-1-42 radioligand with an IC_{50} = 0.32 nM, which indicates a high affinity binding of MZ-J-7-138 to GHRH receptors on PC-3 tumors. However, future investigations are warranted to better characterize the expression of pituitary GHRH-R in PC-3 cell line, especially at protein level.

The effect of treatment with GHRH antagonist MZ-J-7-138 (10 μg/day) on the expression of mRNA for pituitary GHRH-R and SV1 was also investigated. The expression of mRNA for SV1, which is probably the main GHRH receptor expressed at high levels in PC-3 tumors, was slightly and not significantly downregulated after treatment. Conversely, the expression of mRNA for pituitary GHRH-R was significantly upregulated, but it may contribute very little to total binding. Finally, we also studied the expression of GHRH ligand and found that the mRNA level of GHRH peptide was strongly downregulated after treatment with the GHRH antagonist to about one quarter of the level found in control tumors.

Our results demonstrate the effectiveness of a new GHRH antagonist in reducing tumor growth of androgen independent prostate cancer in a dosedependent manner. The reduction of growth factors like VEGF and IGF-II by this GHRH antagonist was evident at higher doses and after prolonged treatment. Further investigations with GHRH antagonists are required to determine their potential utility for the therapy of prostate cancer. It is likely that the synthesis of still more potent GHRH antagonists might be necessary to convert this class of compounds into a therapeutic tool.

5.5. Inhibitory effects of antagonists of growth hormone releasing hormone on experimental prostate cancers are associated with upregulation of wild-type p53 and decrease in p21 and mutant p53 proteins (Study 5)

Mutations of the tumor suppressor gene p53 are among the most common genetic changes found in malignant tumors (94,96). Since p53 protein modulates cellular functions, such as gene transcription, DNA synthesis and repair, cell cycle arrest, and apoptosis, mutations in the p53 gene can abrogate these functions and may lead to genetic instability and progression to cancer (94-99). Alterations of p53 are clearly associated with androgen independent prostate cancer (168,169) and significant overexpression of mt-p53 is found in hormone-refractory and metastatic prostate cancer tissue (97,98). Particularly the bone metastases show p53 alterations in 50-79% of specimens (168-170). Clonal expansion of p53 mutations from the primary tumor to metastases in paired samples of primary cancers and metastases from the same patients was demonstrated (168-170). It was suggested that foci of p53 mutants in the primary tumor may have a selective growth advantage and a higher metastatic potential (97).

Different growth characteristics in vivo and in vitro as well as different responses to the treatment with various anticancer agents observed in androgen independent prostate cancer models such as PC-3 and DU-145, compared to androgen sensitive models MDA-PCa-2b and LNCaP have been attributed to the status of p53 as the former models express mutant type and the latter wt p53 (104,171). The present study demonstrates that inhibition of human experimental prostate cancers by GHRH antagonist MZ-J-7-138 and LHRH antagonist Cetrorelix involves a different effect on wt-p53 and mt-p53 protein levels. MZ-J-7-138 inhibited proliferation of PC-3 and DU-145 tumors inducing a decrease in the levels of mutant p53. MZ-J-7-138 also suppressed MDA-PCa-2b tumors with an upregulation of wt-p53. Cetrorelix also significantly increased the wt-p53 protein expression. Induction of the expression of pro-apoptotic wt-p53 protein may be involved in the inhibitory effect of GHRH and LHRH antagonists on MDA-PCa-2b tumor growth observed in our study. Our results are in accord with recent findings showing an increase of wt-p53 expression after treatment with GHRH antagonists in an experimental BPH model (117), and a decrease of mt-p53 expression after therapy with GHRH antagonists in DMS-153 small cell lung carcinomas (118). In MDA-PCa-2b, combined treatment with LHRH antagonist Cetrorelix and the GHRH antagonist MZ-J-7-138 resulted in a greater tumor inhibition. MZ-J-7-138 is the first GHRH antagonist that significantly decreased growth of MDA-PCa-2b human

androgen sensitive prostate cancers without concomitant androgen deprivation. In previous studies using earlier and less potent GHRH antagonists, the androgen deprivation was required in order to achieve significant tumor inhibition of androgen sensitive experimental prostate cancers by GHRH antagonists (67,84,164). The presence of GHRH receptor and LHRH receptor on PC-3, DU-145 and MDA-PCa-2b human prostate cell lines was demonstrated previously (73,74,153,172).

GHRH antagonists inhibit the growth of various human experimental prostate cancers directly by blocking tumoral GHRH receptors and by decreasing the production of tumoral IGF-I and II (67,84,88). The intracellular signal transduction mechanisms leading to tumor inhibition following treatment with GHRH antagonists include changes in the expression of PKC isoforms, inhibition of the p42/44 MAPK (pERK1/2) – c-jun pathway, and Ca^{2+} entry into the cells which induces apoptosis (164,173).

Most p53 mutations are clustered into the central conserved DNA binding domain, and within this region, a number of hot spot p53 mutations has been observed (174). In DU-145, two mutations are described on the p53 gene. These mutations are found at codon 274 (pro>leu) and codon 223 (val>phe) (104,175). Functionally, one or two of these mutations stabilizes the mutant p53, resulting in its strong expression as shown by Western Blot and staining with immunohistochemistry (171). PC-3 cells are reported to be hemizygous for chromosome 17p. The single copy of the p53 gene has a base pair deletion at codon 138 that generated a frame shift and a new in-frame stop codon at position 169 (171,175). In our experiments PC-3 tumors also expressed detectable mt-p53 protein levels. This is in contrast to earlier studies who described high levels of mutant p53 in DU-145 but no p53 expression in PC-3(171,175).

The detection of p53 expression in our PC-3 line was achieved by three different p53 antibodies with different speciation and all specific for human p53.

In contrast to PC-3 and DU-145 tumors, the androgen sensitive MDA-PCa-2b prostate cancer model was found to express wt-p53 (176). Treatment of MDA-PCa-2b tumors with MZ-J-7-138 led to a non-significant up-regulation of wt-p53.

Based on the role of p53 in the control of apoptosis after DNA damage, the p53 gene has been implicated as a major determinant of tumor responsiveness to cytotoxic therapies. Wild-type p53 protein can suppress tumorigenesis and promote apoptosis, acting as a transcriptional factor while mutant p53 proteins are linked to a number of pathophysiological processes and exert effects that are opposite to those of wild-type p53. The efficacy of chemotherapy with DNA-damaging agents or radiotherapy is influenced by the p53 status of tumors (94,177). It has been shown that transfection of PC-3 and DU-145 with wt p53 restored the chemosensitivity and decreased their excessive growth (97,104). Conversely, gene transfection and expression of mutant p53 proteins in cancer lines that were originally p53-null confers increased resistance to apoptosis (97) and stimulates the transcription of IGFR-I gene, in contrast to wild-type p53, which inhibits it (178). It has also been shown that a

mutation of the p53 gene, in hepatocellular carcinomas, markedly increases the production of IGF-II, which has an antiapoptotic effect, and this could contribute to the selection of transformed hepatocytes with an increased resistance to apoptosis (179). Thus, the inhibition of anti apoptotic mt-p53 by GHRH antagonists observed in PC-3 and DU-145 tumors may offer a strategy to increase chemosensitivity of advanced prostate cancers that respond poorly to chemotherapy and prevent further progression.

The present work, together with the results of several previous studies in our laboratory, indicates that GHRH antagonists could be effective for the treatment of cancers with wt-p53 as well as mt-p53 status. Tumor models that were significantly inhibited by GHRH antagonists in vivo include MDA-PCa-2b and LNCaP prostate cancers, H460 and A549 lung carcinomas, CAKI-1 renal carcinomas and U-87MG glioblastomas with wt-p53 status, as well as PC-3 and DU-145 prostate cancers, DMS-153 lung cancers, MDA-MB-468 and MDA-MB-435 breast cancers, HT29 colorectal and Panc-1 pancreatic cancers that express mt-p53 (67,84,110). GHRH antagonists could offer a distinct advantage for the treatment of cancers with mt-p53 status, since the conventional anticancer drugs, including DNA cross-linking agents, antimetabolites, and topo-isomerase I and II inhibitors, are less effective when mt-p53 is expressed (110). Recent investigations demonstrated, that inhibition of p53 function diminishes the androgen receptor-mediated signaling (180).

To shed more light on the downstream mechanisms of the p53 pathway in prostate cancers treated with GHRH antagonist we investigated the expression of the p53 downstream effector p21 ($p21^{WAF1/Cip1}$). Treatment with GHRH and LHRH antagonists invariably suppressed the p21 protein levels, regardless of whether the tumor models expressed wt- or mt-p53. This indicates that the antagonists possibly influence tumoral p21 levels by mechanisms independent of p53. Thus in MDA-PCa-2b model which contains wt-p53, an upregulation of wt-p53 levels after treatment with antagonists was accompanied by suppression of p21, even though wt-p53 is a well-known positive regulator of p21 expression. Normally, mt-p53 reduces the expression of p21 protein (95,181). The p53 gene mutation and the nuclear accumulation of its mt-p53 protein product have been found to be associated with a down-regulation of p21 (181). It was also reported that ectopic expression of various mt-p53 proteins markedly reduced the expression of p21 and other p53-target genes, whereas silencing of mt-p53 expression by specific siRNAs upregulated the expression of the p21 gene in human cancer lines (95). Nevertheless, in our experiments with PC-3 and DU-145 tumors expressing mt-p53, inhibition of mt-p53 levels by the GHRH antagonist was accompanied by decreased p21 levels. The possible mechanisms by which our antagonists could inhibit tumoral p21 levels in a p53-independent manner are the inhibition of tumoral MAPK (pERK1/2) and pAkt levels, since pERK1/2 and pAkt are positive regulators of p21 (109,182,183) and GHRH antagonists inhibit pERK1/2 and pAkt levels in prostatic and lung cancers (67,84,147,184).

The inhibition of anti-apoptotic p21 levels by antagonists of GHRH and LHRH represents a very favorable molecular mode of action, suggesting that these antagonists could possibly counteract the p21-upregulating effect of conventional chemotherapeutic agents and of radiotherapy, and act as chemotherapy or radiotherapy sensitizers when used with these treatment methods. Similarly it cannot be excluded that antagonists of GHRH and LHRH could exert some protective action against deleterious effects of radiation and chemotherapy. In this respect, we have reported recently that GHRH antagonists in combination with docetaxel produced a synergistic inhibition of human experimental lung and breast cancers (128,147). Similar experiments should be carried out in the future with prostate cancer models in order to fully elucidate the therapeutic potential of GHRH and LHRH antagonists in combination with conventional chemotherapeutic agents such as docetaxel, paclitaxel, doxorubicin, or cisplatin. The decrease of p21 expression, in addition to the earlier described paracrine/autocrine growth factor blockade, could offer a multimodal approach to a new cancer therapy.

Tumor inhibition produced by GHRH antagonists in vivo could be partially explained by a repression of the defective p53 function in PC-3 and DU-145 and by the reduction in p21 protein expression. Further work with these analogs might lead to the development of new therapeutic modalities for patients with relapsed prostate cancer who no longer respond to conventional treatment.

6. Novel findings:

6.1. Experimental benign prostatic hyperplasia studies

- We showed expression of target receptors LHRH-R and GHRH-R and found a single class of high affinity binding sites for LHRH and GHRH in rat prostates
- We localized LHRH-R and GHRH-R on luminal membrane and apical cytoplasm of epithelial cells of rat prostates
- Treatment with LHRH antagonist cetrorelix caused significant reduction of prostate weights in experimental BPH in a dose-dependent manner
- Our findings suggest that the reduction in prostate volume could be due to direct inhibitory effects of cetrorelix exerted through prostatic LHRH receptors as well as transcriptional suppression of proinflammatory cytokines and growth factors
- We demonstrated that the GHRH antagonists JMR-132, MIA-313, and MIA-459 reduce prostate weigths and cellular content in experimental BPH
- Our data suggest that this reduction in prostate volume is caused by the direct inhibitory effects of GHRH antagonists exerted through prostatic GHRH receptors as well as by transcriptional suppression of enumerated growth factors and proinflammatory cytokines.
- We also showed strong inhibition of prostatic IL-1β, NF-κβ, and COX-2 after treatment with GHRH antagonists
- The proapoptotic effects of GHRH antagonists also have been demonstrated.
- We observed the involvement of the mitogenic, hedgehog, PI3/AKT, and phospholipase C pathways and their downstream effectors after treatment of experimental BPH with GHRH antagonists.
- We demonstrated that a combination of GHRH antagonist with LHRH antagonist potentiates reduction in prostate weight in experimental BPH.
- Our data indicate that shrinkage of prostate is induced by direct inhibitory action of GHRH and LHRH antagonists exerted through prostatic receptors.
- We found strong suppression of PSA, STEAP, IL-1β, NF-κβ, and COX-2 after treatment with combination of GHRH and LHRH antagonists.

- Proapoptotic and antiproliferative effects of combination therapy were also demonstrated.
- Our data imply that GHRH and LHRH may serve as a local growth factor in BPH

6.2. Human prostate cancer xenograft studies

- Our work indicates that GHRH antagonist MZ-J-7-138 is effective for the treatment of experimental prostatic cancers with wt-p53 (MDA-PCa-2b) as well as mt-p53 (PC-3 and DU-145) status.
- We showed that treatment with GHRH and LHRH antagonists invariably suppressed the p21 protein levels, regardless of whether the tumor models expressed wt- or mt-p53. This indicates that the antagonists possibly influence tumoral p21 levels by mechanisms independent of p53.
- We also demonstrated that GHRH antagonist MZ-J-7-138 inhibits growth of androgen-independent PC-3 prostate cancer in a dose-dependent manner.
- The reduction of growth factors VEGF and IGF-2 by this GHRH antagonist was evident at higher doses and after prolonged treatment.

7. References

1. Roehrborn CG. Male lower urinary tract symptoms (LUTS) and benign prostatic hyperplasia (BPH). Med Clin North Am 2011;95(1):87-100.
2. Berry SJ, Coffey DS, Walsh PC, Ewing LL. The development of human benign prostatic hyperplasia with age. J Urol 1984;132(3):474-479.
3. Ho CK, Habib FK. Estrogen and androgen signaling in the pathogenesis of BPH. Nat Rev Urol 2011;8(1):29-41.
4. Nicholson TM, Ricke WA. Androgens and estrogens in benign prostatic hyperplasia: Past, present and future. Differentiation 2011.
5. McNeal JE. The zonal anatomy of the prostate. Prostate 1981;2(1):35-49.
6. McNeal JE. Origin and evolution of benign prostatic enlargement. Invest Urol 1978;15(4):340-345.
7. Roehrborn CG. Benign prostatic hyperplasia: an overview. Rev Urol 2005;7 Suppl 9:S3-S14.
8. Abrams P, Chapple C, Khoury S, Roehrborn C, de la Rosette J. Evaluation and treatment of lower urinary tract symptoms in older men. J Urol 2009;181(4):1779-1787.
9. Chapple CR, Roehrborn CG. A shifted paradigm for the further understanding, evaluation, and treatment of lower urinary tract symptoms in men: focus on the bladder. Eur Urol 2006;49(4):651-658.
10. Armitage JN, Sibanda N, Cathcart PJ, Emberton M, van der Meulen JH. Mortality in men admitted to hospital with acute urinary retention: database analysis. BMJ 2007;335(7631):1199-1202.
11. McNeal J. Pathology of benign prostatic hyperplasia. Insight into etiology. Urol Clin North Am 1990;17(3):477-486.
12. Franks LM. Benign nodular hyperplasia of the prostate; a review. Ann R Coll Surg Engl 1953;14(2):92-106.
13. Shapiro E, Becich MJ, Hartanto V, Lepor H. The relative proportion of stromal and epithelial hyperplasia is related to the development of symptomatic benign prostate hyperplasia. J Urol 1992;147(5):1293-1297.
14. McNeal JE. Normal and pathologic anatomy of prostate. Urology 1981;17(Suppl 3):11-16.
15. Coffey DS, Walsh PC. Clinical and experimental studies of benign prostatic hyperplasia. Urol Clin North Am 1990;17(3):461-475.
16. Untergasser G, Madersbacher S, Berger P. Benign prostatic hyperplasia: age-related tissue-remodeling. Exp Gerontol 2005;40(3):121-128.
17. Alonso-Magdalena P, Brossner C, Reiner A, Cheng G, Sugiyama N, Warner M, Gustafsson JA. A role for epithelial-mesenchymal transition in the etiology of benign prostatic hyperplasia. Proc Natl Acad Sci U S A 2009;106(8):2859-2863.
18. Lin VK, Wang SY, Vazquez DV, C CX, Zhang S, Tang L. Prostatic stromal cells derived from benign prostatic hyperplasia specimens possess stem cell like property. Prostate 2007;67(12):1265-1276.
19. Berger AP, Kofler K, Bektic J, Rogatsch H, Steiner H, Bartsch G, Klocker H. Increased growth factor production in a human prostatic stromal cell culture model caused by hypoxia. Prostate 2003;57(1):57-65.
20. Kramer G, Mitteregger D, Marberger M. Is benign prostatic hyperplasia (BPH) an immune inflammatory disease? Eur Urol 2007;51(5):1202-1216.
21. Lucia MS, Lambert JR. Growth Factors in Benign Prostatic Hyperplasia: Basic Science Implications. Curr Urol Rep 2008;9(4):272-278.
22. Cunha GR, Ricke W, Thomson A, Marker PC, Risbridger G, Hayward SW, Wang YZ, Donjacour AA, Kurita T. Hormonal, cellular, and molecular regulation of normal and neoplastic prostatic development. J Steroid Biochem Mol Biol 2004;92(4):221-236.
23. McVary KT. BPH: epidemiology and comorbidities. Am J Manag Care 2006;12(5 Suppl):S122-128.

24. Zhang Z, Duan L, Du X, Ma H, Park I, Lee C, Zhang J, Shi J. The proliferative effect of estradiol on human prostate stromal cells is mediated through activation of ERK. Prostate 2008;68(5):508-516.
25. Park, II, Zhang Q, Liu V, Kozlowski JM, Zhang J, Lee C. 17Beta-estradiol at low concentrations acts through distinct pathways in normal versus benign prostatic hyperplasia-derived prostate stromal cells. Endocrinology 2009;150(10):4594-4605.
26. Tsurusaki T, Aoki D, Kanetake H, Inoue S, Muramatsu M, Hishikawa Y, Koji T. Zone-dependent expression of estrogen receptors alpha and beta in human benign prostatic hyperplasia. J Clin Endocrinol Metab 2003;88(3):1333-1340.
27. Lau KM, LaSpina M, Long J, Ho SM. Expression of estrogen receptor (ER)-alpha and ER-beta in normal and malignant prostatic epithelial cells: regulation by methylation and involvement in growth regulation. Cancer Res 2000;60(12):3175-3182.
28. Zavadil J, Bottinger EP. TGF-beta and epithelial-to-mesenchymal transitions. Oncogene 2005;24(37):5764-5774.
29. Fibbi B, Penna G, Morelli A, Adorini L, Maggi M. Chronic inflammation in the pathogenesis of benign prostatic hyperplasia. Int J Androl 2010;33(3):475-488.
30. Di Silverio F, Gentile V, De Matteis A, Mariotti G, Giuseppe V, Luigi PA, Sciarra A. Distribution of inflammation, pre-malignant lesions, incidental carcinoma in histologically confirmed benign prostatic hyperplasia: a retrospective analysis. Eur Urol 2003;43(2):164-175.
31. Nickel JC, Roehrborn CG, O'Leary M P, Bostwick DG, Somerville MC, Rittmaster RS. Examination of the relationship between symptoms of prostatitis and histological inflammation: baseline data from the REDUCE chemoprevention trial. J Urol 2007;178(3 Pt 1):896-900; discussion 900-891.
32. St Sauver JL, Jacobson DJ, Girman CJ, Lieber MM, McGree ME, Jacobsen SJ. Tracking of longitudinal changes in measures of benign prostatic hyperplasia in a population based cohort. J Urol 2006;175(3 Pt 1):1018-1022; discussion 1022.
33. Kessler OJ, Keisari Y, Servadio C, Abramovici A. Role of chronic inflammation in the promotion of prostatic hyperplasia in rats. J Urol 1998;159(3):1049-1053.
34. Lee KL, Peehl DM. Molecular and cellular pathogenesis of benign prostatic hyperplasia. J Urol 2004;172(5 Pt 1):1784-1791.
35. Kohnen PW, Drach GW. Patterns of inflammation in prostatic hyperplasia: a histologic and bacteriologic study. J Urol 1979;121(6):755-760.
36. Theyer G, Kramer G, Assmann I, Sherwood E, Preinfalk W, Marberger M, Zechner O, Steiner GE. Phenotypic characterization of infiltrating leukocytes in benign prostatic hyperplasia. Lab Invest 1992;66(1):96-107.
37. Kramer G, Steiner GE, Handisurya A, Stix U, Haitel A, Knerer B, Gessl A, Lee C, Marberger M. Increased expression of lymphocyte-derived cytokines in benign hyperplastic prostate tissue, identification of the producing cell types, and effect of differentially expressed cytokines on stromal cell proliferation. Prostate 2002;52(1):43-58.
38. Djavan B, Eckersberger E, Espinosa G, Kramer G, Handisurya A, Lee C, Marberger M, Lepor H, Steiner GE. Complex mechanisms in prostatic inflammatory response. Eur Urol Suppl 2009(8):872-878.
39. Nickel JC, Roehrborn CG, O'Leary MP, Bostwick DG, Somerville MC, Rittmaster RS. The relationship between prostate inflammation and lower urinary tract symptoms: examination of baseline data from the REDUCE trial. Eur Urol 2008;54(6):1379-1384.
40. Steiner GE, Newman ME, Paikl D, Stix U, Memaran-Dagda N, Lee C, Marberger MJ. Expression and function of pro-inflammatory interleukin IL-17 and IL-17 receptor in normal, benign hyperplastic, and malignant prostate. Prostate 2003;56(3):171-182.
41. Handisurya A, Steiner GE, Stix U, Ecker RC, Pfaffeneder-Mantai S, Langer D, Kramer G, Memaran-Dadgar N, Marberger M. Differential expression of interleukin-15, a pro-inflammatory cytokine and T-cell growth factor, and its receptor in human prostate. Prostate 2001;49(4):251-262.

42. Steiner GE, Stix U, Handisurya A, Willheim M, Haitel A, Reithmayr F, Paikl D, Ecker RC, Hrachowitz K, Kramer G, Lee C, Marberger M. Cytokine expression pattern in benign prostatic hyperplasia infiltrating T cells and impact of lymphocytic infiltration on cytokine mRNA profile in prostatic tissue. Lab Invest 2003;83(8):1131-1146.
43. Culig Z, Hobisch A, Cronauer MV, Radmayr C, Hittmair A, Zhang J, Thurnher M, Bartsch G, Klocker H. Regulation of prostatic growth and function by peptide growth factors. Prostate 1996;28(6):392-405.
44. Hieble JP. Animal models for benign prostatic hyperplasia. Handb Exp Pharmacol 2011(202):69-79.
45. Love HD, Booton SE, Boone BE, Breyer JP, Koyama T, Revelo MP, Shappell SB, Smith JR, Hayward SW. Androgen regulated genes in human prostate xenografts in mice: relation to BPH and prostate cancer. PLoS One 2009;4(12):e8384.
46. Barclay WW, Woodruff RD, Hall MC, Cramer SD. A system for studying epithelial-stromal interactions reveals distinct inductive abilities of stromal cells from benign prostatic hyperplasia and prostate cancer. Endocrinology 2005;146(1):13-18.
47. Cunha GR, Lung B. The possible influence of temporal factors in androgenic responsiveness of urogenital tissue recombinants from wild-type and androgen-insensitive (Tfm) mice. J Exp Zool 1978;205(2):181-193.
48. Hayward SW, Dahiya R, Cunha GR, Bartek J, Deshpande N, Narayan P. Establishment and characterization of an immortalized but non-transformed human prostate epithelial cell line: BPH-1. In Vitro Cell Dev Biol Anim 1995;31(1):14-24.
49. Steiner MS, Couch RC, Raghow S, Stauffer D. The chimpanzee as a model of human benign prostatic hyperplasia. J Urol 1999;162(4):1454-1461.
50. Walsh PC, Wilson JD. The induction of prostatic hypertrophy in the dog with androstanediol. J Clin Invest 1976;57(4):1093-1097.
51. Maggi CA, Manzini S, Giuliani S, Meli A. Infravesical outflow obstruction in rats: a comparison of two models. Gen Pharmacol 1989;20(3):345-349.
52. Roehrborn CG. BPH progression: concept and key learning from MTOPS, ALTESS, COMBAT, and ALF-ONE. BJU Int 2008;101 Suppl 3:17-21.
53. Millar RP, Lu ZL, Pawson AJ, Flanagan CA, Morgan K, Maudsley SR. Gonadotropin-releasing hormone receptors. Endocr Rev 2004;25(2):235-275.
54. Bajusz S, Csernus VJ, Janaky T, Bokser L, Fekete M, Schally AV. New antagonists of LHRH. II. Inhibition and potentiation of LHRH by closely related analogues. Int J Pept Protein Res 1988;32(6):425-435.
55. Gonzalez-Barcena D, Vadillo-Buenfil M, Gomez-Orta F, Fuentes Garcia M, Cardenas-Cornejo I, Graef-Sanchez A, Comaru-Schally AM, Schally AV. Responses to the antagonistic analog of LH-RH (SB-75, Cetrorelix) in patients with benign prostatic hyperplasia and prostatic cancer. Prostate 1994;24(2):84-92.
56. Comaru-Schally AM, Brannan W, Schally AV, Colcolough M, Monga M. Efficacy and safety of luteinizing hormone-releasing hormone antagonist cetrorelix in the treatment of symptomatic benign prostatic hyperplasia. J Clin Endocrinol Metab 1998;83(11):3826-3831.
57. Debruyne F, Gres AA, Arustamov DL. Placebo-controlled dose-ranging phase 2 study of subcutaneously administered LHRH antagonist cetrorelix in patients with symptomatic benign prostatic hyperplasia. Eur Urol 2008;54(1):170-177.
58. Debruyne F, Tzvetkov M, Altarac S, Geavlete PA. Dose-ranging study of the luteinizing hormone-releasing hormone receptor antagonist cetrorelix pamoate in the treatment of patients with symptomatic benign prostatic hyperplasia. Urology 2010;76(4):927-933.
59. Horvath JE, Toller GL, Schally AV, Bajo AM, Groot K. Effect of long-term treatment with low doses of the LHRH antagonist Cetrorelix on pituitary receptors for LHRH and gonadal axis in male and female rats. Proc Natl Acad Sci U S A 2004;101(14):4996-5001.
60. Russo A, Castiglione F, Salonia A, Benigni F, Rigatti P, Montorsi F, Andersson KE, Hedlund P. Effects of the gonadotropin-releasing hormone antagonist ganirelix on

normal micturition and prostaglandin e(2)-induced detrusor overactivity in conscious female rats. Eur Urol 2011;59(5):868-874.
61. Engel JB, Schally AV. Drug Insight: clinical use of agonists and antagonists of luteinizing-hormone-releasing hormone. Nat Clin Pract Endocrinol Metab 2007;3(2):157-167.
62. Schally AV. New approaches to the therapy of various tumors based on peptide analogues. Horm Metab Res 2008;40(5):315-322.
63. Jungwirth A, Galvan G, Pinski J, Halmos G, Szepeshazi K, Cai RZ, Groot K, Schally AV. Luteinizing hormone-releasing hormone antagonist Cetrorelix (SB-75) and bombesin antagonist RC-3940-II inhibit the growth of androgen-independent PC-3 prostate cancer in nude mice. Prostate 1997;32(3):164-172.
64. Lamharzi N, Schally AV, Koppan M. Luteinizing hormone-releasing hormone (LH-RH) antagonist Cetrorelix inhibits growth of DU-145 human androgen-independent prostate carcinoma in nude mice and suppresses the levels and mRNA expression of IGF-II in tumors. Regul Pept 1998;77(1-3):185-192.
65. Clementi M, Sanchez C, Benitez DA, Contreras HR, Huidobro C, Cabezas J, Acevedo C, Castellon EA. Gonadotropin releasing hormone analogs induce apoptosis by extrinsic pathway involving p53 phosphorylation in primary cell cultures of human prostatic adenocarcinomas. Prostate 2009;69(10):1025-1033.
66. Siejka A, Schally AV, Block NL, Barabutis N. Mechanisms of inhibition of human benign prostatic hyperplasia in vitro by the luteinizing hormone-releasing hormone antagonist cetrorelix. BJU Int 2010;106(9):1382-1388.
67. Schally AV, Varga JL, Engel JB. Antagonists of growth-hormone-releasing hormone: an emerging new therapy for cancer. Nat Clin Pract Endocrinol Metab 2008;4(1):33-43.
68. Westley BR, May FE. Insulin-like growth factors: the unrecognised oncogenes. Br J Cancer 1995;72(5):1065-1066.
69. Havt A, Schally AV, Halmos G, Varga JL, Toller GL, Horvath JE, Szepeshazi K, Koster F, Kovitz K, Groot K, Zarandi M, Kanashiro CA. The expression of the pituitary growth hormone-releasing hormone receptor and its splice variants in normal and neoplastic human tissues. Proc Natl Acad Sci U S A 2005;102(48):17424-17429.
70. Rekasi Z, Czompoly T, Schally AV, Halmos G. Isolation and sequencing of cDNAs for splice variants of growth hormone-releasing hormone receptors from human cancers. Proc Natl Acad Sci U S A 2000;97(19):10561-10566.
71. Kiaris H, Schally AV, Varga JL, Groot K, Armatis P. Growth hormone-releasing hormone: an autocrine growth factor for small cell lung carcinoma. Proc Natl Acad Sci U S A 1999;96(26):14894-14898.
72. Chopin LK, Herington AC. A potential autocrine pathway for growth hormone releasing hormone (GHRH) and its receptor in human prostate cancer cell lines. Prostate 2001;49(2):116-121.
73. Letsch M, Schally AV, Busto R, Bajo AM, Varga JL. Growth hormone-releasing hormone (GHRH) antagonists inhibit the proliferation of androgen-dependent and -independent prostate cancers. Proc Natl Acad Sci U S A 2003;100(3):1250-1255.
74. Heinrich E, Schally AV, Buchholz S, Rick FG, Halmos G, Mile M, Groot K, Hohla F, Zarandi M, Varga JL. Dose-dependent growth inhibition in vivo of PC-3 prostate cancer with a reduction in tumoral growth factors after therapy with GHRH antagonist MZ-J-7-138. Prostate 2008;68(16):1763-1772.
75. Barabutis N, Schally AV. Antioxidant activity of growth hormone-releasing hormone antagonists in LNCaP human prostate cancer line. Proc Natl Acad Sci U S A 2008;105(51):20470-20475.
76. Siejka A, Schally AV, Block NL, Barabutis N. Antagonists of growth hormone-releasing hormone inhibit the proliferation of human benign prostatic hyperplasia cells. Prostate 2010;70(10):1087-1093.
77. Schally AV, Comaru-Schally AM, Plonowski A, Nagy A, Halmos G, Rekasi Z. Peptide analogs in the therapy of prostate cancer. Prostate 2000;45(2):158-166.

78. Loblaw DA, Mendelson DS, Talcott JA, Virgo KS, Somerfield MR, Ben-Josef E, Middleton R, Porterfield H, Sharp SA, Smith TJ, Taplin ME, Vogelzang NJ, Wade JL, Jr., Bennett CL, Scher HI. American Society of Clinical Oncology recommendations for the initial hormonal management of androgen-sensitive metastatic, recurrent, or progressive prostate cancer. J Clin Oncol 2004;22(14):2927-2941.
79. Tannock IF, de Wit R, Berry WR, Horti J, Pluzanska A, Chi KN, Oudard S, Theodore C, James ND, Turesson I, Rosenthal MA, Eisenberger MA. Docetaxel plus prednisone or mitoxantrone plus prednisone for advanced prostate cancer. N Engl J Med 2004;351(15):1502-1512.
80. Feldman BJ, Feldman D. The development of androgen-independent prostate cancer. Nat Rev Cancer 2001;1(1):34-45.
81. Schally AV C-SA. Hypthalamic and other peptide hormones. In: Holland JF FEI, Bast RC, Jr., editors, editor, 7th Edition ed. Hamilton, Ontario, : BC: Decker; 2006. 802-816 p.
82. Schally AV, Comaru-Schally AM, Nagy A, Kovacs M, Szepeshazi K, Plonowski A, Varga JL, Halmos G. Hypothalamic hormones and cancer. Front Neuroendocrinol 2001;22(4):248-291.
83. Schally AV. Luteinizing hormone-releasing hormone analogs: their impact on the control of tumorigenesis. Peptides 1999;20(10):1247-1262.
84. Schally AV, Varga JL. Antagonists of growth hormone-releasing hormone in oncology. Comb Chem High Throughput Screen 2006;9(3):163-170.
85. Schally AV, Varga JL. Antagonistic Analogs of Growth Hormone-releasing Hormone: New Potential Antitumor Agents. Trends Endocrinol Metab 1999;10(10):383-391.
86. Plonowski A, Schally AV, Varga JL, Rekasi Z, Hebert F, Halmos G, Groot K. Potentiation of the inhibitory effect of growth hormone-releasing hormone antagonists on PC-3 human prostate cancer by bombesin antagonists indicative of interference with both IGF and EGF pathways. Prostate 2000;44(2):172-180.
87. Plonowski A, Schally AV, Letsch M, Krupa M, Hebert F, Busto R, Groot K, Varga JL. Inhibition of proliferation of PC-3 human prostate cancer by antagonists of growth hormone-releasing hormone: lack of correlation with the levels of serum IGF-I and expression of tumoral IGF-II and vascular endothelial growth factor. Prostate 2002;52(3):173-182.
88. Stangelberger A, Schally AV, Varga JL, Hammann BD, Groot K, Halmos G, Cai RZ, Zarandi M. Antagonists of growth hormone releasing hormone (GHRH) and of bombesin/gastrin releasing peptide (BN/GRP) suppress the expression of VEGF, bFGF, and receptors of the EGF/HER family in PC-3 and DU-145 human androgen-independent prostate cancers. Prostate 2005;64(3):303-315.
89. Kiaris H, Schally AV, Busto R, Halmos G, Artavanis-Tsakonas S, Varga JL. Expression of a splice variant of the receptor for GHRH in 3T3 fibroblasts activates cell proliferation responses to GHRH analogs. Proc Natl Acad Sci U S A 2002;99(1):196-200.
90. Halmos G, Schally AV, Czompoly T, Krupa M, Varga JL, Rekasi Z. Expression of growth hormone-releasing hormone and its receptor splice variants in human prostate cancer. J Clin Endocrinol Metab 2002;87(10):4707-4714.
91. Lamharzi N, Schally AV, Koppan M, Groot K. Growth hormone-releasing hormone antagonist MZ-5-156 inhibits growth of DU-145 human androgen-independent prostate carcinoma in nude mice and suppresses the levels and mRNA expression of insulin-like growth factor II in tumors. Proc Natl Acad Sci U S A 1998;95(15):8864-8868.
92. Jungwirth A, Schally AV, Pinski J, Halmos G, Groot K, Armatis P, Vadillo-Buenfil M. Inhibition of in vivo proliferation of androgen-independent prostate cancers by an antagonist of growth hormone-releasing hormone. Br J Cancer 1997;75(11):1585-1592.
93. Zarandi M, Varga JL, Schally AV, Horvath JE, Toller GL, Kovacs M, Letsch M, Groot K, Armatis P, Halmos G. Lipopeptide antagonists of growth hormone-releasing hormone with improved antitumor activities. Proc Natl Acad Sci U S A 2006;103(12):4610-4615.

94. Wallace-Brodeur RR, Lowe SW. Clinical implications of p53 mutations. Cell Mol Life Sci 1999;55(1):64-75.
95. Vikhanskaya F, Lee MK, Mazzoletti M, Broggini M, Sabapathy K. Cancer-derived p53 mutants suppress p53-target gene expression--potential mechanism for gain of function of mutant p53. Nucleic Acids Res 2007;35(6):2093-2104.
96. Smith ND, Rubenstein JN, Eggener SE, Kozlowski JM. The p53 tumor suppressor gene and nuclear protein: basic science review and relevance in the management of bladder cancer. J Urol 2003;169(4):1219-1228.
97. Pisters LL, Pettaway CA, Troncoso P, McDonnell TJ, Stephens LC, Wood CG, Do KA, Brisbay SM, Wang X, Hossan EA, Evans RB, Soto C, Jacobson MG, Parker K, Merritt JA, Steiner MS, Logothetis CJ. Evidence that transfer of functional p53 protein results in increased apoptosis in prostate cancer. Clin Cancer Res 2004;10(8):2587-2593.
98. Navone NM, Rodriquez-Vargas MC, Benedict WF, Troncoso P, McDonnell TJ, Zhou JH, Luthra R, Logothetis CJ. TabBO: a model reflecting common molecular features of androgen-independent prostate cancer. Clin Cancer Res 2000;6(3):1190-1197.
99. Zellweger T, Ninck C, Bloch M, Mirlacher M, Koivisto PA, Helin HJ, Mihatsch MJ, Gasser TC, Bubendorf L. Expression patterns of potential therapeutic targets in prostate cancer. Int J Cancer 2005;113(4):619-628.
100. Bossi G, Lapi E, Strano S, Rinaldo C, Blandino G, Sacchi A. Mutant p53 gain of function: reduction of tumor malignancy of human cancer cell lines through abrogation of mutant p53 expression. Oncogene 2006;25(2):304-309.
101. Scian MJ, Stagliano KE, Ellis MA, Hassan S, Bowman M, Miles MF, Deb SP, Deb S. Modulation of gene expression by tumor-derived p53 mutants. Cancer Res 2004;64(20):7447-7454.
102. Blagosklonny MV, Trostel S, Kayastha G, Demidenko ZN, Vassilev LT, Romanova LY, Bates S, Fojo T. Depletion of mutant p53 and cytotoxicity of histone deacetylase inhibitors. Cancer Res 2005;65(16):7386-7392.
103. Lee JT, Lehmann BD, Terrian DM, Chappell WH, Stivala F, Libra M, Martelli AM, Steelman LS, McCubrey JA. Targeting prostate cancer based on signal transduction and cell cycle pathways. Cell Cycle 2008;7(12):1745-1762.
104. Isaacs WB, Carter BS, Ewing CM. Wild-type p53 suppresses growth of human prostate cancer cells containing mutant p53 alleles. Cancer Res 1991;51(17):4716-4720.
105. Li R, Hannon GJ, Beach D, Stillman B. Subcellular distribution of p21 and PCNA in normal and repair-deficient cells following DNA damage. Curr Biol 1996;6(2):189-199.
106. Martinez LA, Yang J, Vazquez ES, Rodriguez-Vargas Mdel C, Olive M, Hsieh JT, Logothetis CJ, Navone NM. p21 modulates threshold of apoptosis induced by DNA-damage and growth factor withdrawal in prostate cancer cells. Carcinogenesis 2002;23(8):1289-1296.
107. Janicke RU, Sohn D, Essmann F, Schulze-Osthoff K. The multiple battles fought by anti-apoptotic p21. Cell Cycle 2007;6(4):407-413.
108. Kim CG, Choi BH, Son SW, Yi SJ, Shin SY, Lee YH. Tamoxifen-induced activation of p21Waf1/Cip1 gene transcription is mediated by Early Growth Response-1 protein through the JNK and p38 MAP kinase/Elk-1 cascades in MDA-MB-361 breast carcinoma cells. Cell Signal 2007;19(6):1290-1300.
109. Lin PY, Fosmire SP, Park SH, Park JY, Baksh S, Modiano JF, Weiss RH. Attenuation of PTEN increases p21 stability and cytosolic localization in kidney cancer cells: a potential mechanism of apoptosis resistance. Mol Cancer 2007;6:16.
110. O'Connor PM, Jackman J, Bae I, Myers TG, Fan S, Mutoh M, Scudiero DA, Monks A, Sausville EA, Weinstein JN, Friend S, Fornace AJ, Jr., Kohn KW. Characterization of the p53 tumor suppressor pathway in cell lines of the National Cancer Institute anticancer drug screen and correlations with the growth-inhibitory potency of 123 anticancer agents. Cancer Res 1997;57(19):4285-4300.
111. Rohlff C, Blagosklonny MV, Kyle E, Kesari A, Kim IY, Zelner DJ, Hakim F, Trepel J, Bergan RC. Prostate cancer cell growth inhibition by tamoxifen is associated with

inhibition of protein kinase C and induction of p21(waf1/cip1). Prostate 1998;37(1):51-59.
112. Levkau B, Koyama H, Raines EW, Clurman BE, Herren B, Orth K, Roberts JM, Ross R. Cleavage of p21Cip1/Waf1 and p27Kip1 mediates apoptosis in endothelial cells through activation of Cdk2: role of a caspase cascade. Mol Cell 1998;1(4):553-563.
113. Fizazi K, Martinez LA, Sikes CR, Johnston DA, Stephens LC, McDonnell TJ, Logothetis CJ, Trapman J, Pisters LL, Ordonez NG, Troncoso P, Navone NM. The association of p21((WAF-1/CIP1)) with progression to androgen-independent prostate cancer. Clin Cancer Res 2002;8(3):775-781.
114. Aaltomaa S, Lipponen P, Eskelinen M, Ala-Opas M, Kosma VM. Prognostic value and expression of p21(waf1/cip1) protein in prostate cancer. Prostate 1999;39(1):8-15.
115. Baretton GB, Klenk U, Diebold J, Schmeller N, Lohrs U. Proliferation- and apoptosis-associated factors in advanced prostatic carcinomas before and after androgen deprivation therapy: prognostic significance of p21/WAF1/CIP1 expression. Br J Cancer 1999;80(3-4):546-555.
116. Lacombe L, Maillette A, Meyer F, Veilleux C, Moore L, Fradet Y. Expression of p21 predicts PSA failure in locally advanced prostate cancer treated by prostatectomy. Int J Cancer 2001;95(3):135-139.
117. Rick FG, Schally AV, Block NL, Nadji M, Szepeshazi K, Zarandi M, Vidaurre I, Perez R, Halmos G, Szalontay L. Antagonists of growth hormone-releasing hormone (GHRH) reduce prostate size in experimental benign prostatic hyperplasia. Proc Natl Acad Sci U S A 2011;108(9):3755-3760.
118. Kanashiro CA, Schally AV, Groot K, Armatis P, Bernardino AL, Varga JL. Inhibition of mutant p53 expression and growth of DMS-153 small cell lung carcinoma by antagonists of growth hormone-releasing hormone and bombesin. Proc Natl Acad Sci U S A 2003;100(26):15836-15841.
119. Zarandi M, Horvath JE, Halmos G, Pinski J, Nagy A, Groot K, Rekasi Z, Schally AV. Synthesis and biological activities of highly potent antagonists of growth hormone-releasing hormone. Proc Natl Acad Sci U S A 1994;91(25):12298-12302.
120. Varga JL, Schally AV, Horvath JE, Kovacs M, Halmos G, Groot K, Toller GL, Rekasi Z, Zarandi M. Increased activity of antagonists of growth hormone-releasing hormone substituted at positions 8, 9, and 10. Proc Natl Acad Sci U S A 2004;101(6):1708-1713.
121. McConnell JD. Benign prostatic hyperplasia. Hormonal treatment. Urol Clin North Am 1995;22(2):387-400.
122. Wemyss-Holden SA, Hamdy FC, Hastie KJ. Steroid abuse in athletes, prostatic enlargement and bladder outflow obstruction--is there a relationship? Br J Urol 1994;74(4):476-478.
123. Constantinou CE. Influence of hormone treatment on prostate growth and micturition characteristics of the rat. Prostate 1996;29(1):30-35.
124. Liu HP, Chen GL, Liu P, Xu XP. Amlodipine alone or combined with terazosin improves lower urinary tract disorder in rat models of benign prostatic hyperplasia or detrusor instability: focus on detrusor overactivity. BJU Int 2009;104(11):1752-1757.
125. Pandita RK, Persson K, Hedlund P, Andersson KE. Testosterone-induced prostatic growth in the rat causes bladder overactivity unrelated to detrusor hypertrophy. Prostate 1998;35(2):102-108.
126. Scolnik MD, Servadio C, Abramovici A. Comparative study of experimentally induced benign and atypical hyperplasia in the ventral prostate of different rat strains. J Androl 1994;15(4):287-297.
127. Kojima Y, Sasaki S, Oda N, Koshimizu TA, Hayashi Y, Kiniwa M, Tsujimoto G, Kohri K. Prostate growth inhibition by subtype-selective alpha(1)-adrenoceptor antagonist naftopidil in benign prostatic hyperplasia. Prostate 2009;69(14):1521-1528.
128. Buchholz S, Schally AV, Engel JB, Hohla F, Heinrich E, Koester F, Varga JL, Halmos G. Potentiation of mammary cancer inhibition by combination of antagonists of growth

hormone-releasing hormone with docetaxel. Proc Natl Acad Sci U S A 2007;104(6):1943-1946.
129. Rick FG, Schally AV, Block NL, Halmos G, Perez R, Fernandez JB, Vidaurre I, Szalontay L. LHRH antagonist Cetrorelix reduces prostate size and gene expression of proinflammatory cytokines and growth factors in a rat model of benign prostatic hyperplasia. Prostate 2011;71(7):736-747.
130. Stangelberger A, Schally AV, Rick FG, Varga J, Baker B, Zarandi M, Halmos G. Inhibitory effects of antagonists of growth hormone releasing hormone on experimental prostate cancers are associated with upregulation of wild-type p53 and decrease in p21 and mutant p53 proteins. Prostate 2011.
131. Nemeth JA, Lee C. Prostatic ductal system in rats: regional variation in stromal organization. Prostate 1996;28(2):124-128.
132. Rick FG, Szalontay L, Schally AV, Block NL, Nadji M, Szepeshazi K, Vidaurre I, Kovacs M, Rekasi Z. Combining antagonist of GHRH with antagonist of LHRH greatly augments BPH shrinkage. J Urol 2011.
133. Pfaffl MW. A new mathematical model for relative quantification in real-time RT-PCR. Nucleic Acids Res 2001;29(9):e45.
134. Breier BH, Gallaher BW, Gluckman PD. Radioimmunoassay for insulin-like growth factor-I: solutions to some potential problems and pitfalls. J Endocrinol 1991;128(3):347-357.
135. Halmos G, Arencibia JM, Schally AV, Davis R, Bostwick DG. High incidence of receptors for luteinizing hormone-releasing hormone (LHRH) and LHRH receptor gene expression in human prostate cancers. J Urol 2000;163(2):623-629.
136. Plonowski A, Schally AV, Busto R, Krupa M, Varga JL, Halmos G. Expression of growth hormone-releasing hormone (GHRH) and splice variants of GHRH receptors in human experimental prostate cancers. Peptides 2002;23(6):1127-1133.
137. Emons G, Grundker C, Gunthert AR, Westphalen S, Kavanagh J, Verschraegen C. GnRH antagonists in the treatment of gynecological and breast cancers. Endocr Relat Cancer 2003;10(2):291-299.
138. Nickel JC, Downey J, Young I, Boag S. Asymptomatic inflammation and/or infection in benign prostatic hyperplasia. BJU Int 1999;84(9):976-981.
139. Tagaya M, Oka M, Ueda M, Takagaki K, Tanaka M, Ohgi T, Yano J. Eviprostat suppresses proinflammatory gene expression in the prostate of rats with partial bladder-outlet obstruction: a genome-wide DNA microarray analysis. Cytokine 2009;47(3):185-193.
140. Konig JE, Senge T, Allhoff EP, Konig W. Analysis of the inflammatory network in benign prostate hyperplasia and prostate cancer. Prostate 2004;58(2):121-129.
141. Schulz S, Rocken C. Immunocytochemical localisation of plasma membrane GHRH receptors in human tumours using a novel anti-peptide antibody. Eur J Cancer 2006;42(14):2390-2396.
142. Vykhovanets EV, Shukla S, MacLennan GT, Vykhovanets OV, Bodner DR, Gupta S. Il-1 beta-induced post-transition effect of NF-kappaB provides time-dependent wave of signals for initial phase of intrapostatic inflammation. Prostate 2009;69(6):633-643.
143. Barnes PJ, Karin M. Nuclear factor-kappaB: a pivotal transcription factor in chronic inflammatory diseases. N Engl J Med 1997;336(15):1066-1071.
144. Morisset S, Patry C, Lora M, de Brum-Fernandes AJ. Regulation of cyclooxygenase-2 expression in bovine chondrocytes in culture by interleukin 1alpha, tumor necrosis factor-alpha, glucocorticoids, and 17beta-estradiol. J Rheumatol 1998;25(6):1146-1153.
145. Smith WL, DeWitt DL, Garavito RM. Cyclooxygenases: structural, cellular, and molecular biology. Annu Rev Biochem 2000;69:145-182.
146. Kirschenbaum A, Klausner AP, Lee R, Unger P, Yao S, Liu XH, Levine AC. Expression of cyclooxygenase-1 and cyclooxygenase-2 in the human prostate. Urology 2000;56(4):671-676.

147. Hohla F, Schally AV, Szepeshazi K, Varga JL, Buchholz S, Koster F, Heinrich E, Halmos G, Rick FG, Kannadka C, Datz C, Kanashiro CA. Synergistic inhibition of growth of lung carcinomas by antagonists of growth hormone-releasing hormone in combination with docetaxel. Proc Natl Acad Sci U S A 2006;103(39):14513-14518.
148. Tsujii M, DuBois RN. Alterations in cellular adhesion and apoptosis in epithelial cells overexpressing prostaglandin endoperoxide synthase 2. Cell 1995;83(3):493-501.
149. Hohla F, Buchholz S, Schally AV, Seitz S, Rick FG, Szalontay L, Varga JL, Zarandi M, Halmos G, Vidaurre I, Krishan A, Kurtoglu M, Chandna S, Aigner E, Datz C. GHRH antagonist causes DNA damage leading to p21 mediated cell cycle arrest and apoptosis in human colon cancer cells. Cell Cycle 2009;8(19):3149-3156.
150. Kanashiro CA, Schally AV, Zarandi M, Hammann BD, Varga JL. Suppression of growth of H-69 small cell lung carcinoma by antagonists of growth hormone releasing hormone and bombesin is associated with an inhibition of protein kinase C signaling. Int J Cancer 2004;112(4):570-576.
151. Hubert RS, Vivanco I, Chen E, Rastegar S, Leong K, Mitchell SC, Madraswala R, Zhou Y, Kuo J, Raitano AB, Jakobovits A, Saffran DC, Afar DE. STEAP: a prostate-specific cell-surface antigen highly expressed in human prostate tumors. Proc Natl Acad Sci U S A 1999;96(25):14523-14528.
152. Azumi M, Kobayashi H, Aoki N, Sato K, Kimura S, Kakizaki H, Tateno M. Six-transmembrane epithelial antigen of the prostate as an immunotherapeutic target for renal cell and bladder cancer. J Urol 2010;183(5):2036-2044.
153. Stangelberger A, Schally AV, Zarandi M, Heinrich E, Groot K, Havt A, Kanashiro CA, Varga JL, Halmos G. The combination of antagonists of LHRH with antagonists of GHRH improves inhibition of androgen sensitive MDA-PCa-2b and LuCaP-35 prostate cancers. Prostate 2007;67(12):1339-1353.
154. Stangelberger A, Schally AV, Djavan B. New treatment approaches for prostate cancer based on peptide analogues. Eur Urol 2008;53(5):890-900.
155. Djakiew D. Dysregulated expression of growth factors and their receptors in the development of prostate cancer. Prostate 2000;42(2):150-160.
156. Hellawell GO, Turner GD, Davies DR, Poulsom R, Brewster SF, Macaulay VM. Expression of the type 1 insulin-like growth factor receptor is up-regulated in primary prostate cancer and commonly persists in metastatic disease. Cancer Res 2002;62(10):2942-2950.
157. Culig Z, Hobisch A, Cronauer MV, Radmayr C, Trapman J, Hittmair A, Bartsch G, Klocker H. Androgen receptor activation in prostatic tumor cell lines by insulin-like growth factor-I, keratinocyte growth factor, and epidermal growth factor. Cancer Res 1994;54(20):5474-5478.
158. Hoosein NM, Logothetis CJ, Chung LW. Differential effects of peptide hormones bombesin, vasoactive intestinal polypeptide and somatostatin analog RC-160 on the invasive capacity of human prostatic carcinoma cells. J Urol 1993;149(5):1209-1213.
159. Mimeault M, Pommery N, Henichart JP. New advances on prostate carcinogenesis and therapies: involvement of EGF-EGFR transduction system. Growth Factors 2003;21(1):1-14.
160. Culig Z, Hobisch A, Cronauer MV, Cato AC, Hittmair A, Radmayr C, Eberle J, Bartsch G, Klocker H. Mutant androgen receptor detected in an advanced-stage prostatic carcinoma is activated by adrenal androgens and progesterone. Mol Endocrinol 1993;7(12):1541-1550.
161. Stangelberger A, Schally AV, Varga JL, Zarandi M, Szepeshazi K, Armatis P, Halmos G. Inhibitory effect of antagonists of bombesin and growth hormone-releasing hormone on orthotopic and intraosseous growth and invasiveness of PC-3 human prostate cancer in nude mice. Clin Cancer Res 2005;11(1):49-57.
162. Kvols LK, Woltering EA. Role of somatostatin analogs in the clinical management of non-neuroendocrine solid tumors. Anticancer Drugs 2006;17(6):601-608.

163. Keller G, Schally AV, Groot K, Toller GL, Havt A, Koster F, Armatis P, Halmos G, Zarandi M, Varga JL, Engel JB. Effective treatment of experimental human non-Hodgkin's lymphomas with antagonists of growth hormone-releasing hormone. Proc Natl Acad Sci U S A 2005;102(30):10628-10633.
164. Letsch M, Schally AV, Stangelberger A, Groot K, Varga JL. Antagonists of growth hormone-releasing hormone (GH-RH) enhance tumour growth inhibition induced by androgen deprivation in human MDA-Pca-2b prostate cancers. Eur J Cancer 2004;40(3):436-444.
165. Pinski J, Schally AV, Halmos G, Szepeshazi K. Effect of somatostatin analog RC-160 and bombesin/gastrin releasing peptide antagonist RC-3095 on growth of PC-3 human prostate-cancer xenografts in nude mice. Int J Cancer 1993;55(6):963-967.
166. Gonzalez-Barcena D, Vadillo-Buenfil M, Cortez-Morales A, Fuentes-Garcia M, Cardenas-Cornejo I, Comaru-Schally AM, Schally AV. Luteinizing hormone-releasing hormone antagonist cetrorelix as primary single therapy in patients with advanced prostatic cancer and paraplegia due to metastatic invasion of spinal cord. Urology 1995;45(2):275-281.
167. Gonzalez-Barcena D, Schally AV, Vadillo-Buenfil M, Cortez-Morales A, Hernandez LV, Cardenas-Cornejo I, Comaru-Schally AM. Response of patients with advanced prostatic cancer to administration of somatostatin analog RC-160 (vapreotide) at the time of relapse. Prostate 2003;56(3):183-191.
168. McDonnell TJ, Navone NM, Troncoso P, Pisters LL, Conti C, von Eschenbach AC, Brisbay S, Logothetis CJ. Expression of bcl-2 oncoprotein and p53 protein accumulation in bone marrow metastases of androgen independent prostate cancer. J Urol 1997;157(2):569-574.
169. Navone NM, Troncoso P, Pisters LL, Goodrow TL, Palmer JL, Nichols WW, von Eschenbach AC, Conti CJ. p53 protein accumulation and gene mutation in the progression of human prostate carcinoma. J Natl Cancer Inst 1993;85(20):1657-1669.
170. Stapleton AM, Timme TL, Gousse AE, Li QF, Tobon AA, Kattan MW, Slawin KM, Wheeler TM, Scardino PT, Thompson TC. Primary human prostate cancer cells harboring p53 mutations are clonally expanded in metastases. Clin Cancer Res 1997;3(8):1389-1397.
171. Carroll AG, Voeller HJ, Sugars L, Gelmann EP. p53 oncogene mutations in three human prostate cancer cell lines. Prostate 1993;23(2):123-134.
172. Leuschner C, Enright FM, Gawronska-Kozak B, Hansel W. Human prostate cancer cells and xenografts are targeted and destroyed through luteinizing hormone releasing hormone receptors. Prostate 2003;56(4):239-249.
173. Rekasi Z, Czompoly T, Schally AV, Boldizsar F, Varga JL, Zarandi M, Berki T, Horvath RA, Nemeth P. Antagonist of growth hormone-releasing hormone induces apoptosis in LNCaP human prostate cancer cells through a Ca2+-dependent pathway. Proc Natl Acad Sci U S A 2005;102(9):3435-3440.
174. Greenblatt MS, Bennett WP, Hollstein M, Harris CC. Mutations in the p53 tumor suppressor gene: clues to cancer etiology and molecular pathogenesis. Cancer Res 1994;54(18):4855-4878.
175. van Bokhoven A, Varella-Garcia M, Korch C, Johannes WU, Smith EE, Miller HL, Nordeen SK, Miller GJ, Lucia MS. Molecular characterization of human prostate carcinoma cell lines. Prostate 2003;57(3):205-225.
176. Navone NM, Olive M, Ozen M, Davis R, Troncoso P, Tu SM, Johnston D, Pollack A, Pathak S, von Eschenbach AC, Logothetis CJ. Establishment of two human prostate cancer cell lines derived from a single bone metastasis. Clin Cancer Res 1997;3(12 Pt 1):2493-2500.
177. Natsume T, Kobayashi M, Fujimoto S. Association of p53 gene mutations with sensitivity to TZT-1027 in patients with clinical lung and renal carcinoma. Cancer 2001;92(2):386-394.

178. Werner H, Karnieli E, Rauscher FJ, LeRoith D. Wild-type and mutant p53 differentially regulate transcription of the insulin-like growth factor I receptor gene. Proc Natl Acad Sci U S A 1996;93(16):8318-8323.
179. Lee YI, Lee S, Das GC, Park US, Park SM. Activation of the insulin-like growth factor II transcription by aflatoxin B1 induced p53 mutant 249 is caused by activation of transcription complexes; implications for a gain-of-function during the formation of hepatocellular carcinoma. Oncogene 2000;19(33):3717-3726.
180. Cronauer MV, Schulz WA, Burchardt T, Ackermann R, Burchardt M. Inhibition of p53 function diminishes androgen receptor-mediated signaling in prostate cancer cell lines. Oncogene 2004;23(20):3541-3549.
181. Hu YX, Watanabe H, Ohtsubo K, Yamaguchi Y, Ha A, Motoo Y, Okai T, Sawabu N. Infrequent expression of p21 is related to altered p53 protein in pancreatic carcinoma. Clin Cancer Res 1998;4(5):1147-1152.
182. Tu Y, Wu W, Wu T, Cao Z, Wilkins R, Toh BH, Cooper ME, Chai Z. Antiproliferative autoantigen CDA1 transcriptionally up-regulates p21(Waf1/Cip1) by activating p53 and MEK/ERK1/2 MAPK pathways. J Biol Chem 2007;282(16):11722-11731.
183. Meng LH, Kohn KW, Pommier Y. Dose-response transition from cell cycle arrest to apoptosis with selective degradation of Mdm2 and p21WAF1/CIP1 in response to the novel anticancer agent, aminoflavone (NSC 686,288). Oncogene 2007;26(33):4806-4816.
184. Stangelberger A, Schally AV, Varga JL, Zarandi M, Cai RZ, Baker B, Hammann BD, Armatis P, Kanashiro CA. Inhibition of human androgen-independent PC-3 and DU-145 prostate cancers by antagonists of bombesin and growth hormone releasing hormone is linked to PKC, MAPK and c-jun intracellular signalling. Eur J Cancer 2005;41(17):2735-2744.

8. List of publications

Cumulative impact factor of publications related to the dissertation: articles: 23.456; abstracts: 2.365

Cumulative impact factor of all publications: articles: 69.256; abstracts: 117.95

Publications related to the dissertation

1. Peer-reviewed journal articles:

1. **Rick FG**, Schally AV, Block NL, Nadji M, Szepeshazi K, Zarandi M, Vidaurre I, Perez R, Halmos G, Szalontay L. Antagonists of growth hormone-releasing hormone (GHRH) reduce prostate size in experimental benign prostatic hyperplasia. *Proc Natl Acad Sci USA.* 2011 Mar 1;108(9):3755-60. [IF: 9.771] (2010)

2. **Rick FG**, Schally AV, Block NL, Halmos G, Perez R, Fernandez JB, Vidaurre I, Szalontay L. LHRH antagonist Cetrorelix reduces prostate size and gene expression of proinflammatory cytokines in a rat model of benign prostatic hyperplasia. *Prostate.* 2011 May 15;71(7):736-47. [IF: 3.377] (2010)

3. **Rick FG**, Szalontay L, Schally AV, Block NL, Nadji M, Szepeshazi K, Vidaurre I, Zarandi M, Kovacs M, Rekasi Z. Combining antagonist of GHRH with antagonist of LHRH greatly augments BPH shrinkage. *J Urol*. Accepted for publication. [IF: 3.862] (2010)

4. Stangelberger A, Schally AV, **Rick FG**, Varga JL, Baker B, Zarandi M, Halmos G. Inhibitory effects of antagonists of growth hormone releasing hormone on experimental prostate cancers are associated with upregulation of wild-type p53 and decrease in p21 and mutant p53 proteins. *Prostate.* 2011 July 27. doi: 10.1002/pros.21458. [Epub ahead of print] [IF: 3.377] (2010)

5. Heinrich E, Schally AV, Buchholz S, **Rick FG**, Halmos G Mile M, Groot K, Hohla F, Zarandi M, Varga JL. Dose-dependent growth inhibition in vivo of PC-3 prostate cancer with a reduction in tumoral growth factors after therapy with GHRH antagonist MZ-J-7-138. *Prostate.* 2008 Dec 1;68(16):1763-72. **[**IF: 3.069]

2. Citable abstracts:

1. **Rick FG**, Schally AV, Block NL, Szalontay L, Siejka A, Rincon R, Fensterle J, Engel J. Reduction in prostate size after treatment with Cetrorelix in a rat model of bening prostatic hyperplasia (BPH). *Urology*. 2009;74(4) S45. [IF: 2.365]

Further publications

1. Peer-reviewed journal articles:

1. Pozsgai E, Schally AV, Hocsak E, Zarandi M, **Rick F**, Bellyei S. The effect of a novel antagonist of growth hormone releasing hormone on cell proliferation and on the key cell signaling pathways in nine different breast cancer cell lines. *Int J Oncol*. 2011 Oct;39(4):1025-32. [IF: 2.571] (2010)

2. Papadia A, Schally AV, Halmos G, Varga JL, Seitz S, Buchholz S, Rick FG, Zarandi M, Bellyei S, Treszl A,. Lucci JA. Growth hormone releasing-hormone antagonist JMR-132 inhibits growth of ES-2 clear cell human ovarian cancer. *Horm Metab Res*. 2011. Accepted for publication. [IF: 2.414] (2010)

3. Kovacs M, Schally AV, Hohla F, **Rick FG**, Pozsgai E, Szalontay L,. Varga JL, Zarandi M. A correlation of endocrine and anticancer effects of some antagonists of GHRH. *Peptides*. 2010 Oct;31(10):1839-46**.** **[**IF: 2.654]

4. Pozsgai E, Schally AV, Varga JL, Halmos G, **Rick F**, Bellyei S. The inhibitory effect of a novel cytotoxic somatostatin analogue AN-162 on experimental glioblastoma. *Horm Metab Res*. 2010 Oct;42(11):781-6. [IF: 2.414]

5. Hohla F, Buchholz S, Schally AV, Krishan A, **Rick FG**, Szalontay L, Papadia A, Halmos G, Koster F, Aigner E, Datz C, Seitz S. Targeted cytotoxic somatostatin analog AN-162 inhibits growth of human colon carcinomas and increases sensitivity of doxorubicin resistant murine leukemia cells. *Cancer Lett.* 2010 Aug 1;294(1):35-42. [IF: 4.864]

6. Kanashiro-Takeuchi RM, Tziomalos K, Takeuchi LM, Treuer AV, Lamirault G, Dulce R, Hurtado M, Song Y, Block NL, **Rick F**, Klukovits A, Hu Q, Varga JL, Schally AV, Hare JM. Cardioprotective effects of growth hormone-releasing hormone agonist after myocardial infarction. *Proc Natl Acad Sci USA.* 2010 Feb 9;107(6):2604-9. [IF: 9.771]

7. Hohla F, Buchholz S, Schally AV, Seitz S, **Rick FG**, Szalontay L, Varga JL, Zarandi M, Halmos G, Vidaurre I, Krishan A, Kurtoglu M, Chandna S, Aigner E, Datz C.GHRH antagonist causes DNA damage leading to p21 mediated cell cycle arrest and apoptosis in human colon cancer cells. *Cell Cycle*. 2009 Oct 1;8(19):3149-56. [IF: 4.087]

8. Buchholz S, Seitz S, Schally AV, Engel JB, **Rick FG**, Szalontay L, Hohla F, Krishan A, Papadia A, Gaiser T, Ortmann O, Brockhoff G, Koster F. Triple negative breast cancers express receptors for LHRH and their growth can be inhibited by the LHRH antagonist Cetrorelix. *Int J Oncol.* 2009 Oct;35(4):789-96. [IF: 2.447]

9. Treszl A, Schally AV, Seitz S, Szalontay L, **Rick FG**, Halmos G. Inhibition of Human Non-Small Cell Lung Cancers with a Targeted Cytotoxic Somatostatin Analog, AN-162. *Peptides*. 2009 Sep;30(9):1643-50. [IF: 2.705]

10. Seitz S, Schally AV, Treszl A, Papadia A, **Rick F**, Szalontay L, Szepeshazi K, Ortmann O, Halmos G, Buchholz S. Preclinical evaluation of properties of new targeted-cytotoxic somatostatin analogue AN-162 [AEZS-124] and its effects on tumor growth inhibition. *Anticancer Drugs.* 2009 Aug;20(7):553-8. [IF: 2.23]

11. Hohla F, Schally AV, Szepeshazi K, Varga JL, Buchholz S, Koster F, Heinrich E, Halmos G, **Rick FG**, Kannadka C, Datz C, Kanashiro CA. Synergistic inhibition of growth of lung carcinomas by antagonists of growthhormone-releasing hormone in combination with docetaxel. *Proc Natl Acad Sci USA.* 2006 Sep 26;103(39):14513-8. [IF: 9.643]

2. Citable abstracts:

1. Kanashiro-Takeuchi RM, Takeuchi LM, **Rick FG,** Dulce RA, Treuer A, Paulino EC, Hatzistergos KE, Gonzalez DR, Hu Q, Block NL, Schally AV, Hare JM. Growth hormone relasing hormone (GHRH) receptor dependency for cardioprotective repair. *American Heart Association Scientific*

Sessions, November 12-16 2011, Orlando, FL. Abstract No. 2011-SS-A-13849-AHA. Published in *Circulation* 2011. [IF: 14.429] (2010)

2. Kovacs M, Schally AV, Hohla F, **Rick FG**, Pozsgai E, Szalontay L, Varga J, Zarandi M. *A correlation of endocrine and anticancer effects of some antagonists of GHRH*. *Endocrine Reviews*, Supplement 1, June 2010, 31(3):S1293. [IF: 22.469]

3. Abdel Wahab M, Schally AV, **Rick FG**, Szalontay L, Mahmoud O, Shi Y-F, Zarandi M, Varga JL. Antagonists of growth hormone releasing hormone (GHRH-A) given after radiation for prostate cancer tumors enhance tumor response through gene regulation. *International Journal of Radiation Oncology Biology Physics.* 2010 78(3):S649. [IF: 4.503]

4. Abdel-Wahab M, Schally AV, **Rick FG**, Szalontay L, Varga J, Shi Y, Zarandi M, Pollack A. Antagonists of growth hormone releasing hormone potentiate radiation response in prostate cancer. *J Clin Oncol* 2010;28(15). [IF: 18.97]

5. Papadia A, Schally AV, Seitz S, Buchhols S, **Rick FG**, Szalontay L, Bellyei S, Pozsgai E, Halmos G, Block N, Lucci J. Inhibition of growth of HEC-1-A and HEC-1-B human endometrial cancer by growth hormone releasing hormone antagonist JMR-132. *Gynecologic Oncology* 2010;116(3):596. [IF: 3.76]

6. Seitz S, Schally AV, **Rick F**, Weber F, Ortmann O, Buchholz S. Wirkung der kombinierten Behandlung mit dem GHRH-Antagonisten JMR 132 und Docetaxel in triple negativen Mammakarzinomen. *Senologie - Zeitschrift für Mammadiagnostik und –therapie* 2010;7:A166.

7. Kanashiro-Takeuchi RM, Tziomalos K, Takeuchi LM, Hurtado M, Song Y, Treuer A, Dulce R, Block NL, **Rick FG**, Hu Q, Varga JL, Schally AV, Hare JM. Growth-Hormone-Releasing-Hormone (GHRH) Agonist as a Potential Cardioprotective Agent in Rats with Post-Myocardial Infarction (MI). *Circulation* 2009;120:S868. [IF: 14.816]

8. Abdel-Wahab M, Schally AV, Szalontay L, **Rick FG**, Varga JL, Y-F Shi, Zarandi M, A Pollack, Duncan R. Radioprotection by Antagonists of Growth Hormone Releasing Hormone given before Whole Body Radiation is dependent on the Radiation Dose. *Int J Radiat Oncol Biol Phys* 2009;75(3):S552-553. [IF: 4.592]

9. Abdel-Wahab M, Schally AV, Szalontay L, Zarandi M, Varga JL, Pollack A, **Rick FG.** The use of antagonists of growth hormone releasing hormone (GHRH) radioprotect tumors in vivo. *Radiother Oncol* 2009;90(suppl 3):S113. [IF: 4.343]

10. Abdel-Wahab M, Schally AV, Szalontay L, **Rick FG** , Varga JL, Zarandi M, Pollack A. Use of antagonists of growth hormone releasing hormone for protection during whole body radiation. *Radiother Oncol* 2009; 90(suppl 3):S107. [IF: 4.343]

11. Seitz S, Schally AV, **Rick FG**, Szalontay L, Ortmann O, Buchholz S. Effective treatment of triple negative breast cancer with targeted cytotoxic somatostatin analogue AN-162 [AEZS-124]. *Journal of Clinical Oncology* 2009;27(15). [F: 17.793]

12. Seitz S, Schally AV, Papadia A, **Rick FG**, Szalontay L, Ortmann O, Engel J, Koster F, Buchholz S. Combination of antagonists of growth hormone-releasing hormone with docetaxel as potential therapy in breast cancer in a preclinical study. *Breast* 2009;18:S54. [IF: 2.087]

13. Papadia A, Schally AV, Seitz S, Buchholz S, Holha F, Szalontay L, **Rick FG**, Lucci J. Experimental therapy of ES-2 human platinum-resistant ovarian cancer with growth hormone-

releasing hormone antagonist JMR-132 or with targeted cytotoxic analog of somatostatin AN-162. *Gynecologic Oncology* 2009;112(2):S128-9. [IF: 3.733]

14. Seitz S, Schally AV, **Rick F**, Papadia A, Köster F, Engel J, Hönig A, Ortmann O, Buchholz S. Präklinische Studie zu dem zytotoxischen Somatostatinanalog AN-162 [AEZS-124] in der Therapie des rezeptornegativen Mammakarzinoms. *Senologie - Zeitschrift für Mammadiagnostik und –therapie* 2009; 6:A113.

15. Seitz S, **Rick F**, Papadia A, Schally AV, Köster F, Engel J, Ortmann O, Buchholz S. Potente Tumorinhibition des neuen GHRH Antagonisten JMR-132 im Östrogen Rezeptor negativen Mammakarzinom. *Senologie - Zeitschrift für Mammadiagnostik und –therapie* 2008;5:A133.

16. Abdel-Wahab M, Schally AV, Szalontay L, Zarandi M, Varga JL, Pollack A, **Rick FG.** Antagonists of growth hormone releasing hormone prostect tumors in vivo when given before radiation. *Indian J Radiat Res* 2008;5(3-4):203.

17. Abdel-Wahab M, Schally AV, Szalontay L, **Rick FG** , Varga JL, Zarandi M, Pollack A. Antagonists of growth hormone releasing hormone given before whole body radiation have protectivce effects. *Indian J Radiat Res* 2008;5(3-4):203.

3. Further abstracts:

1. Abdel-Wahab M, Schally AV, Szalontay L, **Rick FG**, Varga JL, Y-F Shi, Zarandi M, Pollack A, Duncan R. Dose-dependent Radioprotection by Antagonists of Growth Hormone Releasing Hormone given before Whole Body Radiation is dependent on organ-specific upregulation of target genes. *American Radium Society 92nd Annual Meeting*, May 1-5, 2010, Cancun, Mexico. Also printed in *Oncology*. [IF: 2.112]

9. Acknowledgements

I am grateful to **Professor Magdolna Kovacs**, who has introduced me to academic research when I was a medical student and has been a wonderful mentor over the years. Without her persistent encouragement, support and helpful advices I would not have been able to accomplish what I have achieved.

I would like to express the deepest appreciation to **Dr. Andrew V. Schally**, my chief and mentor, who has supported me and my work and continually conveyed a spirit of adventure in regard to research. This dissertation would not have been possible without his guidance and kind support.

Here I would like to express my appreciation to **Dr. Norman L. Block** for his support and guidance in urologic research.

I wish to thank to **Dr. Zoltan Rekasi**, my mentor for his encouraging support and teaching.

I am also thankful to all my colleagues at the Department of Pathology, University of Miami, Miller School of Medicine and Endocrine, Polypeptide and Cancer Institute, Veterans Affairs Medical Center and South Florida Veterans Affairs Foundation for Research and Education, Miami, especially to **Dr. Luca Szalontay, Dr. Karoly Szepeshazi, Dr. Marta Zarandi, Dr. Roberto Perez, Dr. Mehrdad Nadji, Dr. Ren-Zhi Cai, Dr. Jozsef L. Varga, Irving Vidaurre, Ricardo Rincon** and **Benny Fernandez** for their friendly support and helpful advices.

Last, but not least, I express my most sincere thank and eternal gratitude to my family for their love, sacrifice and encouraging support.